Universidade do Minho
Escola de Engenharia

Hugo Alexandre Mendes de Oliveira

Molecular studies on bacteriophage endolysins and their potential to control Gram-negative bacteria

April, 2014

Universidade do Minho
Escola de Engenharia

Hugo Alexandre Mendes de Oliveira

Molecular studies on bacteriophage endolysins and their potential to control Gram-negative bacteria

Thesis for PhD degree in Chemical and Biological Engineering

SUPERVISOR:
Professor Joana Cecília Valente Rodrigues Azeredo

CO-SUPERVISOR:
Doctor Leonardus Dorothea Kluskens

April, 2014

AUTHOR: Hugo Alexandre Mendes de Oliveira

E-MAIL: hugooliveira@deb.uminho.pt

TITLE OF THE THESIS: Molecular studies on bacteriophage endolysins and their potential to control Gram-negative bacteria

SUPERVISOR: Professor Joana Cecília Valente Rodrigues Azeredo

CO-SUPERVISOR: Doctor Leonardus Dorothea Kluskens

CONCLUSION YEAR: 2014

PhD in Chemical and Biological Engineering

University of Minho, April 2014

_____

“The true sign of intelligence is not knowledge but imagination”

Albert Einstein

Acknowledgments

I would like to acknowledge all persons that, made this work possible to accomplish for their disposal and kindness provided.

First and foremost, I would like to thank my Supervisors, Doctor Joana Azeredo and Doctor Leon Kluskens. Without their support, flexibility, and guidance, I would never have extended myself so far or achieved so much.

To my mentors and co-supervisors abroad, Craig Billington (Institution of Environmental Science and Research, Christchurch), Rob Lavigne (Katholieke Universiteit, Leuven), Teresa Petersen (International Iberian Nanotechnology Laboratory, Braga), and Francesco Secundo (Istituto di chimica del riconoscimento molecolare, Milan) and colleagues that became friends, Maarten Walmagh, Pieter-Jan Ceyssens and Thiagarajan Viruthachalam, for their teaching and leadership related to this thesis.

Many thanks go to all my colleagues at the Centre of Biological Engineering, for their collaboration, sympathy, availability and assistance.

Finally, I'd like to extend a special thanks to family and friends outside the University for their love and friendship, making it possible to finish my doctoral degree.

I would like to acknowledge "Fundação para a Ciência e Tecnologia" (FCT), Portugal for supporting this thesis though the Grant SFRH/BD/63734/2009 and the projects FCOMP-01-0124-FEDER-019446, FCOMP-01-0124-FEDER-027462 and PEst-OE/EQB/LA0023/2013. I would also like to acknowledge the financial support from the project "BioHealth - Biotechnology and Bioengineering approaches to improve health quality", Ref. NORTE-07-0124-FEDER-000027, co-funded by the Programa Operacional Regional do Norte (ON.2 – O Novo Norte), QREN, FEDER.

FCT Fundação para a Ciência e a Tecnologia
MINISTÉRIO DA CIÊNCIA, TECNOLOGIA E ENSINO SUPERIOR Portugal

Abstract

Bacteriophages are viruses that specifically infect bacterial hosts to reproduce. At the end of the infection cycle, progeny virions are confronted with a rigid cell wall that impedes their release into the environment. Consequently, bacteriophages encode hydrolytic enzymes, called endolysins, to digest the peptidoglycan and cause bacteriolysis.

In contrast to their extensively studied counterparts, active against Gram-positives, endolysins from bacteriophages from a Gram-negative background remain less explored. This knowledge gap is largely due to their limited potential as an antimicrobial, which is related to the presence of an impermeable outer membrane in Gram-negatives that blocks the exogenous endolysin action. The experimental work developed in the scope of this thesis aimed at developing efficient strategies to potentiate the endolysin action against these pathogens.

An extensive *in silico* analysis was performed to provide new insights about endolysins structure and function and bacteriophage-endolysin-host ecology. It was possible to identify and analyze 723 putative endolysins sequences from 5 distinct bacteriophages families, infecting 64 different bacterial genera. These endolysins are tremendously diverse in terms of enzymatic function (24 different enzymatic and 13 binding domains), architecture arrangements (89 different types with either globular or modular design) and length (72 to 578 amino acid residues).

Three different novel endolysins (Lys68, ABgp46 and PVP-SE1gp146) were studied in detail. Biochemical characterization of Lys68 (from a *Salmonella*-infecting bacteriophage) showed that it is highly thermostable, withstanding temperatures up to 100°C, and able to refold to its original conformation upon thermal denaturation. Lys68 was able to lyse a wide panel of Gram-negative bacteria in combination with outer membrane permeabilizers. While the Lys68/EDTA combination could only inactivate *Pseudomonas* strains, the use of citric or malic acid as permeabilizer broadened and increased its antibacterial effect. Particularly against *Salmonella*, the combinatory effect of malic or citric acid with Lys68 led to approximately 3 to 5 log reductions after 2 hours, respectively. During an acid-promoted effect, weak acids permeabilized the lipopolysaccharide of most bacteria to Lys68, which retained a relative high activity under these acidic conditions. In case of EDTA, its chelation effect was only observed against

Pseudomonas membranes, where ionic interactions are crucial stabilizing forces.

The endolysin ABgp46 (from an *Acinetobacter*-infecting bacteriophage) was shown to naturally inactivate 1 log of certain *Acinetobacter* strains. Tests in the presence of a number of weak acids (citric, malic, lactic, benzoic and acetic acid) resulted in a powerful antibacterial effect when combined with Abgp46. Higher bactericidal activity was consistently obtained when ABgp46 was combined with citric and malic acid, reducing all planktonic *Cronobacter*, *Klebsiella* and *E. coli* O157 (reductions of 1 to 3 logs) and *Pseudomonas*, *Acinetobacter* and *Salmonella* (reduction of more than 4 logs) species tested. It can be speculated that the major weak acid differences observed are related to their acid dissociated constant, that seems to favor compounds (with lower pKa values) that tend be more ionized. The same combinations did not have significant antibacterial activity when applied against *Pseudomonas* and *Acinetobacter* biofilms.

To enhance the activity of endolysins against Gram-negative cells, modified endolysins where constructed by fusing PVP-SE1gp146 (from a *Salmonella*-infecting bacteriophage) with different LPS-destabilizing peptides of polycationic, hydrophobic and amphipathic nature. This strategy resulted in an improvement of the activity of the modified endolysin compared to the native one (1 log reduction on *Pseudomonas* and *Salmonella* cells was obtained). The bactericidal activity of all modified variants was increased further in the presence of EDTA. A polycationic nonapeptide was the most efficient tag (maximum reduction of 5 logs). With a different purpose, attempts of increasing the endolysin (in this case Lys68) action against *Listeria monocytogenes* cells, by inserting species-specific peptidoglycan-binding peptides, did not result in a higher activity.

From the moment their genetic identity became known, endolysins have sparked the interest as alternatives for existing antibiotics. Here it was shown that endolysins can be used to kill not only Gram-positive, but also Gram-negative bacterial pathogens. These obtained results underline the great potential of using an endolysin-based strategy for prevention and/or control of Gram-negative pathogens in foodstuff, food processing surfaces, veterinary and medical applications.

Sumário

Os bacteriófagos são vírus que especificamente infectam bactérias para se reproduzirem. No fim do ciclo de infecção, os vírus descendentes são confrontados com uma parede celular rígida que impede a sua libertação para o meio ambiente. Consequentemente, os bacteriófagos codificam enzimas hidrolíticas, chamados endolisinas, para digerir o peptidoglicano e causar lise bacteriana.

Em oposição às suas homólogas extensivamente estudadas contra bactérias Gram-positivas, as endolisinas de bacteriófagos que infectam bactérias Gram-negativas permanecem menos exploradas. Este facto está relacionado com o seu potencial antibacteriano limitado, devido à presença de uma membrana externa que bloqueia a sua acção exógena. O trabalho desenvolvido nesta dissertação teve como objectivo o desenvolvimento de estratégias eficientes para potenciar a acção das endolisina contra estes agentes patogénicos.

A partir de bibliotecas genómicas públicas, foi realizada uma extensa análise bioinformática sobre endolisinas e a ecologia estabelecida entre o bacteriófago-endolisina-hospedeiro bacteriano. Foi possível analisar 723 sequências que codificam endolisinas de bacteriófagos de 5 famílias distintas e que infectam 64 géneros bacterianos diferentes. Estas endolisinas são tremendamente diversas em termos de sua função enzimática (encontrados 24 domínios enzimáticos e 13 domínios de ligação diferentes), estrutura molecular (89 tipos diferentes identificadas) e do seu tamanho (72-578 resíduos de aminoácidos).

Foram estudados em detalhe três endolisinas diferentes (Lys68, ABgp46 e PVP-SE1gp146). A Lys68 (isolada de um bacteriófago que infecta *Salmonella*) mostrou ser altamente termoestável, resistindo temperaturas até 100°C, sendo capaz de renaturar para a sua conformação original após um efeito térmico desnaturante. A Lys68 foi capaz de lisar um painel alargado de bactérias Gram-negativas, em combinação com permeabilizantes de membrana externa. Enquanto da combinação Lys68/EDTA apenas resultou na inactivação de estirpes de *Pseudomonas*, o uso de ácido cítrico ou ácido como permeabilizantes, aumentou e alargou o espetro da sua acção antibacteriana. Particularmente contra *Salmonella*, a combinação Lys68/cítrico e Lys68/málico levou a reduções aproximadamente de 3 a 5 logs ao fim de 2 horas, respectivamente. Os ácidos fracos permeabilizam os lipopolissacáridos das bactérias, permitindo a entrada da Lys68 que permanece com uma elevada actividade nestas condições ácidas. No caso do EDTA, o seu

efeito quelante apenas é eficaz contra as membranas da *Pseudomonas* que são essencialmente estabilizadas por interacções iónicas.

A endolisina ABgp46 (isolada de um bacteriófago que infecta *Acinetobacter*) mostrou ter uma capacidade natural de eliminar células de *Acinetobacter*. O seu efeito bactericida foi testado na presença de uma lista extensa de ácidos fracos (cítrico, málico, láctico, benzóico e ácido acético), mostrando ter um poderoso efeito antibacteriano. A actividade bactericida foi sempre superior quando ABgp46 foi combinada com o ácido cítrico ou málico, reduzindo populações planctónicas pertencentes as células de *Cronobacter*, *Klebsiella* e *E. coli* O157 (reduções de 1 a 3 logs) e de *Pseudomonas*, *Acinetobacter* e *Salmonella* (reduções de mais de 4 logs). Pensa-se que as diferenças observadas entre os ácidos fracos usados estão relacionados com a sua constante de dissociação, que parece favorecer os compostos (com valores mais baixos de pKa), que tendem ficar mais ionizados. As mesmas combinações não tiveram actividade antibacteriana significativa quando aplicada contra biofilmes de *Pseudomonas* e *Acinetobacter*.

Para melhorar a actividade, a endolisina PVP-SE1gp146 (isolada de um bacteriófago que infecta *Salmonella*) foi geneticamente alterada, adicionando péptidos de natureza policatiónica, hidrofóbica e anfipática que destabilizam os lipopolissacáridos da membrana de células Gram-negativas. Estas proteínas quiméricas tiveram melhor actividade antibacteriana quando comparada com a proteína nativa (reduções de 1 log em células de *Pseudomonas* e *Salmonella*). A actividade bactericida foi ainda melhorada na presença de EDTA. O péptido policatiónico (contendo nove aminoácidos) foi a fusão mais eficiente (reduções máximas de 5 logs). Com um objectivo diferente, tentou-se melhorar a actividade da endolisina (neste caso a Lys68) contra células de *Listeria monocytogenes*, inserindo péptidos que especificamente reconhecem o peptidoglicano de células de *Listeria*, contudo sem nenhum efeito positivo alcançado.

Desde o momento da sua descoberta, as endolisinas têm despertado o interesse como agentes antibacterianos alternativos. Aqui mostrou-se que as endolisinas podem não só ser usadas para matar bactérias Gram-positivas, mas também patogénicos Gram-negativos. Os resultados obtidos sublinham o grande potencial do uso de uma estratégia baseada em endolisinas para a prevenção e/ou controlo de patogénicos Gram-negativos em alimentos, superfícies de processamento alimentar, na veterinária e em aplicações médicas.

Table of contents

List of publications

Peer reviewed articles

Submitted

Oliveira H; Viruthachalam T; Walmagh M; Sillankorva S; Lavigne R; Petersen T; Kluskens LD; Azeredo J (2014). A highly thermostable *Salmonella* phage endolysin, Lys68, with broad anti-Gram-negative activity in the presence of weak acids.

Briers Y; Walmagh M; Puyenbroeck V; Cornelissen A; **Oliveira H**; Azeredo J; Verween G; Pirnay JP; Miller S; Volckaert G; Lavigne R (2014). Engineered endolysin-based "Artilysins" to combat multidrug resistant Gram-negative pathogens.

Published

Oliveira H; Azeredo J; Lavigne R; Kluskens LD (2012). Bacteriophage endolysins as a response to emerging foodborne pathogens. *Trends in Food Science & Technology* 28: 103-115.

Oliveira H; Melo L; Santos S; Nóbrega F; Ferreira E; Cerca N; Azeredo J; Kluskens, L (2013). Molecular aspects and comparative genomics of bacteriophage endolysins. *J Virol* 87: 4558-4570.

Other scientific output

Oral presentations

Oliveira H; Melo L; Santos S; Nóbrega F; Ferreira E; Cerca N; Azeredo, J; Kluskens L. Molecular and functional aspects of bacteriophage endolysins. BioMicroWorld 2013 - V International Conferenec on Environmental, Industrial and Applied Microbiology, Madrid, Spain, October 2-4th, 2013.

Invited oral presentations

Oliveira H. Development of Bacteriophage Endolysins to Control Gram-negative Pathogens, at the Istituto di Chimica del Riconoscimento Molecolare CNR, Milan, Italy, January 28th, 2014.

Posters in conferences

Oliveira H; Walmagh M; Kluskens LD; Sillankorva S; Lavigne R; Azeredo J. Biochemical and antibacterial characterization of a novel phage endolysin against the Gram-negative pathogen *Pseudomonas aeruginosa.* 19th Evergreen International Phage Biology Meeting, August 7-12th, 2011.

Oliveira H; Walmagh M; Kluskens LD; Sillankorva S; Lavigne R; Azeredo J. Antibacterial activity on opportunistic *Pseudomonas aeruginosa* pathogen by a novel *Salmonella* phage endolysin. MicroBiotec'11 - Book of Abstracts, Braga, Portugal, 1-3th December, 2011. - **Best poster prize**

Oliveira H; Melo, L; Nóbrega F; Santos SB; Cerca N; Ferreira EC; Azeredo J; Kluskens LD. Unraveling the insights into phage endolysin association. Viruses of Microbes - EMBO Conference, Brussels, Belgium, 16-20th July, 2012.

List of abbreviations

AMP	Antimicrobial Peptide
α4	α-helix 4 of T4 lysozyme (amino acids 143-155)
bp	Base Pair(s)
CBD	Cell Binding Domain
CEB	Centre of Biological Engineering
CD	Circular Dichroism
CFU	Colony Forming Unit
CHAP	Cysteine-, Histidine-dependent Aminohydrolase/Peptidase
CPP	Cell-Penetrating Peptide
dCTP	Deoxycytidine Triphosphate
DNA	Desoxyribonucleic Acid
ds	Double-stranded
ECD	Enzymatic Catalytic Domain
EDTA	Ethylene Diamine Tetra Acetic acid
(E)GFP	(Enhanced) Green Fluorescent Protein
G^-/ G^+	Gram-negative / Gram-positive
GHxx	Glycoside Hydrolase xx family
HEWL	Hen Egg White Lysozyme
HEPES	4-(2-HydroxyEthyl)-1-Piperazine-EthaneSulfonic acid
IPTG	Isopropyl-β-D-1-thiogalactopyranoside
LB	Lysogeny Broth
LIC	Ligation Independent Cloning
LPS	Lipopolysaccharide
kDa	Kilodalton
NAG or GluNAc	N-acetylglucosamine
NAM or MurNAc	N-acetylmuramic acid
Ni^{2+}-NTA	Nickel-Nitrilotriacetic Acid
OD_{xxxnm}	Optical Density at xxx nm wavelength
OM	Outer Membrane
OMP	Outer Membrane Permeabilizer
ORF	Open Reading Frame
PBS	Phosphate Buffered Saline
PCR	Polymerase Chain Reaction
PG	Peptidoglycan
PGH	Peptidoglycan Hydrolases
SDS-PAGE	Sodium Dodecyl Sulfate Polyacrylamide Gel Electrophoresis
ss	Single-Stranded
T_m	Melting temperature
Tris	Tris(hydroxymethyl)aminomethane
wt	Wild-Type

List of figures

List of tables

Chapter 1

Introduction and Background

This chapter is adapted from the following paper: Oliveira H; Azeredo J; Lavigne R; Kluskens LD (2012). Bacteriophage endolysins as a response to emerging foodborne pathogens. *Trends in Food Science & Technology* 28:103-115.

1.1 General introduction

Bacterial infections have always been a threat to human health. Gram-negative (G^-) bacterial pathogens in particular prevail in various surroundings, from food to clinical settings. A possible way to prevent or control such pathogens is by using bacteriophage (phages) lytic enzymes, called endolysins, evolved to destroy the peptidoglycan (PG), the structural component of the bacterial cell wall. However, part of the G^- bacterial resilience originates from the presence of a protective outer membrane (OM) that prevents toxic substances, such as endolysins, from entering the cell. This literature review starts by addressing the G^- bacterial infection problems, and gives a detailed overview of a possible solution involving endolysins to control these pathogens. Subsequently, the natural diffusion barrier of G^- bacterial OM for external endolysins is discussed as well as possible strategies to cross and overcome it.

1.1.1 The problem - Gram-negative bacterial infections

Foodborne contaminations that are dominated by G^- bacteria, represent a global incidence, causing 9.4 million acquired illnesses on a yearly basis in the United States alone (Scallan et al, 2011). With an estimated cost of $6 billion dollars each year in medical expenses and lost productivity, according to the United States Department of Agriculture's Economic Research Service (USDA-ERS, 2011), control of foodborne outbreaks has become a vital issue in the last decade. The actual figure is higher since this estimate reflects illnesses caused only by the major foodborne pathogens like *Salmonella*, *Escherichia coli* O157:H7, *Shigella sonnei* and *Campylobacter*. According to several food regulatory entities, there are other less common G^- foodborne infectious species like *Cronobacter sakazakii*, *Pantoea agglomerans* and *Pseudomonas fluorescens* that contribute to yearly costs related to foodborne outbreaks (EFSA, 2009; CDC, 2011) .

In clinical settings, hospital-acquired infections represent one of the most important leading causes of death worldwide, often associated with mechanical ventilation, invasive medical devices, or surgical procedures. With total of 1.7 million episodes and almost 99,000 deaths annually (Klevens et al, 2007; Kung et al, 2008), hospital-acquired infections lead to an estimated United States health care budget of more than $5 billion every year (Chopra et al, 2008). G^- bacteria represent more than 30% of hospital-acquired infections, and these bacteria predominate in cases of ventilator-associated pneumonia (47%) and urinary tract infections (45%). *Pseudomonas aeruginosa*, *Acinetobacter baumannii*, *Klebsiella oxycota* and *Proteus mirabilis* species are the most important G^- nosocomial infections reported.

Today, several antimicrobial agents are used to prevent food spoilage (chemical preservatives such as benzoates, nitrites, sulphites) or to treat infectious diseases (naturally produced antibiotics or synthetic chemotherapeutic agents). However, the beneficial, efficient and safety aspects of many applied antimicrobials are one of the hottest topics of debate among researchers specialized in food and medical science. For instance, sodium nitrite and nitrate are synthetic food preservatives that have been associated to cause chest tightness, elevated pulse rate and cancer among other adverse health effects (US EPA, 2006). The alarming emergence of bacteria resistant to antibiotics (*P. aeruginosa*, *A. baumannii* and *E. coli* are prevalent examples), acquired from foodborne or nosocomial infections, is considered one of the greatest threats to human health of the new millennium, as considered by the Infectious Diseases Society of America and the European Society of Clinical Microbiology and Infectious Diseases, hampering the effectiveness of everyday applied antibiotics (El-Tahawy, 2004; Gandhi et al, 2010).

Thus, despite the vast number of preservation methodologies adopted by the food industry and hospitals, contaminations by pathogens still occur, leading to serious economic consequences and threats associated with outbreaks. One

promising approach to prevent or destroy pathogenic bacteria is the use of PG-degrading enzymes of phage origin as alternative bacteriolytic agents to currently applied antimicrobials. This topic will be discussed in detail in the next section.

1.1.2 A "possible" solution - Bacteriophage lytic proteins

Phages are viruses that specifically infect bacteria and are harmless to humans, animals and plants. They are the most abundant living entities on Earth, outnumbering bacteria by an estimated tenfold, and accounting for a total population size of 10^{31} phage particles able to infect 10^{8} bacterial species (Brussow & Hendrix, 2002; Rohwer, 2003). Since their discovery, first by Hankin in 1896 and later rediscovered by Twort (1915) and d`Herelle (1917) (Summers, 2004), phage research has contributed to some of most important scientific breakthroughs in history of biological science, from molecular biology to genetic regulation.

The morphology of phage particles and the type of nucleic acids form the basis of their classification, a responsibility attributed to the International Committee on the Taxonomy of Viruses. The major order of phages is the *Caudovirales*, with 96% of all reported phages (Ackermann, 2003). *Caudovirales* virions possess double-stranded (ds) DNA genomes enclosed in heads with icosahedral symmetry, and with tails that vary in length. These tailed phages are subdivided in three families: *Siphoviridae* (61%) with long, flexible and noncontractile tails; *Myoviridae* (25%) having long, rigid and contractile tails; and *Podoviridae* (14%) with short and noncontractile tails. The remaining non-tailed phages belong to a small and highly variable group, with single-stranded (ss) DNA, ssRNA, or dsRNA (Ackermann, 2007).

In terms of reproduction cycle, being obligatory parasites, upon bacterial infection, phages can either cause cell lysis to release the newly formed virus

particles (lytic pathway) or lead to integration of the genetic information into the bacterial chromosome without cell death (lysogenic pathway). The lytic life cycle, illustrated in **Figure 1.1**, is predominantly found in all double-stranded nucleic acid (dsNA) phages.

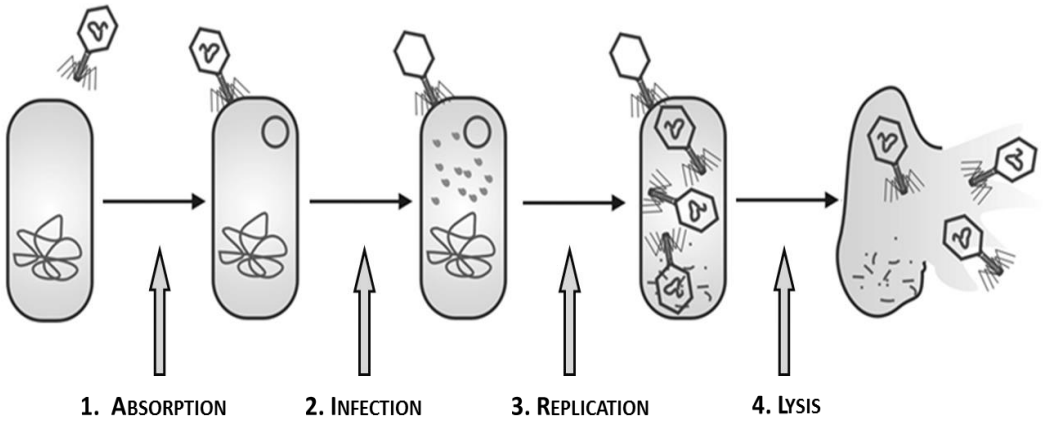

Figure 1.1. Lytic life cycle found in most double-stranded nucleic acid phages. Phages attach to cells (absorption), inject their DNA and hijack the host protein machinery (infection), to produce new phage particles (replication), causing bacterial disruption and subsequent release of their progeny (lysis) to initiate a new life cycle. The schematic drawing was kindly provided by Dr. Rob Lavigne, head of the Laboratory of Gene Technology at Katholieke Universiteit Leuven.

To be able to enter the cell and replicate, phages rely on random motion to attach to specific receptors (e.g. lipopolysaccharides, teichoic acids, proteins) on the surface of bacteria that narrows the host range of bacterial infection. The attachment can occur by a variety of mechanisms, depending on the morphology of the virus, often involving tail contraction and enzymatic degradation of a small portion of the cell membrane, to allow genetic material injection. Intracellularly, the phages multiply by taking advantage of the host's DNA replication and protein synthesis machinery, manufacturing and assembling new virus particles. At the end of the infection cycle, progeny virions are confronted with a rigid cell wall that

hinders their release into the environment and the opportunity to start a new infection cycle.

In this last step, phage encodes lytic proteins (discussed in detail in the next section) responsible for the bacterial lysis and subsequent release of new phage particles. The regulation of the lysis event has evolved individually to optimize phage fitness. Consequently, a diverse lysis cassette is found in dsNA phage genomes, although all contain a common lytic enzyme to degrade the bacterial cell wall - the endolysin.

1.1.2.1 Endolysin-mediated lysis

Phage replication demands a strategy for progeny release and dispersion to enable infection of new hosts. Two general strategies (holin-dependent and holin-independent export) to accomplish lysis have been described and are illustrated in **Figure 1.2**. They are exclusively reported for dsNA *Caudovirales* phages, as not much is known about lytic systems present in cassettes of phages outside this order.

Holin-dependent export

The holin-endolysin two-component cell lysis system, known as the lambda paradigm, is thought to be universal in almost all dsNA phages, with some exceptions (Sao-Jose et al, 2000; Kakikawa et al, 2002). In this system, soluble and active endolysins, lacking secretory signals, accumulate in the intracellular space due to the bacterial inner membrane. To gain access to the PG, small hydrophobic membrane-spanning proteins called holins are expressed at a genetically predetermined time and accumulate in clusters, producing homo-oligomeric pores in the inner membrane (340 nm - 1 μm diameter width) and thereby exposing the PG layer to the endolysins (Young, 1992; Young & Blasi, 1995).

Consequently, by degrading the PG, the endolysins compromise the mechanical strength and resistance of the cell wall that is needed to withstand the internal cytoplasmic turgor (osmotic) pressure, causing bacteriolysis and the subsequent release of the phage progeny. The lysis is then solely determined by the holin, but in some cases further fine-tuned by the presence of a holin inhibitor (Young & Blasi, 1995). This complex system illustrates the evolutionary pressure to optimize lysis timing, which is crucial for phage fitness. On the one hand, the vegetative cycle should be extended to allow sufficient accumulation and maturation of new phage particles. On the other hand, the vegetative cycle should be shortened, partially sacrificing the phage maturation period, to release early progeny viruses with better opportunity to infect more hosts and multiply exponentially.

Holin-independent export

Two holin-independent lytic systems are found in phages. In the first system, endolysins present N-terminal signal peptides that enable them to pass the cytoplasmic membrane and reach the PG, by making use of the host Sec system. Examples are endolysins found in *Bacillus cereus* phage TP21-L, *Oenococcus oeni* phage fOg44 and *Lactobacillus plantarum* phage Øg1e (Sao-Jose et al, 2000; Kakikawa et al, 2002). Secreted endolysins are translocated in an inactive form, after which the N-terminal signal is subjected to proteolytic cleavage. Already in the periplasm, the endolysins are only activated after dissipation of the proton motive force, triggered by holins that accumulate till an allele-specific time. So, rather than permeabilizing the endolysins through the cytoplasmic membrane, holins play here an endolysin activation role to control the lysis timing event.

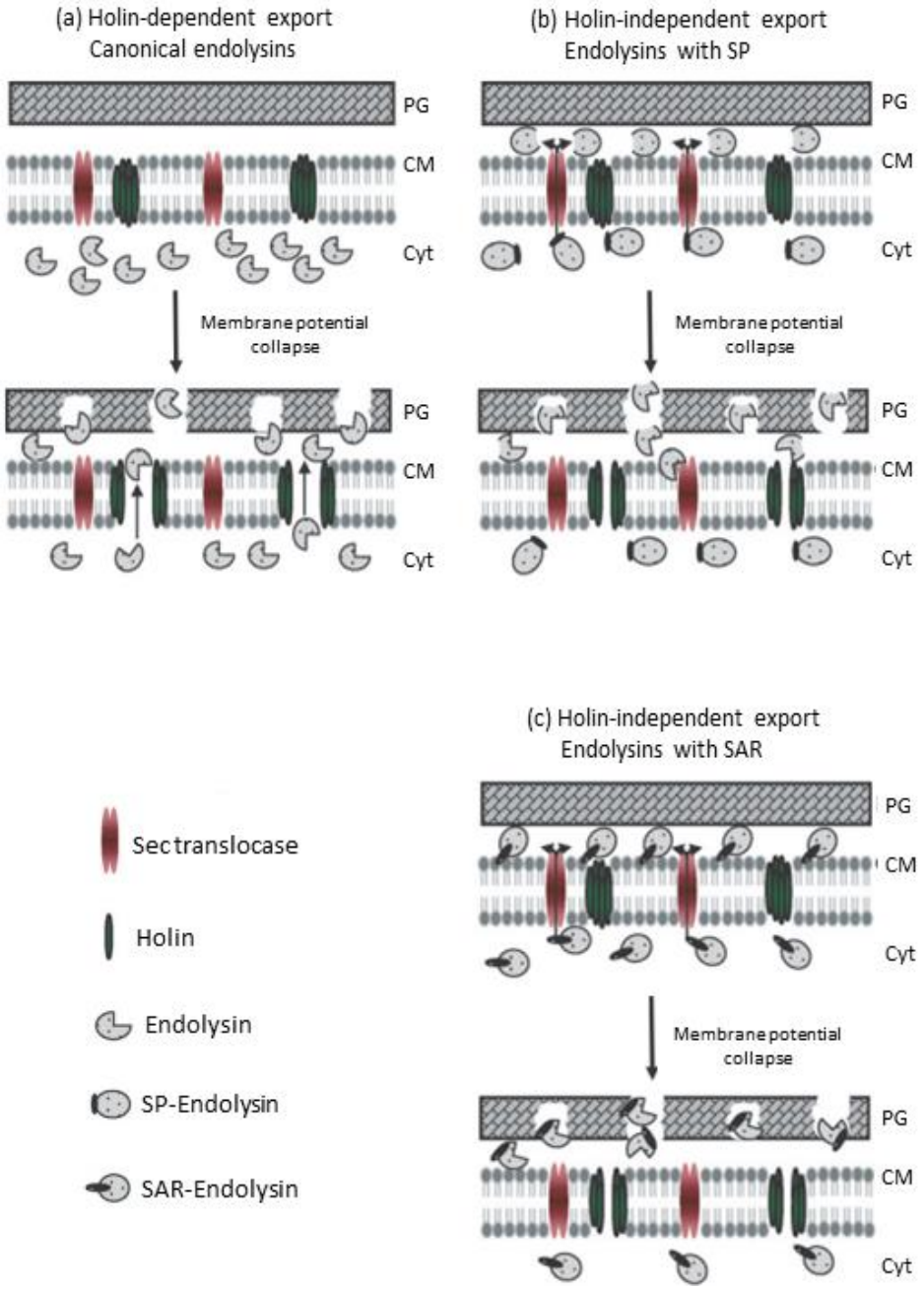

Figure 1.2. Schematic representation of how phage endolysins gain access to the peptidoglycan at the end of the phage lytic cycle through a holin dependent and independent manner. a) Holin-dependent export containing canonical endolysins; b) Holin-independent export with endolysins containing a SP, and c) Holin-independent export with endolysin containing SAR. Abbreviations: SP, signal peptide; SAR, signal-arrest-release; PG, peptidoglycan; CM, cytoplasmic membrane; Cyt, cytosol. Adapted from (Catalao et al, 2012).

The signal-arrest-release sequence is the second system found that uses the host Sec system for the secretion of endolysins. However in this case, the endolysin possesses a noncleavable N-terminal type II signal anchor that remains part of the mature endolysin and stays embedded in the inner cell membrane in an inactive form (Xu et al, 2004; Briers et al, 2011a). Consequently, these endolysins require pinholins to cause a membrane depolarization to release the SAR anchor, triggering endolysin activation and its access to the cell wall (Park et al, 2007; Pang et al, 2009). Pinholins are here distinguished from holins for their role of only promoting lesions (small pores < 2 nm) large enough to depolarize de cytoplasmic membrane in order to control the timing of lysis.

More recently, a new model of holin-independent endolysin export was found in Mycobacteriophage Ms6 (Catalao et al, 2012). Although not yet completely understood, evidence shows that Ms6 endolysins, lacking any predicted Sec-type or signal-arrest-release sequence, are assisted in their export by a chaperone-like protein (*gp1*). Endolysin regulation and activation is assumed to be a combined effort between two genes (*gp4 and gp5*), suggested to encode a holin and holin-inhibitor proteins.

Overall, lysis is accomplished by two steps: the holin permeabilization of the cytoplasmic membrane or signal-arrest-release endolysin activation (first step), followed by PG degradation by endolysins (second step). Additionally, G^- infecting dsNA phages have also acquired accessory proteins (spanins and LysB) in what can be considered a third step of host lysis - degradation of the OM (last barrier for progeny phage egress) (Catalao et al, 2012). Spanins (Rz/Rz1), first discovered in lambda phage, are proteins involved in the fusion of both inner/outer membranes. As for LysB, it has only been observed in Mycobacteriophages and their role is to digest bonds between the mycolic acids and the arabinogalactan, a particular content of *Mycobacterium* OM.

1.2 Endolysins as murein hydrolases

The rigid PG layer, also known as murein, is responsible for the physical integrity and shape of bacteria. It is composed of several chains of alternating residues of N-acetylmuramic acid (MurNAc) and N-acetylglucosamine (GlcNAc), connected by β-1,4 glycosidic bonds, linked to a short stem tetrapeptide. Whereas the carbohydrate backbone is conserved in all bacteria, the peptide moiety made of L- and D-amino acids is only conserved in G^- organisms (Vollmer & Born, 2009). In Gram-positives (G^+), it is considerably more diverse in terms of length and composition.

The amino acid residue in position 3 defines two types of PG: a meso-2,6-diaminopimelic acid type (mDAP-type) in G^- and some G^+ species (i.e. *Bacillus* and *Listeria* spp.) and an L-lysine type (Lys-type) typical for G^+ organisms. In the mDAP-type the peptide stem is usually directly linked via an amide bond, while in the Lys-type they are connected through an interpeptide bridge, such as in pentaglycine (*Staphylococcus aureus*) or dialanine (*Streptococcus pyogenes*).

This complexity and variety of more than 100 different reported eubacterial PG chemotypes has resulted in an evolutionary pressure on phages to refine their lytic cassette in order to compromise the host cell wall (Schleifer & Kandler, 1972). Toward this end, phages have acquired a huge diversity endolysins, varying in structure, type of domain and number, all discussed in detail in the next sections.

1.2.1 Endolysin structure organization

Depending on their origin, endolysins can vary in their molecular structure. Endolysins can either be globular proteins, with an enzymatic catalytic domain (ECD) alone responsible for the PG bonds cleavage, or modular proteins with an extra cell wall (or PG) binding domain (CBD) to help with substrate recognition.

Endolysins from G^+ infecting phages possess a typical, well-defined modular architecture, with an N-terminal ECD and a C-terminal CBD, separated by a short linker. In some cases, endolysins can also contain more than one ECD or CBDs. A unique example is the streptococcal C1 phage endolysin (PlyC). While in general endolysins have a molecular mass of 25 to 40 kDa (Fischetti, 2008), this peculiar endolysin weighs 114 kDa. PlyC is a multimeric protein that consists of one heavy chain representing the catalytic site (PlyCA), and eight PlyCB chains that bind to the cell wall (Nelson et al, 2006). In contrast to their G^+ counterparts, endolysins active against G^- generally display a globular structure (i.e. only contain the ECD) and rarely show a modular organization. Few examples of modular structure are reported to have inverted molecular orientations compared to G^+ endolysins, with the ECD at the C-terminal and the CBD at the N-terminal side (e.g. KZ144 of phiKZ) (Briers et al, 2007b).

1.2.1.1 Enzymatic catalytic domain

Depending on their ECD and the bonds that they hydrolyse, endolysins can be divided into different classes (**Figure 1.3**). Glycosidases cleave the glycan component at the reducing end of GlcNAc (**Fig. 1.3, target 1**), as shown for the streptococcal LambdaSa2 endolysin (Pritchard et al, 2007), or at the reducing end of MurNAc (**Fig. 1.3, target 2**), as described for the streptococcal B30 endolysin (Pritchard et al, 2004). The N-acetyl-β-D-muramidases (often called lysozymes or muramidases) share the same glycan target as the lytic transglycosidases (**Fig. 1.3, target 3**), however both deliver different end products: transglycosidases do not work as genuine hydrolases since no water is involved in the cleavage of the glycoside bond, and a 1,6-anhydro bond is formed instead in the muramic acid residue (Vollmer et al, 2008). This is an uncommon class among the phage endolysins with the *P. aeruginosa* phage phiKZ gp144 endolysin as an example

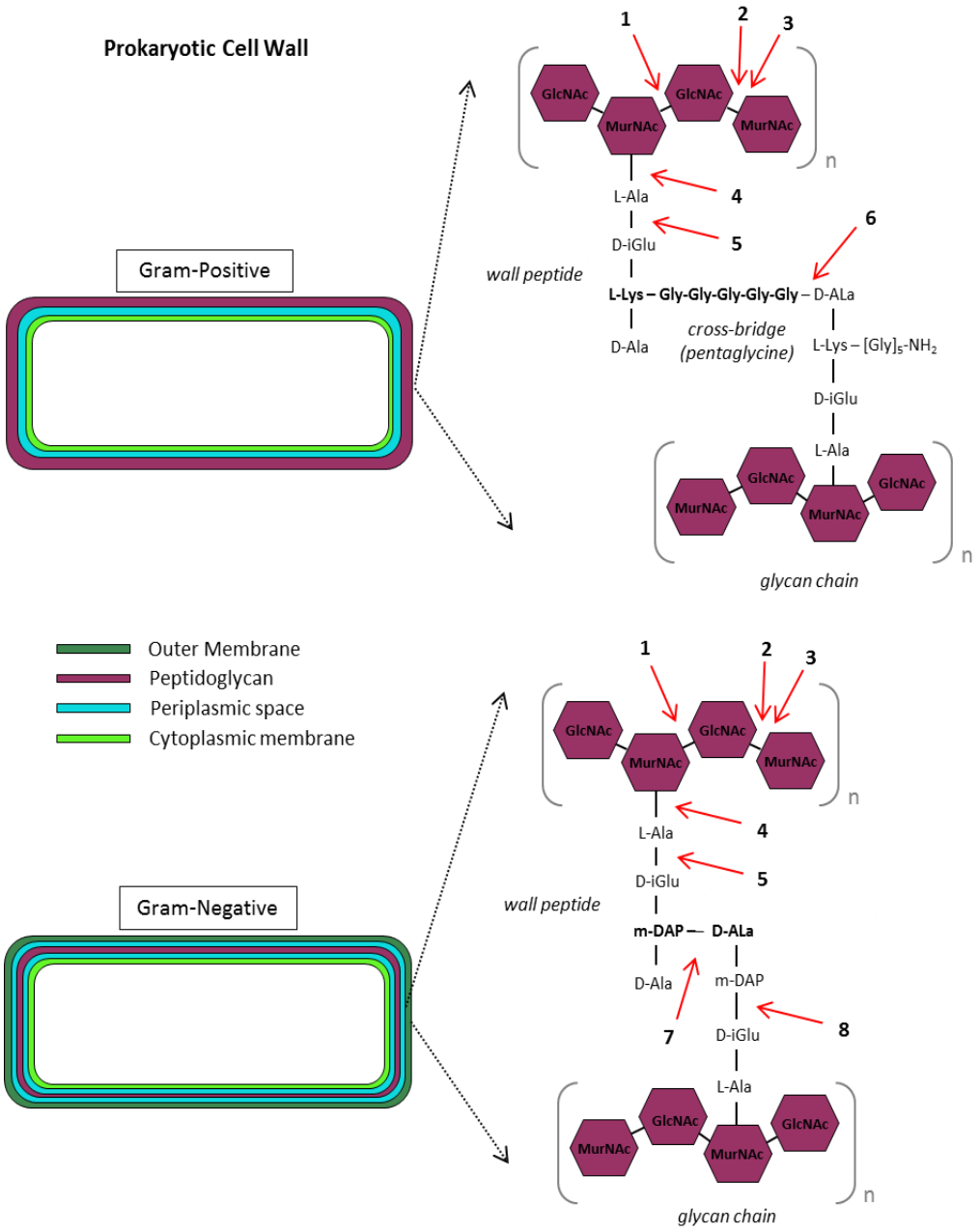

Figure 1.3. Schematic representation of the main peptidoglycan differences (in bold) between a Gram-positive and Gram-negative bacteria and endolysin mode of action according to their murein activity. Legend: 1) N-acetyl-β-D-glucosaminidase; 2) N-acetyl-β-D-muramidase; 3) lytic transglycosylase; 4) N-acetylmuramoyl-L-alanine amidase; 5) L-alanoyl-D-glutamate endopeptidase; 6) D-alanyl-glycyl endopeptidase. Abbreviations: GlcNAc, N-acetyl glucosamine; MurNAc, N-acetyl muramic acid.

(Fokine et al, 2008). Distinct classes of amidases catalyze the hydrolysis of the critical amide bond between MurNAc and the L-alanine (**Fig 1.3, target 4**), separating the glycan strand from the stem peptide. Therefore, amidases are predicted to cause the strongest destabilization effect in the PG. In addition, distinct classes of endopeptidases and carboxypeptidases attack the LD- and DD-bonds in the stem peptides, as has been demonstrated for *Listeria* Ply500 and the Ply118 L-alanyl-D-glutamate endopeptidases (Loessner et al, 1995) (**Fig. 1.3, target 5**). Other endopeptidases, like the staphylococcal phi11 D-alanyl-glycyl endopeptidase, also cleave within peptides that crosslink the cell wall (Navarre et al, 1999) (**Fig. 1.3, target 6**).

Related with the possibility to cleave more than one PG bond, some endolysins have even acquired more than one ECD, such as the endopeptidase/muramidase from the *Streptococcus agalactiae* phage B30 (Pritchard et al, 2004), the muramidase/endopeptidase of a pneumococcal phage Cpl-1 lytic enzyme (Hermoso et al, 2003), the endopeptidase/amidase of the phage phi11 endolysin (Navarre et al, 1999) and the endopeptidase/glucosaminidase of a streptococcal LambdaSa2 endolysin (Donovan & Foster-Frey, 2008). However, the presence of two ECDs does not necessarily mean that they are equally active. For instance, the D-glutaminyl-L-lysine endopeptidase of the streptococcal lambdaSa2 was found to be responsible for almost the entire hydrolytic activity of the protein (Donovan & Foster-Frey, 2008).

1.2.1.2 Cell binding domain

Endolysin modularity is represented when ECDs are accompanied by a CBD to target different receptors (e.g. PG subunits, saccharides, proteins, lipoteichoic acid, choline, and PG itself). The pneumococcal phage endolysin Cpl-1 CBD recognizes choline decorations on teichoic acids, resulting in a very narrow activity spectrum (Fernandez-Tornero et al, 2005). The CBDs of the *Listeria*

monocytogenes phage endolysins Ply118 and Ply500 can bind to different *Listeria* serovars, with an extremely high, nanomolar range affinity, comparable with levels of affinity-matured antibodies (Loessner et al, 2002). Another example is the action of an endolysin against *Streptococcus* group A that binds to polyrhamnose, which is a molecule indispensable for the growth of these bacteria (Fischetti, 2003). In the case of PlyC, the total CBD consists of 8 monomeric subunits which are able to specifically bind certain group A (*S. pyogenes*) and C (*S. equi, S. dysgalactiae*) streptococci with high affinity using an unknown cell wall epitope (McGowan et al, 2012). Notably, CBDs are mostly present in endolysins from G^+-infecting phages and are often found in double motifs. While it is shown that, generally, CBDs of endolysins targeting G^+ are highly specific, those found in G^-, like the endolysins KZ144 and EL188, show a broad binding spectrum (Briers et al, 2007b).

1.2.1.3 Domain swapping, truncation and addition

The urge to develop endolysins with desired or enhanced properties for several biotechnological applications has led to the creation of tailor-made enzymes. In this approach, the emphasis is laid on adding, truncating or swapping endolysin domains to obtain enzymes with optimized applications. Domain swapping can be done to enhance the endolysin`s lytic activity, overcome insolubility problems or for labelling purposes. Exchanging catalytic domains of a *Streptococcus pneumoniae* phage endolysins resulted in enzymes with the same binding characteristics but with multiple PG targets (Garcia et al, 1990). In the case of the staphyloccocal P16 endolysin, a similar modification was made with the intention to overcome solubility problems (Manoharadas et al, 2009). Probably, the most representative case of domain swapping studies lies in exchanging the ECD for a fluorescent protein (e.g. GFP). By exploiting the high affinity and specificity of the CBDs, these CBD-GFP proteins are used to label and capture different bacterial

cells, e.g. *Listeria* and *Bacillus* cells (Low et al, 2005; Kretzer et al, 2007). In case of endolysins from G^- phages, their CBDs (that bind to G^- PG unspecifically) fused with GFPs are also applied, but now as biomarkers, to assess the G^- OM permeability (Briers et al, 2009).

Domain truncations of both the ECD and the CBD have been carried out. CBD truncations have resulted in mixed successes. For instance, CBD truncation of the *Listeria* phage Ply118 and Ply500 endolysins (Loessner et al, 2002) or the *Clostridium perfringens* phage phi3626 endolysin (Zimmer et al, 2002) abolished its antibacterial activity, while for the Mur endolysin lytic activity remained unaltered (Vasala et al, 1995). In some cases, the truncation of the endolysin`s CBD resulted in a decrease of muralytic activity (Walmagh et al, 2012). For other studies, a higher bacteriolytic activity was achieved (Loessner et al, 1998; Loessner et al, 1999; Gaeng et al, 2000; Low et al, 2005) and in the case of the CBD-truncated LysK and PlyGBS endolysins, a 2-fold and approximately 25-fold increase in muralytic activity was attained, respectively (Cheng & Fischetti, 2007; Horgan et al, 2009). Interestingly, despite that CBDs are responsible for targeting the bacterial cell wall, they do not always seem to be essential for endolysin antibacterial activity.

Finally, constructs containing extra repetitive CBDs to increase affinity have also been made. This was the case for *Listeria* endolysins where duplicating the CBD500 increased the equilibrium cell wall binding affinity by approximately 50-fold (Schmelcher et al, 2011).

1.2.2 Endolysin biotechnological characteristics

Before considering the application of endolysins as a means to control foodborne and clinical diseases (see compilation of biotechnological applications in **Table 1.1**), an analysis of their physiochemical properties should be considered,

alongside other aspects concerning antimicrobial efficiency and safety. The following section debates relevant endolysin biotechnology features, giving examples of their positive impact in food and clinical *in situ* applications.

1.2.2.1 Host specificity

Endolysins only cleave PG linkages that are exclusively present in bacteria; however by displaying dissimilar lytic spectra they can be exploited differently. When a wide range of bacteria has to be controlled, endolysins with a broad host range will be required. For instance, in agriculture, endolysins targeting different bacterial species could play an important role as biopesticides, preventing tomato scabs, wilts and spots caused by *Streptomyces scabies*, *Clavibacter michiganensis* and *Xanthomonas campestris*, respectively. In health care units, endolysins could act as sanitizers targeting etilological agents of hospital-acquired infections (e.g. *S. aureus* or *P. aeruginosa*).

Endolysins with a narrower range of action, targeting a specific species or at least closely related bacterial species or genus, could prove useful for the elimination or control of specific pathogens or spoilage organisms. In livestock, endolysin - prebiotic - products could be administered to control enteric diseases in the cattle and poultry gastro-intestinal tract (e.g. with *C. perfringens* Ply2626 endolysin on poultry), while leaving the gut microflora unaltered (Zimmer et al, 2002). Alternatively, endolysins can control mastitis-causing bacteria in mammary glands of dairy cattle (e.g. with *Streptococcus uberis* Ply700 and *S. aureus* LysH5 endolysins) (Celia et al, 2008; Obeso et al, 2008), preventing cross-contamination of dairy products and animal carcasses during milking and slaughtering procedures, respectively. In industrial fermentations, endolysins like Ply511 could be secreted *in situ* in modified starter cultures, to control *L. monocytogenes* spoilage in milk (Gaeng et al, 2000), or used as a food additive, like the clostridial-

specific CTP1 endolysin preventing cheese spoilage and blowing (Mayer et al, 2010).

1.2.2.2 Temperature

The effect of thermal stress on endolysins can be variable. It is important to determine their antimicrobial activity under different temperatures (e.g. chilled food of approximately 4°C), to allow for efficient biocontrol. Surprisingly, endolysins have been shown to be active at a wide temperature range. While the T4 lysozyme retains only a minor fraction of its activity after a 5 min treatment at 65°C (Nakagawa et al, 1985), KZ144 and EL188 endolysin activities remain high even when exposed for 10 min to 50°C (Briers et al, 2007b). Others are shown to be stable for 30 min at 45°C (Loeffler et al, 2003), or exhibit only a 30% decrease in activity when exposed for 30 min to 90°C (Schmelcher et al, 2012b). Even higher thermostability has been described for the lysozyme domain of gp36 from a *P. aeruginosa* phage phiKMV, which is resistant to temperatures up to 100°C (Lavigne et al, 2004). However, it is likely that phages isolated from more thermostable bacteria will contain endolysins that are even more thermostable. Good examples of sources of potentially thermostable endolysins are *Bacillus* phage W1 and *Geobacillus* phage E1, isolated from deep-sea thermophilic bacteria, or the phage phiTMA isolated from the extreme thermophile *Thermus thermophilus*, originating from hot springs (Liu et al, 2006; Tamakoshi et al, 2011). Endorsing this hypothesis is the characterized *Thermus aquaticus* phage phiIN93 endolysin with an optimal activity between 60 and 120°C (Matsushita & Yanase, 2008).

Some bacteria, such as *Listeria* spp., are able to multiply even in refrigerated conditions. However, little is known about endolysin activity on this side of the temperature spectrum. Recently, an endolysin LysZ5 report showed the ability to reduce *Listeria* contamination at 4°C on soya milk (Zhang et al, 2012). It is

therefore estimated that with the characterization of more phages, novel thermo- and cryo-resistant endolysins will be identified and new potential biotechnology applications that require cryo/thermal processing will be established.

1.2.2.3 pH tolerance

Phage endolysin studies have indicated that their optimum pH can vary, ranging from acidic to basic. While some have an optimal pH within 4.0-6.0 (Borysowski et al, 2006), other have a better antibacterial activity at pH 7.0 (Walmagh et al, 2012) and even between pH 8.0-9.0 (Schmelcher et al, 2012b). In addition, the endolysin PlyPH, with a specific activity against *Bacillus cereus* and *B. anthracis*, remains active over an unusually broad pH range of 4.0 to 10.5 (Yoong et al, 2006).

1.2.2.4 Long-term storage (shelf life)

A good food antimicrobial extends the shelf-life of food products. Several endolysins demonstrate an extraordinarily long-term stability, such as Cpl-1, which showed no loss in activity over 6 months at 4°C and 3 weeks at 37°C (Loeffler et al, 2003). Other examples of endolysins with a long-term stability are KZ144 and EL188, which can be stored for 4 months at 4°C without loss of activity (Briers et al, 2007b).

1.2.2.5 Antimicrobial efficiency

Nanogram quantities of endolysin are able to eliminate bacteria from suspensions in seconds (Loeffler et al, 2001). To date, no other known biological compound has been found to kill microorganisms so quickly. In addition, affinity detection methods using nanomolar amounts of CBDs have been described (Loessner et al, 2002).

The possibility to eradicate antibiotic-resistant bacteria makes endolysins attractive antimicrobials. This has been shown, for example, on methicillin-resistant and multidrug-resistant *S. aureus* (endolysins LysK and MV-L, respectively) (O'Flaherty et al, 2005; Rashel et al, 2007), on vancomycin-resistant *E. faecalis* and *E. faecium* (endolysin PlyV12) (Yoong et al, 2004) and against multi-resistant *P. aeruginosa* strains (endolysin OBPgp279) (Walmagh et al, 2012). To further improve the antimicrobial efficacy, an endolysin cocktail or a combination with antibiotics could be employed to eliminate less accessible bacteria. Consistent with this, antibiotic-resistant *S. pneumoniae* strains have been targeted using Cpl-1 and Pal endolysins with the same target specificity, but different catalytic activities *in vitro* (Loeffler & Fischetti, 2003) and *in vivo* (Jado et al, 2003). Also, synergistic effects have also been demonstrated with the Cpl-1 endolysin and penicillin or gentamicin antibiotics against *S. pneumoniae* strains with different levels of susceptibilities to penicillin (Djurkovic et al, 2005).

Still regarding to antimicrobial efficiency, endolysins can also eliminate bacterial biofilms, which are often associated with potential problems in food and clinical processing units. Despite the higher resistance of biofilms to antimicrobials, compared to planktonic cells, three staphylococcal (phi11, phi12 and SAL-2) and one streptococcal phage endolysin (PlyC) were shown to successfully remove biofilms (Sass & Bierbaum, 2007; Son et al, 2010; Shen et al, 2013). In addition, endolysin activity has been shown in the presence of nonionic detergents (i.e. hard water and organic compounds), as well as its enzymatic disinfectant capacities on surfaces (Hoopes et al, 2009), potentiating even more the endolysins antimicrobial efficiency.

1.2.2.6 Safety

Several successful preclinical treatments with endolysins have been carried out in animal models and thus far no potential toxicity was observed (Loeffler et al, 2003; McCullers et al, 2007). Moreover, since phages are daily ingested via water and food without any associated health problems, endolysins may be regarded as safe to humans and animals. Additionally, in contrast to the several antiviral mechanisms of bacteria described against phages (Labrie et al, 2010), to date, resistance to endolysins has not yet been reported. Repetitive exposure of bacteria grown on agar plates to low concentrations of endolysin did not lead to the recovery of resistant strains; neither did bacterial resistance occur after several cycles of exposure to low concentrations of enzyme in liquid conditions (Loeffler et al, 2001; Rodriguez-Rubio et al, 2013). It has been postulated that the lack of bacterial resistance towards endolysins is due to their unique mode of action on targeting essential molecules that are difficult to be altered by bacteria (Loeffler et al, 2001; Fischetti, 2005).

Since their discovery, phage-encoded endolysins have been exploited in many fields. **Table 1.1** shows, however, an overwhelming application of endolysins in combating G^+ pathogens. The absence of their use against G^- bacteria is explained by the presence of an impermeable OM that hinders the action of external endolysins. Because G^- bacteria are also an important group of foodborne and hospital related infections, the next sections introduce the bacterial OM composition and diversity, which acts as a natural barrier for external endolysins. Furthermore, a set of different strategies are discussed to show how to permeabilize the bacterial membrane to endolysins.

Table 1.1. Endolysins that have been tested in animal models and food samples since 2000.

Gram -type	Bacterial pathogen	Endolysin or CBD	Animal model or Food Sample	Reference
G^+	*Listeria monocytogenes*	Ply511	Food Sample (milk fermentation)	(Gaeng et al, 2000)
G^+	*Streptococcus pneumoniae*	Cpl-1	Animal model (mouse model induced bacteremia)	(Loeffler et al, 2003)
G^+	*Streptococcus pyogenes*	Pal	Animal model (mouse model of pharyngitis)	(Nelson et al, 2001)
G^+	*Bacillus anthracis*	PlyG	Animal model (mouse model of nasopharyngeal carriage)	(Schuch et al, 2002)
G^+	*Clostridium perfringens*	Phi3626	Food Sample (poultry intestines)	(Zimmer et al, 2002)
G^+	*Streptococcus pneumoniae*	Pal	Animal model (murine sepsis)	(Jado et al, 2003)
G^-	*Erwinia amylovora*	phiEalh	Food Sample (Pears surface)	(Kim et al, 2004)
G^+	Group B streptococci	PlyGBS	Animal model (mouse model vagina and oropharynx)	(Cheng et al, 2005)
G^+	*Staphylococcus aureus*	phi11	Food Sample (bovine milk)	(Donovan et al, 2006b)
G^+	*Bacillus anthracis*	PlyPH	Animal model (*B. cereus* RSVF1 model of peritonitis)	(Yoong et al, 2006)
G^+	*Staphylococcus aureus*	MV-L	Animal model (mouse of systemic MRSA disease)	(Rashel et al, 2007)
G^+	*Listeria monocytogenes*	CBD118 or CBD500	Food Sample (meat, dairy and ready-to-eat products)	(Kretzer et al, 2007)
G^+	*Streptococcus uberis*	Ply700	Food Sample (bovine milk)	(Celia et al, 2008)
G^+	*Staphylococcus aureus*	LysH5	Food Sample (pasteurized milk)	(Obeso et al, 2008)
G^+	*Streptococcus equi*	PlyC	Food Sample (horse-related material surfaces)	(Hoopes et al, 2009)
G^+	*Clostridium tyrobutyricum*	phiCTP1	Food Sample (semi-skim milk)	(Mayer et al, 2010)
G^+	*Staphylococcus aureus*	LysH5	Food Sample (pasteurized milk)	(Garcia et al, 2010)
G^+	*Listeria monocytogenes*	CBDP40	Food Sample (milk and cheese)	(Schmelcher et al, 2010)
G^+	*Staphylococcus aureus*	P-27 or HP	Animal model (mouse model induced bacteremia)	(Gupta & Prasad, 2011)
G^+	*Listeria monocytogenes*	Lys	Food Sample (soya milk)	(Zhang et al, 2012)
G^+	*Staphylococcus aureus*	λSA2	Animal model (mouse model of bovine mastitis)	(Schmelcher et al, 2012a)
G^+	*Staphylococcus aureus*	SAL-1	Animal model (mouse model of MRSA infection)	(Jun et al, 2013)
G^+	*Streptococcus Pneumonia*	Cpl-1	Animal model (mouse model)	(Doehn et al, 2013)

1.3 Gram-negative outer membrane barrier for external endolysins

Although G^- bacteria class is represented by a variety of genera, the cell envelope of these bacteria has a common general architecture, comprising of a cytoplasmic membrane (symmetric membrane of mainly phospholipids in both leaflets) separated by a periplasmic space (containing the PG and some transport-proteins), from the OM. With a few exceptions, the OM consists of an asymmetric membrane of phospholipids (inner leaflet), lipopolysaccharides (LPS) (outer leaflet) and proteins, like porins, serving as defusing channels, and lipoproteins, covalently bound to the PG and anchored to the inner leaflet (**Figure 1.4 a**).

The LPS is the major component of the OM and represents the major virulence factor, providing the bacterium a permeability barrier for many external agents, such as endolysins. An overview of the LPS structure typically seen in G^- bacteria is presented, giving specific examples within the *Enterobacteriaceae* (*Salmonella*, *E. coli*) and *Pseudomonadaceae* (*P. aeruginosa*). Furthermore, OM permeabilization strategies to potentiate the endolysins` antibacterial activity are discussed.

1.3.1 LPS structure and diversity

The LPS is an extremely diverse structure that can be modified in response to prevailing environmental conditions (Nikaido, 2003). Three different regions can be distinguished according to their chemical structure, biosynthesis, genetics and function: *i*) the lipid A component, *ii*) the core region and *iii*) the O-antigen, also known as O-specific polysaccharides or O-side chains, illustrated in **Figure 1.4 b**. The LPS may be presented in a rough (R-type, without O-antigen), smooth (S-type, with O-antigen) or a mixture (SR-type).

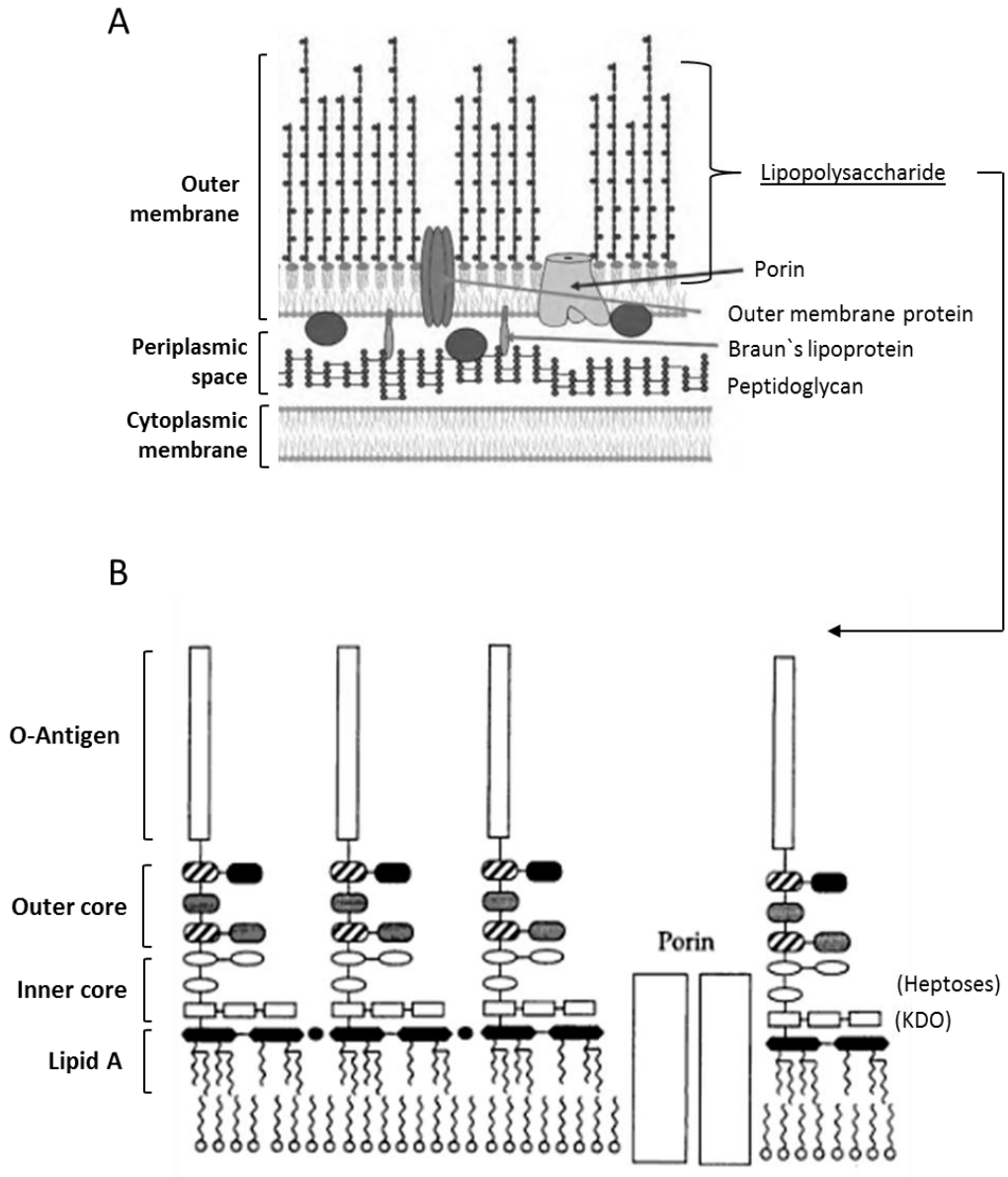

Figure 1.4. Schematic representation of a typical Gram-negative cell envelope. a) Illustration of the main cell envelope components (cytoplasmic membrane, the periplasmic space and the outer membrane). b) A zoomed image of a typical *E. coli* and *S.* Typhimurium LPS chemical structure is illustrated. Two different sub-regions (inner and outer) are found in core oligosaccharide based on their chemical composition. Small black dots represents divalent cations (Mg^{2+}, Ca^{2+}) that bridge LPS molecules via ionic linkages to form a network. Abbreviation: KDO, 2-keto-3-deoxy-octonic acid. Adapted from (Vaara, 1999).

1.3.1.1 O-polysaccharide or O-antigen

The O-antigen, the major component of the LPS surface, is a highly antigenic structure consisting of a linear chain of oligosaccharide units, attached to the lipid A-core molecules by a ligase (**Figure 1.4 b**). The O-antigen is a highly diverse structure that provides the bacterium with an extra shelter against external factors. Contributing to this diversity are the chain length (up to 50 mono- or oligosaccharides), the sugar composition (containing 2-8 monosaccharide residues of which D-glucose and D-galactose are more common), their modifications (O-acetylation, epimerization, glycosylation and amidation) and the glycosyl linkages between the repeating units (i.e. by α-(1→2)-, α-(1→3)- or β-(1→3)). This is reflected by the polymorphisms presented in the genes responsible for the biosynthesis of these structures (Knirel, 2009).

1.3.1.2 Core oligosaccharide

The core oligosaccharide is a short chain of oligosaccharides of ≈15 sugars. Being chemically diverse (although to a lesser extent than the O-antigen), the core region can be divided into an inner and outer core. The basis of the inner core consists of keto-deoxyoctanoate, also known as 3-deoxy-D-manno-2-octulosonic acid (Kdo) and L-glycero-D-manno-heptose (Hep) residues. Their number, linkages and substituent units present (e.g. other sugars or phosphate residues, or sometimes by acetyl groups or amino acids) account for structural diversity of this core region. Common to all is the Kdo residue that covalently links the inner core to the Lipid A (**Figure 1.5**) (Holst & Molinaro, 2009). The outer core is made of hexose residues attaching the O-antigen to the last heptose of the inner core. Common sugar residues found here are D-glucose, D-mannose and D-galactose. In particular, the *P. aeruginosa* inner core contains a higher amount of Kdo and phosphate residues, which gives an average of 6.5 formal negative charges per LPS molecule, compared to the 5.5 formal negative charges of the *E. coli* Lipid A.

This indicates that ionic interactions in the *P. aeruginosa* Lipid A with surrounding divalent cations have a stronger contribution for the stabilization of LPS molecules (Nikaido, 2003; Pier, 2007).

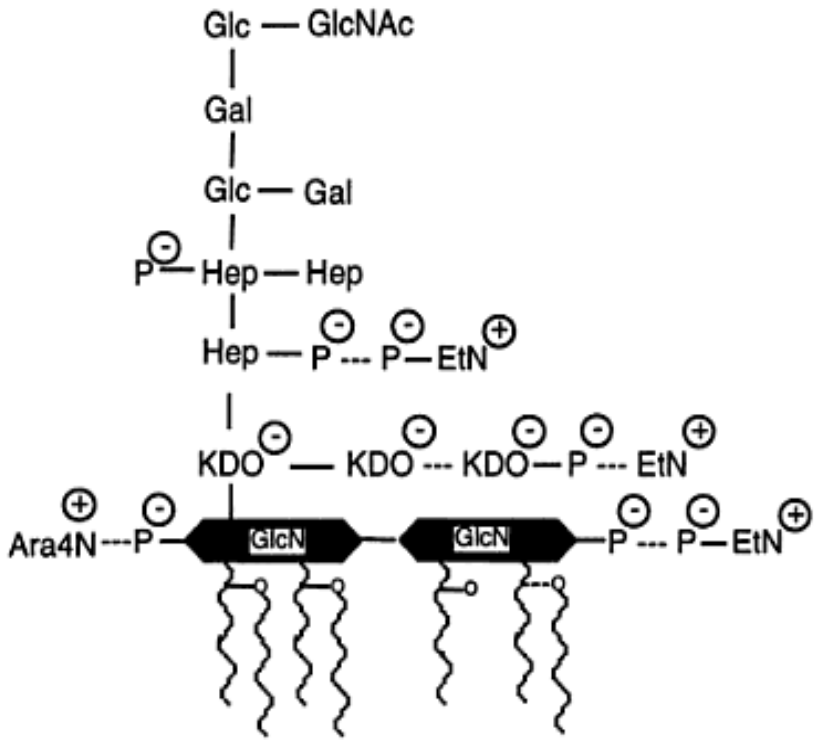

Figure 1.5. Detailed view of the inner core oligosaccharide and Lipid A components of *S.* Typhimurium. Dotted lines represent incomplete substitutions. Abbreviations: Glc, D-glucose; Gal, D-galactose, GlcN, D-glucosamine; P, phosphate; Hep, L-glycero-D-mannoheptose; EtN, 2-aminoethanol; Ara4N, 4-amino-4-deoxy-L-arabinose; KDO, 2-keto-3-deoxy-octonic acid; GlcN, D-glucosamine; GlcNAc, N-acetyl-D-glucosamine. Retrieved from (Vaara, 1999).

1.3.1.3 Lipid A

Lipid A is the innermost of the three regions of the LPS that anchors the whole molecule to the OM. It represents the endotoxic centre of the LPS, which is responsible for the pyrogenicity of LPS. Lipid A is known to possess a rather conservative structure which is characterized by a β (1',6) linked disaccharide of D-glucosamine backbone, phosphorylated (at C_1 and $C_{4'}$) and acetylated on different positions (C_2, C_3, $C_{2'}$ and $C_{3'}$) by primary hydroxy and non-hydroxy acyl groups (**Figure 1.5**). Heterogeneity found in lipid A can arise from the type of sugar present, the degree of phosphorylation, the presence of phosphate substitutes, ethanolamine or other groups, and nature, chain length, number, and position of the acyl groups (Raetz & Whitfield, 2002; Holst & Molinaro, 2009) (**Figure 1.5).** Particularly, lateral interaction between the neighbouring Lipid A moieties is responsible for the LPS stability and subsequent permeabilizing efficiency. First, the negatively charged phosphate groups presented throughout the Lipid A (and also the core oligosaccharide) are important for strengthening the LPS monolayer by linking molecules via ionic bridges with divalent cations (Vaara, 1999). However, Lipid A phosphate group substitutes can occur, lowering the overall negative charge of the LPS. Second, the presence of a higher number and length of acyl chains (fatty acids) in lipid A increases intermolecular hydrophobic stacking, also contributing to a more stabilized OM (Nikaido, 2003). A higher acylated lipid A is found in *E. coli* and *Salmonella* (composed of hexa- or hepta-acylations, with a minimum of 14 carbon atoms long), compared to the less acylated Lipid A of *P. aeruginosa* (composed of penta-acylations, with a 12 carbon atoms long), favouring the *E. coli* and *Salmonella* for a more stabilized LPS structure (Nikaido, 2003).

1.4 Strategies to overcome the outer membrane

In view of the conserved G^- bacterial PG structure, the application of endolysins on these bacteria is considered to be the ”holy grail” in endolysin-based microbial control (Schleifer & Kandler, 1972). As mentioned before, two main OM-stabilizing forces, the LPS cation-binding sites (ionic interactions) and the dense hydrophobic stacking of the Lipid A acyl chain groups (hydrophobic interactions), are present. Possible strategies to weaken the OM are: *i*) the use of outer membrane permeabilizing (OMP) compounds (such as EDTA and organic acids) or *ii*) covalent modification of endolysins by inserting LPS-destabilizing peptides (like antimicrobial peptides. Their OMP mechanisms are illustrated in **Figure 1.6**. Liposome delivery, OM vesicle-delivery and pressure-promoted permeabilization are other possible OMP techniques that are not discussed here, as they are beyond the scope of this research.

1.4.1 Outer membrane permeabilizer agents

The G^- bacteria OM functions as a natural barrier against external harmful agents. Its integrity can be challenged by targeting the aforementioned stabilizing divalent cations interactions with the ionic LPS structure. Polycations, chelators and organic acids form three distinct groups of OMPs interacting with the OM in a different way.

Polycations (mostly represented by polymyxin B and their derivatives, lysine polymers and aminoglycosides) compete with the stabilizing cations to bind to the ionic sites of the LPS. This results in displacement of the divalent cations and destabilization and/or permeation of the OM (Vaara, 1992). Among polymyxin groups, polymyxin B (four net positive charges) is the strongest OMP because it not only weakens the OM by cation-binding competition in range of 0.3-1 µg/mL (sublethal effect) but also can cause leakage of cytoplasmic components (lethal

effect) with a minimal inhibitory concentration of 1 µg/mL in *E. coli* and *S.* Typhimurium (Vaara & Vaara, 1983). As for lysine polymers, $lysine_{20}$ (20 lysine residues) has the strongest permeabilizing effect in the range of 0.3 to 3 µL/mL (Vaara & Vaara, 1983). In case of aminoglycosides (three to six net positive charges), they are weaker permeabilizers, strongly dependent on the ionic strength (Vaara, 1992).

Chelators (mostly represented by EDTA) remove the stabilizing Mg^{2+} and Ca^{2+} cations from the LPS (**Figure 1.6**). Consequently, LPS components are released to the extracellular environment (Leive et al, 1968) and this results in an uptake of phospholipids that migrate from the inner layers, creating patches that facilitate transport of hydrophobic/lipophilic agents (Nikaido & Vaara, 1985). Like most chelators, EDTA has a weak bactericidal effect, able to, for example, sensitize G^- bacteria to several hydrophobic antibiotics (e.g. erythromycin, rifampin, cloxacillin) (Scudamore et al, 1979). To date, EDTA is the only OMP agent described to act synergistically with endolysins, permeabilizing the OM of *P. aeruginosa* to these enzymes (Briers et al, 2007b).

Recently, weak organic acids (e.g. citric, malic, benzoic and lactic acid) have been considered as another group of OMPs. Although some agents, such as citric acid, have, to a lesser extent, chelating properties, additional acidity can contribute to OM disruption (Alakomi et al, 2000; Theron & Lues, 2011) (**Figure 1.6**). It has been proposed that the LPS disintegration is accomplished by the ability of undissociated acid groups to interact/pass through the negatively charged LPS (where negatively charged acid forms are repulsed) and migrate inside the cells to cause sublethal injuries. Intracellularly, the organic acid meets a higher internal pH (7.2) and dissociates to produce protons (that can exit through specific proton channels) and anions (Breidt et al, 2004). The persistent presence of the higher concentration of protons increases the cytoplasmic acidity, compromising some enzymatic functions (e.g. inactivation of acid-sensitive enzymes) (Roe et al, 2002; Hirshfield et al, 2003). The presence of anion parts that cannot exit also

contributes to the inhibition of several metabolic reactions (e.g. increase of turgor pressure) (Roe et al, 1998; Kirkpatrick et al, 2001). Citric, malic and lactic acid are examples of weak organic acids reported to possess OM-disrupting activity against *P. aeruginosa*, *S.* Typhimurium and *E. coli* O157 (Alakomi et al, 2000; Kim & Rhee, 2013). They can become active antimicrobial agents against G^- bacteria at higher concentrations or when combined with fatty acids (In et al, 2013; Kim & Rhee, 2013).

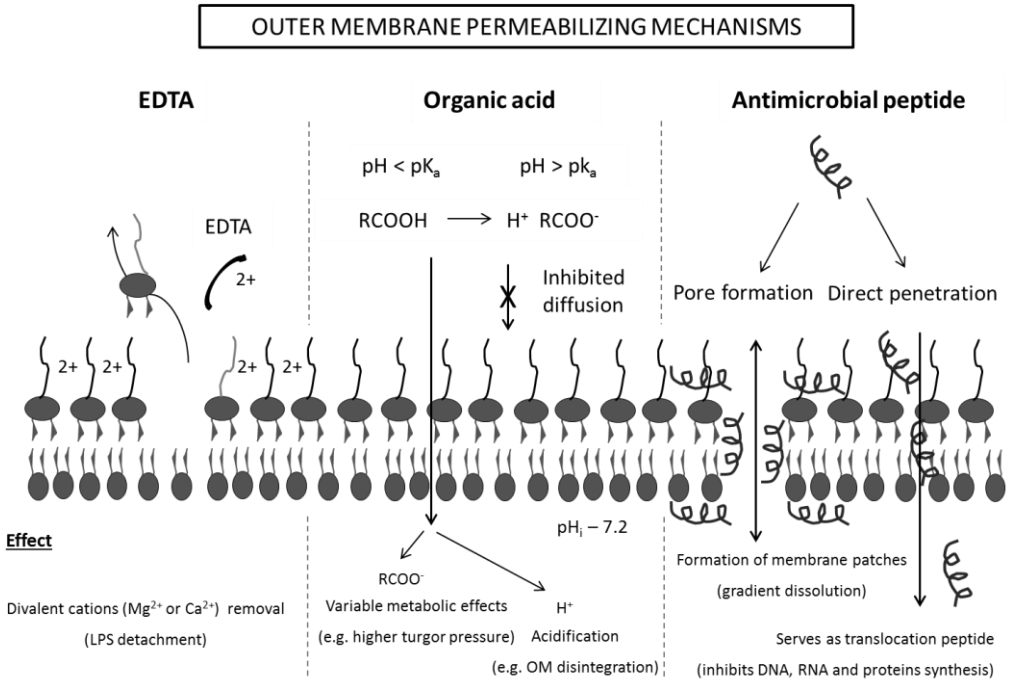

Figure 1.6. Simplified view of the Gram-negative bilayer with an overview of its destabilization by using different membrane active agents (EDTA, organic acid and antimicrobial peptide). EDTA chelates outer membrane-bound stabilizing divalent cations, causing dispersion of LPS molecules from the cells. Organic acids can diffuse freely into intracellular spaces in their undissosiated form (oppositely, dissociated acids are limited to secondary transport). Increase of anion as well as proton concentrations affects several metabolic processes (e.g. enzyme inhibitions, amino acid decarboxylation, membrane disruption). Antimicrobial peptides have a binary mode of action. They can either lyse the cell by disruption of cytoplasmic membrane (pore formation) or translocate inside the cells (direct penetration) to lethally interfere with several cellular processes (e.g. DNA, RNA synthesis). Abbreviations: RCOOH, undissociated acid; H^+ $RCOO^-$, dissociated acid; pH_i, intracellular pH; pK_a, acid dissociation constant; OM, outer membrane.

1.4.2 Covalent modification - inserting LPS-destabilizing peptides

Covalent modification by the addition of (LPS-destabilizing) peptides with a polycationic, hydrophobic or amphipathic nature can allow the passage of external proteins through the bacterial OM barrier. Antimicrobial peptides (AMPs) are short peptides with such characteristics that could be fused to endolysins. The OM-AMP interaction is not completely understood and several mechanisms have been proposed. Generally, two different AMP modes of action have been described: they can make OM pores and lyse the cells upon contact; or penetrate through the OM, exerting its antimicrobial effect intracellularly by inhibition of various vital cellular processes (Splith & Neundorf, 2011). **Figure 1.6** illustrates all membrane active agents (EDTA, organic acid and AMPs, representing sources of LPS-destabilizing peptides) used in this study to permeabilize the G^- OM for endolysins. Polycatonic peptides (such as polymyxin B or poly-L-lysine) compromise the OM integrity by displacement of the divalent cations responsible for the normal packing between phosphate groups of phospholipids and LPS (Vaara, 1992). A similar peptide with positively charged amino acids has been found in the *Bacillus amyloliquefaciens* phage IAM1521 endolysin C-terminal side, thought to be responsible for its spontaneous antibacterial activity against G^- cells (Morita et al, 2001). Hydrophobic peptides are able to intercalate and disorder the lipid A acyl chain-phospholipid moieties of the OM. This leads to a reduced hydrophobic stacking and subsequent OM destabilization, no longer acting as an efficient diffusion barrier (Nikaido, 2003). In the past, several modifications of the hen egg white lysozyme (HEWL) with increased hydrophobic content expanded its activity to G^- bacteria. The addition of a hydrophobic Phe-Phe-Val-Ala-Pro pentapeptide, which was shown to adopt β-strand conformation and interact with the bacterial OMs, is an example of enhanced HEWL bactericidal effect, reducing 85% of *E. coli* cells (Ibrahim et al, 1994). Amphipathic peptides are α-helical structures that contain both cationic and hydrophobic amino acids on opposite sides of the helical axis, thereby exerting a powerful permeabilization effect on

the bacterial membranes (Oren & Shai, 1998). An example is found within the C-terminal sequence of the T4 lysozyme. The 13-mer peptide located between the amino acids 143-155, corresponds to a typical positively charged amphipathic α-helix (named α4), enabling the enzyme to interact with the negatively charged LPS groups of G^- bacteria. Synthetic α4, is highly active on different biological membranes, and its antibacterial properties is apparently more important that the enzymatic PG degradation (During et al, 1999).

.

Chapter 2

Roadmap of the Thesis

G^- pathogenic bacteria are a global human health concern as they are common causes of foodborne, environmental and zoonotic infectious diseases. This problem is exacerbated by their ability to display intrinsic (natural) or acquired antibiotic resistant mechanisms. Therefore there is an urgent need to develop efficient mechanisms to combat harmful G^- bacteria. The work developed in the scope of this thesis aimed at developing innovative methods of G^- control, based on phage endolysins. The scientific challenge behind this approach is to make endolysins accessible to the bacterial OM that naturally acts as protective barrier for external agents.

This thesis comprises 7 different chapters grouped in 5 main parts, each presenting:

1- An extensive literature review on phage endolysin functions and their biotechnological interest to fight the problematic G^- bacterial infections. A detailed discussion was given on the structure and composition of the protective G^- OM, introducing several strategies to permeabilize it for endolysins and facilitate access to the PG (chapter 1).

2- A deep *in silico* analysis of all available endolysins genes covering the endolysins distribution in phages/infecting hosts and their molecular differences, particularly those from a G^- background, aiming at indicating the best endolysin candidates to prevent or destroy pathogenic bacteria (chapter 3).

3- The characterization of two novel phage-encoded endolysins (Lys68 and ABgp46) to expand the knowledge on the few endolysins described from G^- background. Their antibacterial effect in combination with different kind of OMPs (chelators and organic acids) was evaluated against a broad range of G^- pathogens in planktonic and biofilm cultures (chapter 4 and 5).

4- A description of an engineered class of endolysins (PVP-SE1gp146 and Lys68) fused with a set of different tags (LPS-destabilizing peptides and

CBDs), to enhance the endolysin`s antibacterial properties. Modified PVPSE1-gp146 with different LPS-destabilizing peptides was tested against G^- pathogens. With a different objective, Lys68 variants possessing different PG-binding peptides, derived from listerial phage endolysin CBDs, were used to direct and amplify their activity against *L. monocytogenes*, illustrating an additional usage of G^--like endolysins (chapter 6).

5- Major conclusions of the work, addressing the main advantages and limitations of the developed endolysin strategies to kill G^- bacterial pathogens, suggesting important issues that should be clarified in future works (chapter 7).

Chapter 3

In silico analysis of bacteriophage endolysins

The work presented in this chapter was published in the following paper: Oliveira H*; Melo L*; Santos S; Nóbrega F; Ferreira E; Cerca N; Azeredo J; Kluskens L (2013). Molecular aspects and comparative genomics of bacteriophage endolysins. *J Virol* 87:4558-4570.

*Oliveira, H. and Melo, L. contributed equally to this article

3.1 Introduction

Phages are the most abundant living entities on Earth and can be found in every conceivable habitat (Rohwer, 2003). Regarding their diversity, phages can exist with different morphotype (e.g. *Myoviridae*, *Siphoviridae* and *Podoviridae* with different tail types), nucleic acid (double- or single-stranded DNA), genome size and type of replication mechanisms (lytic or lysogenic pathway). Tremendously diversified, they constitute a reservoir of great genetic diversity, which is supported by the high frequency of novel genes found in newly characterized phage genomes. This high diversification in phage population can be attributed to the high number of different bacterial hosts available for phage infection and the ability of phages to rapidly evolve in order to circumvent bacterial resistance mechanisms (Sturino & Klaenhammer, 2006; Labrie et al, 2010). Therefore, among other proteins, phages potentially encoded a diverse group of PG hydrolases (PGHs) - endolysins - worth of exploring.

This chapter presents a deep *in silico* study of all known endolysins encoded by double-stranded nucleic acid (dsNA) completely sequenced phage genomes. There domains (ECDs/CBDs), structure (globular and modular design), as well as their distribution through phage families and bacterial hosts was assessed. With this analysis it was intended not only to resolve previous misconception regarding endolysins nomenclature (simply calling all endolysins lysozymes as a generic term for PGHs) but also to better understand the phage-endolysin-host ecology. This will allow in the future the study of novel uncharacterized endolysins and selection of the best endolysin candidates to fight specific bacterial pathogens.

3.2 Materials and methods

3.2.1 Endolysin search and database

To identify endolysin genes and create a database, a comprehensive list of all endolysins from 890 retrieved dsNA phages with completed genome sequences deposited in the NCBI database was gathered. An *in silic*o analysis of all putative endolysin sequences were screened by the HHpred webserver (URL http://toolkit.tuebingen.mpg.de/hhpred) using Pfam, InterProScan and COG; with an E-value cut-off of $1x10^{-5}$ and at least 80% of query coverage. The MSA generation method used was HHblits (Remmert et al, 2012). To indicate a given ORF as a probable endolysin, two criteria were followed: (*i*) the presence of a putative ECD and (*ii*) the absence of additional domains with extraneous function. The latter allowed distinguishing endolysins involved in programmed lysis from a second phage-associated muralytic activity often found to be involved in DNA-injection (structural lysins, also known as exolysins). For each putative encoded endolysin found, the following information was gathered: (*i*) presence and position of ECD/CBD; (*ii*) phage family type; (*iii*) Gram reaction corresponding host; and (*iv*) host genus.

3.2.2 Cladogram of bacteriophage-endolysin-host

Phage-endolysin-host cladogram was constructed using putative endolysin sequences of only completely sequenced dsNA phage genomes. All these protein sequences were retrieved from our database in FASTA format, aligned using Clustal Omega (beta version for proteins only, v1.1.0) with the -o output.aln -MAC-RAM=30000 –v –v parameters. The conversion to the PHYLIP format was done using ClustalX multiple alignment software (version 2.0). The phylogenetic construction was obtained using the Phylogeny Inference Package (PHYLIP v3.68). The phylogenic analysis was performed using the following algorithms: Maximum

Likelihood, Neighbor-Joining and Parsimony. These methods were applied to the PHYLIP sequences base using PROML, PROTDIST+NEIGHBOR and PROTPARS, with SEQBOOT programmed to 100 replicates to bootstrap and number seed variation (the trees were compared to address similarity). Bootstrap values were calculated using CONSENSE. In all methods, the jumble number used was 10 and the bootstrap values were all above 80%. Although more than one method was used to construct the trees, the Maximum Likelihood method was selected since it chooses those trees that maximize the probability of observing the data. Phylogenetic trees obtained from PHYLIP were represented and arranged, without being altered, using the FigTree software (version 1.3.1).

3.3 Results

3.3.1 Outline - Endolysins structure diversity and distribution

With an *in silico* analysis of a total of 890 complete phage sequences found in the NCBI, 723 putative endolysins were identified, from phages infecting 64 different bacterial genera. The endolysins were identified in 136 *Myoviridae*, 378 *Siphoviridae*, 97 *Podoviridae*, and nine *Tectiviridae* (all dsDNA), four *Cystoviridae* (dsRNA) and 99 unclassified phages. Despite their conserved biological function, phage endolysins are enzymatically and architecturally tremendously diverse and vary hugely in length and size. With a remarkable number of 24 different ECDs and 13 CBD types (**Table 3.1**), these specialized enzymes comprehend 89 different types of architectural organizations (**Figure 3.1**) ranging from 72 to 578 amino acids residues (on average around 177 and 390 amino acids for endolysins from a G^- and G^+ background, respectively). All the information mentioned above was gathered in a database available at http://dx.doi.org/10.1128/JVI.03277-12.

For a systematic analysis, predicted similar domains found in different databases (CHW and LYSM from both Pfam and SMART databases) were referred to as the same domain. It is important to note that, despite AMI-5 being a domain similar to other amidases, this bioinformatic analysis showed a similarity with the peptidase NLPC-P60 domain (E-values differ at most 5 log). Additionally, *in vitro* studies with AMI-5-endolysin from streptococcal phage Dp-1 indicate a peptidase activity (Sheehan et al, 1997). Since the 16 Ami-5 domains found were all from *Streptococcus* spp., they were further considered as NLPC-P60.

Table 3.1. Identified putative endolysin catalytic and binding domains.

PREDICTED CATALYTIC DOMAIN	CONSERVED DOMAINS	PHAGE EXAMPLE	HHpred probability/E-value
Phage_lysozyme (LYSO)	PF00959 / IPR002196	*Burkholderia* phage Bcep176	100.0 / 3.1E-34
Muramidase (MURA)	COG4678	*Enterobacteria* phage lambda	100.0 / 6.2E-52
Glyco_hydro_19 (GH19)	PF00182 / IPR000726	*Pseudomonas* phage F10	100.0 / 6.8E-42
Glyco_hydro_25 (GH25)	PF01183 / IPR002053	*Clostridium* phage phiCTP1	100.0 / 4.9E-48
Glyco_hydro_108 (GH108)	PF05838 / IPR008565	*Vibrio* phage VP882	100.0 / 1.5E-37
SLT (SLT)	PF01464 / IPR008258	*Pseudomonas* phage B3	99.9 / 2.9E-23
Transglycosylase (TRANG)	PF06737 / IPR010618	*Mycobacterium* phage Blue7	100.0 / 8.3E-31
Glucosaminidase (GLUCO)	PF01832 / IPR002901	*Bacillus* phage Bam35c	100.0 / 6.8E-32
Amidase02_C (AMI02-C)	PF12123/ IPR021976	*Clostridium* phage phiCD38-2	98.2 / 1.2E-06
Amidase_5 (AMI-5)	PF05382 / IPR008044	*Streptococcus* phage 858	99.9 / 3.0E-26
Amidase_3 (AMI-3)	PF01520 / IPR002508	*Listeria* phage 2389	100.0 / 6.4E-44
Amidase_2 (AMI-2)	PF01510 / IPR002502	*Gordonia* phage GTE7	100.0 / 2.4E-29
NlpD (NLPD)	COG0739	*Mycobacterium* phage Timshel	97.8 / 2E-05
VanY (VANY)	PF02557 / IPR003709	*Yersinia* phage PY100	99.9 / 1.2E-24
Peptidase_U40 (PET-U40)	PF10464 / IPR19505	*Pseudomonas* phage phi-6	100.0 / 2E-138
Peptidase_M15_3 (PET-15-3)	PF08291 / IPR013230	*Bacteroides* phage B40-8	100.0 / 1.1E-38
Peptidase_M15_4 (PET-15-4)	PF13539	*Salmonella* phage ST64T	99.7 / 8.2E-17
Peptidase_M23 (PET-M23)	PF01551 / IPR016047	*Thermus* phage P23-45	100.0 / 2E-28
YkuD (YKUD)	PF03734 / IPR005490	*Synechococcus* phage S-CBS4	99.7 / 7.1E-18
NLPC_P60 (NLPC-P60)	PF00877 / IPR000064	*Mycobacterium* phage Dori	99.8 / 2.9E-19
Peptidase_C39_2 (PET-C39-2)	PF13529	*Rhodococcus* phage REQ3	99.8 / 1.8E-17
CHAP (CHAP)	PF05257 / IPR007921	*Staphylococcus* phage phi13	99.8 / 9.4E-22
DUF3597 (DUF)	PF12200 / IPR022016	*Listeria* phage A188	99.5 / 7.6E-15
PREDICTED BINDING DOMAIN			
PG_binding_3 (PG-3)	PF09374 / IPR018537	*Vibrio* phage VP882	99.9 / 7.9E-25
LysM (LYSM)	PF01476/ IPR018392	*Enterococcus* phage phiEf11	99.0 / 1.4E-10
LysM (LYSM)	smart00257	*Lactobacillus* phage Lb338-1	99.5 / 5.0E-14
SH3_3 (SH3-3)	PF08239/ IPR013247	*Lactobacillus* phage Lv-1	97.6 / 5.3E-05
SH3_5 (SH3-5)	PF08460 / IPR013667	*Staphylococcus* phage phi2958PVL	99.5 / 1.5E-14
PG_binding_1 (PG-1)	PF01471 / IPR002477	*Mycobacterium* phage Hertubise	99.5 / 8.7E-14
ChW (CHW)	smart00728	*Lactobacillus* phage A2	99.3 / 2.3E-12
ChW (CHW)	PF07538 / IPR006637	*Lactococcus* phage 949	99.2 / 7.1E-12
Cpl-7 (CPL7)	PF08230/ IPR013168	*Streptococcus* phage SMP	99.5 / 2.4E-14
LGFP (LGFP)	PF08310/ IPR013207	*Nocardia* phage NBR1	99.7 / 1.6E-17
SH3-related (SH3-r)	SUPFAM0051050	*Listeria* phage A500	100.0 / 4.4E-54
FOG (FOG)	COG5263	*Listeria* phage B054	99.8 / 4.0E-19
SH3b (SH3b)	smart00287	*Lactococcus* phage P087	97.5 / 4.4E-05
SPOR (SPOR)	PF05036/ IPR007730	*Bacillus* phage AP50	99.1 / 1.8E-10
SLAP (SLAP)	PF03217/ IPR004903	*Bacillus* phage 0305phi8-36	98.9 / 3.0E-08

The acronyms used in all ECDs and CBDs are illustrated in parentheses. Domain abbreviations: Glyco_hydro, Glycoside hydrolase; SLT, Soluble Lytic Transglycosylase; CHAP, Cysteine, Histidine-dependent Amidohydrolases/Peptidases; DUF, Domain of Unknown Function; LYSM, Lysin motif; CHW, Clostridial hydrophobic with conserved W (Trp); SPOR, Sporulation related domain; SLAP, bacterial Surface LAyer Protein. Databases: PF, Pfam; COG, Clusters of Orthologous Groups of proteins; IPR, InterProScan; Smart, Simple Modular Architecture Research Tool. AMI-5 is further considered as NLPC-P60.

3.3.2 Enzymatic catalytic domains

3.3.2.1 Phage glycosidase PGHs

This group of enzymes belongs to the lysozyme-like superfamily that catalyzes the glycolytic cleavage of the O-glycosidic bond of the bacterial PG. The PGHs are very diverse and can be defined by sequence similarity according to the Carbohydrate-Active Enzymes database (Cantarel et al, 2009). GH24, GH25 and GH108 (EC 3.2.1.17) are a structurally diverse set of phage endolysin members with the same lysozyme activity cleaving the MurNAc-N-GlcNAc bond of the carbohydrate backbone. GH24 are the most predominant PGHs, generally containing globular MURA or LYSO domains that are only present in lytic cassettes of phages infecting G^- bacteria. GH25 endolysins, on the other hand, are acquired by *Siphoviridae* viruses targeting G^+ organisms, mostly belonging to the *Firmicutes* family (e.g. *Bacillus* spp., *Staphylococcus* spp., *Streptococcus* spp.) that can be linked to several distinct C-terminal CBDs (SLAP, CPL-7, LYSM, SH3 and FOG). The GH108 class contains just nine endolysins with an enzymatic activity restricted to phages infecting only seven G^- genera and have never been characterized *in vitro*. Other SLT and TRANG domains belong to the lytic transglycosylase group of enzymes. Although degrading the same PG covalent bond as the previous group, they are not hydrolases. SLT-encoding endolysins are globular and acquired by phages to target G^- PG (found in *Burkholderia*, *Campylobacter*, *Escherichia* and *Pseudomonas* phage endolysins), while the TRANG-type enzymes are modular and specialized in G^+ PG degradation (only found in Mycobacteriophages Gladiator, Da Vinci, Hammer, Trixie, Jeffabunny, Blue7 and Turbido). *P. aeruginosa* phage phiKZ endolysin is an example of a (SLT) lytic transglycosylase for which activity has been biochemically confirmed (Paradis-Bleau et al, 2007). GH19 (EC 3.2.1.14) is a distinct class cleaving the glycosidic β-1,4 linkages of unbranched chains of N-acetylglucosamine polymers. This structure is uncommon in bacterial cell walls; therefore one can speculate that GH19-identified endolysins can have glycosidase activity, acting either as N-acetylglucosaminidase or as N-acetylmuramidase. They

are mainly found in phages infecting *Mycobacterium* spp., *Gordonia* spp. and *Corynebacterium* spp. and have been recently characterized in the *P. fluorescens* OBP and *S.* Enteritidis phage PVP-SE1 (Lai et al, 2011; Walmagh et al, 2012). Finally, glucosaminidases (GLUCO) (EC.3.2.1.52) are core-specific lysosomal enzymes cleaving the GlcNAc-(β-1,4)-MurNAc bond. In phage endolysins, this domain is repeatedly found in *Siphoviridae* phage lytic cassettes that mostly target hosts within the *Firmicutes* family. Although this catalytic class is frequently present in *Staphylococcus* infecting phages containing three domains in a CHAP/AMI-2/GLUCO module, only the *Streptococcus agalactiae* prophage LambdaSa2 was shown to display β-D-N-acetylglucosaminidase activity (Pritchard et al, 2007).

3.3.2.2 Phage amidase PGHs

N-acetylmuramoyl-L-alanine amidases (EC 3.5.1.28) are endolysins composed of domains of the AMI-2, AMI-3, AMI-5 and AMI02-C type, cleaving the same PG bond between the N-acetylmuramoyl residues and L-amino acid residues. AMI-2, the most predominant domain (representing 28.22%), found in *Mycobacterium*-like and *Staphylococcus*-like endolysins, is usually located as a central domain. *Escherichia* phage T7 and *Staphylococcus* phage Twort endolysins are well studied enzymes (Cheng et al, 1994; Loessner et al, 1998). AMI-3 domains are predominantly found in G^+-like endolysins. It is important to highlight that all staphylococcal phage endolysins bearing AMI-3 have a CHAP/AMI-3/SH3-5 structure. Finally, AMI02-C is located at the C-terminal side and is merely present in some *Bacillus* and *Clostridium*-like endolysins. To our knowledge, no *in vitro* studies have yet been performed to confirm lytic activity of this domain.

3.3.2.3 Phage carboxy/endopeptidases

Phage carboxy/endopeptidase PGHs form the larger group of ECDs that cleave short peptides that link the sugar polymers of the PG. A total of nine different peptidases were found: endopeptidase domains PET-M23, NLPC-P60, NLPD, PET-U40 and PET-C39-2; and the carboxypeptidase domains VANY, PET-M15-4, PET-M15-3 and YKUD. PET-M23 is found in phage endolysins from several genera. It has been reported that the *Bacillus subtilis* prophage Sp-β endolysin (named CwlP) contains a related domain that has been shown to function as a DD-endopeptidase cleaving 4R3 D-Ala–m-DAP interpeptide linkages (Sudiarta et al, 2010). The NLPC-P60 domain is described as a superfamily with a very different range of activities. Only found in G^+-like endolysins, they can cleave N-acetylmuramate-L-alanine linkages, as was shown for the *Streptococcus* phage Dp-1 and *Lactococcus lactis* phage BK5-T endolysins (Boyce et al, 1995; Sheehan et al, 1997). More recently, NLPC-P60, found in some Mycobacteriophage endolysins, was described as a cysteine proteinase cleaving the 4→3 linkage between D-Glu and m-DAP residues (Payne & Hatfull, 2012). PET-C39-2 was first identified in Lysin A proteins (Mycobacteriophage cell wall hydrolytic enzymes), cleaving the D-Glu-m-DAP linkages (Payne & Hatfull, 2012). This peptidase is also a cysteine proteinase and is mainly present in Mycobacteriophages. VANY is described in the Pfam database as a D-alanyl-D-alanine carboxypeptidase, possibly due to the *Enterococcus faecium* vancomycin resistance protein VanY (Wright et al, 1992). Concerning its phage origin, this domain was identified both in G^+ and G^--like endolysins, particularly in phages infecting *Listeria*, *Bacillus* and *Escherichia* organisms. In opposition to what is described by Pfam, the *Listeria* phage endolysins Ply118 and Ply500 and the enterobacteriophage T5 endolysin classified as VANY carboxypeptidases act as L-alanyl-D-glutamate endopeptidases (Loessner et al, 1995; Mikoulinskaia et al, 2009). PET-M15-4 is a domain also described as D-alanyl-D-alanine carboxypeptidases, however it has been predicted to display L-Ala-D-Glu activity (Payne & Hatfull, 2012). This domain was found in several

Mycobacteriophages and in some phages infecting G^- organisms, such as *Salmonella*. PET-M15-3 peptidase domains are metallopeptidase domains belonging to family M15A, found in only nine different endolysins, mainly from G^- infecting phages. The exact cleavage site has not yet been identified, due to the lack of biochemical evidence. CHAP is a common domain found in phage endolysins identified in 87 proteins. This CHAP domain is strictly encoded in phages infecting G^+ hosts, predominantly in phages infecting *Streptococcus* spp. and *Staphylococcus* spp. Of particular interest is their association with several other families of amidases, which suggests that they might act in a cooperative manner to cleave multiple PG substrates. Reports have shown that CHAP can serve as a peptidase or amidase, acting as D-alanyl-L-alanyl endopeptidase (in *Streptococcus* phage B30), as a D-alanyl-glycyl endopeptidase (in *Staphylococcus* phage phi11) or as an N-acetylmuramoyl-L-analine amidase (in *Streptococcus* phage C1). This latter endolysin (PlyC) is a unique multimeric protein composed of two separate gene products (PlyA and PlyB) (Navarre et al, 1999; Baker et al, 2006; Nelson et al, 2006). The remaining NLPD, PET-U40 and YKUD have only been found in one phage endolysin each, Mycobacteriophage Timshel (PET-M15-4/NLPD), *Cystoviridae Pseudomonas* phage phi-6 (PET-U40), and *Synechococcus* phage S-CBS4 (GLUCO/YKUD) endolysins, respectively. NLPD and YKUD remain experimentally uncharacterized.

Phage endolysins with multi-catalytic activities

Through evolution, endolysins appear to have acquired certain substrate specificities by obtaining multiple ECDs found in phages infecting a range of 11 different genera, but predominantly present in *Staphylococcus* and *Mycobacterium*-like phages. The latter have 26 different types of structures, 14 of which combine two ECDs. The most prevalent ones contain an N-terminal predicted peptidase, a centrally located AMI-2, MURA, and TRANG, and a C-

terminal PG-1. Less frequently, staphylococcal-like endolysins with multiple ECDs can contain up to three ECDs with alternating CHAP/AMI-3/SH3-5, CHAP/AMI-2/SH3-5 or CHAP/AMI-2/GLUCO modules. An unusual double amidase activity was found with an AMI-2/AMI-2C and an AMI-3/AMI-2C structure in six *Bacillus* phages and two *Clostridium* phages, respectively. In G^--like endolysins, the few multi-ECDs found belong to the *Prochlorococcus marinus* phage PSS2 and 4 *Synechococcus* phages with an N-terminal GH activity (MURA or GLUCO) and an additional peptidase activity (PET-C39-2, YKUD or PET-M15-3). Another notable detail is that 150 (77%) of the 196 annotated multi-ECDs phage endolysins belong to *Siphoviridae* viruses, mostly infecting G^+ hosts. Studied examples including plural active lytic domains are the staphylococcal phi11 (Navarre et al, 1999), the Group B streptococcal endolysin B30 (Pritchard et al, 2004) and the streptococcal lSa2 phage endolysin (Pritchard et al, 2007).

3.3.3 Cell binding domains

Endolysin modularity can also associate ECDs with a selected CBD (**Table 3.1**). Notably, CBDs are predominantly present in *Bacillus*, *Lactobacillus*, *Lactococcus*, *Mycobacterium*, *Staphylococcus* and *Streptococcus* phage endolysins (**Figure 3.1**). Among the great variety of CBD motifs found, only PG-1, SH3, LYSM and CPL-7 have been characterized *in vitro* (Loessner et al, 2002; Hu et al, 2010; Walmagh et al, 2012). PG-1 is almost only restricted to phages infecting G^+ genera with few exceptions detected in G^--like endolysins (*Salmonella* phage PVP-SE1 and *Pseudomonas* phages phiKZ, EL, 201phi21 and OBP), where they occur in a unique inverse rearrangement (one or more PG-1 CBDs at the N-termini). PG-3 type has been acquired from phages with a rare modular arrangement (GH108/PG-3), infecting G^- counterparts. SH3 domains commonly found in autolysins and phage endolysins often belong to the SH3b, SH3-3 or SH3-5 type. This CBD, shared by lysostaphin (a bacteriocin from *Staphylococcus simulans* bv. *staphylolyticus*) and

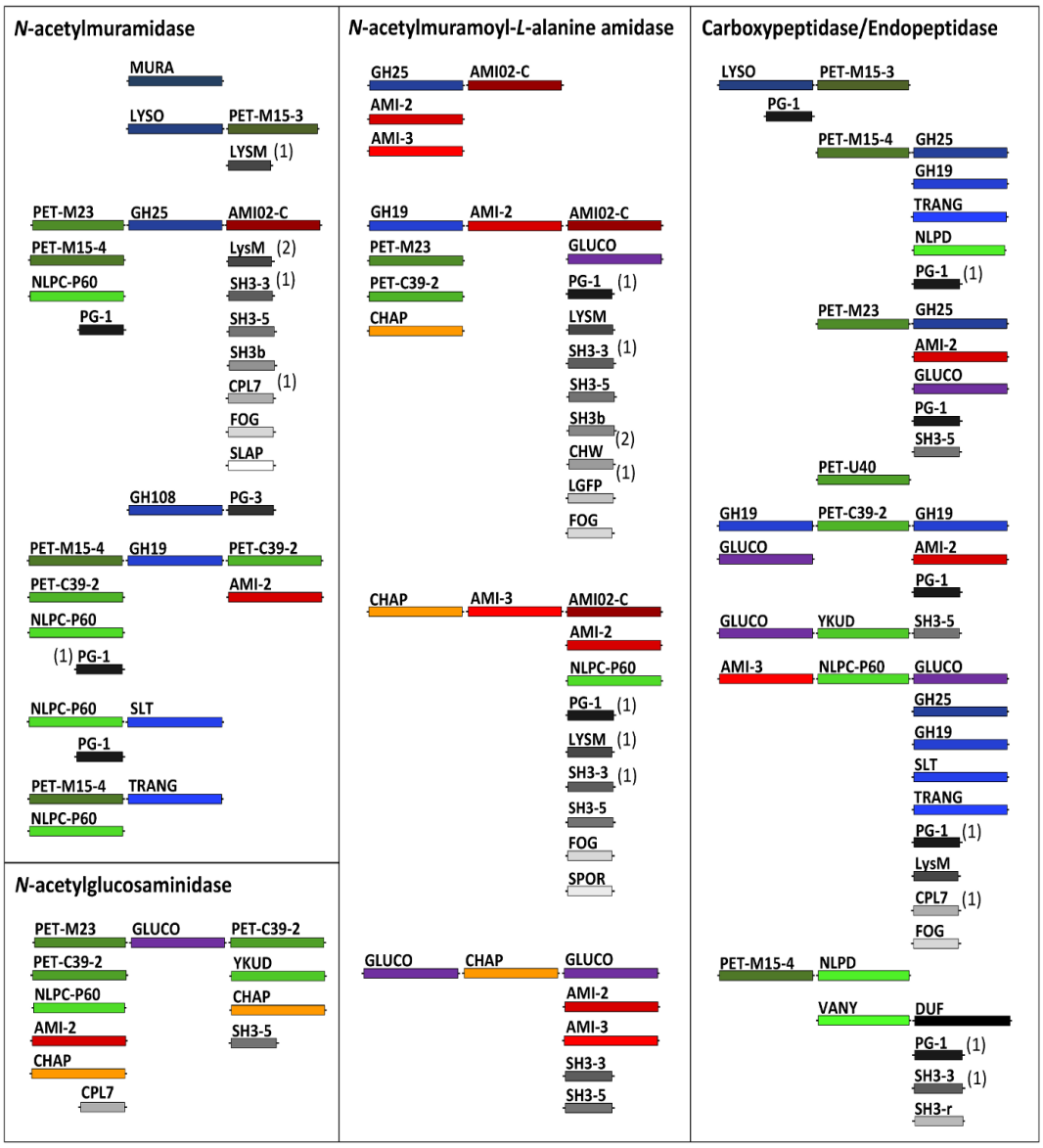

(1) Can have one extra repeated motif
(2) Can have two extra repeated motifs

Figure 3.1. Diversity of enzymatic catalytic domains/cell binding domains found at the N- and C-terminus of the four major endolysin classes centrally located (from all 723 putative endolysins): N-acetylmuramidases (blue scale), N-acetylglucoaminidases (purple), N-acetylmuramoyl-L-alanine and carboxy/endopeptidases (green scale). CHAP (orange) can act as an amidase or peptidase. These four major classes have been centrally located to show all ECDs (with colours mentioned above) and CBDs (gray scale) found attached to their N- and C-termini. For the correct interpretation of the schematic representation: of all endolysins found with a CHAP domain, a GLUCO at their N-terminus was observed. In some proteins a GLUCO, AMI-2 and AMI-3 domain at the C-terminus was identified.

its homologue, hydrolase ALE-1, has been uncovered to recognize pentaglycine cross bridges in PG (Grundling & Schneewind, 2006; Lu et al, 2006). Therefore, the fact that most of SH3 domains are found in *Staphylococcus*-like endolysins is not surprising. The LysM domain is considered to be the CBD with the widest range of receptors identified in more than 4000 proteins of both prokaryotes and eukaryotes. It has been postulated that this domain binds to various types of PG and most likely recognizes the N-acetylglucosamine moiety (Buist et al, 2008). This is in agreement with the findings presented herein that show that LysM is always correlated to MurNAc-N-GlcNAc glycosidase activity (LYSO or GH25), with the exception of three endolysins, in which LysM is joined with an amidase domain (AMI-2 or AMI-3 type). Interestingly, the LysM domain is often found in double motifs, having a unique architecture of three motifs in the *Lactobacillus* phage Lb338-1 endolysin (GH25/LYSM/LYSM/LYSM). Endolysin modules containing the less abundant CPL-7 are GH25/Cpl-7/Cpl-7, NLPC-P60/GH25/Cpl-7 and NLPC-P60/Cpl-7/GLUCO present in *Clostridium* phage (phiCTP1), *Mycobacterium* phages (Optimus and Baka) and in *Streptococcus* phages (SMP and 315.3), respectively. Although CBD location is usually found at the N- or C-terminus, the aforementioned CBDs (LYSM, CPL-7 and PG-1) can also be located as central domains (e.g. Mycobacteriophage Adjutor with NLPC-P60/PG-1/PG-1/GH19, *Streptococcus* phage SMP with NLPC/CPL-7/CPL-7/GLUCO and *Streptococcus* phage phi-SsUD.1 with AMI-3/LYSM/LYSM/NLPC-P60). Concerning CHW, it has been stated that this protein family is almost exclusively limited to the *Clostridium acetobutylicum* bacterial species (Sullivan et al, 2007). The present results reveal only nine CHW domains detected in three *Lactococcus* and six *Lactobacillus* phage endolysins. Curiously, this domain is always present in endolysins attached to an AMI-2 type domain and bears multi-CHW motif copies. The *Lactococcus* phage A2 endolysin has an AMI-2/CHW/CHW/CHW arrangement while *Lactococcus* phages 949, asccphi28 and KSY1 contain the AMI-2/CHW/CHW modules. The acquirement of other uncommon CBD motifs, like LGFP, SPOR, FOG and SLAP, can

represent alternative ways for tighter binding, by directing the catalytic cavity into target muropeptides or changes in species specificity. Remarkably, FOG motifs are characterized by having six CBD (PF01473) repeats found only in six streptococcal phages (Cp-1, Dp-1, EJ-1, MM1, PH10 and SM1) and one *Listeria* phage (B054). To our knowledge these CBDs have never been characterized *in vitro* in the big pool of phage PGHs.

Altogether, the structural endolysin design (ECD and CBD), their distribution through phage genomes (dsDNA or dsRNA genomes) and phage infecting hosts (different bacterial genera) are summarized in **Figure 3.2**. The diverse nature and repartition of endolysin domains observed, is a reflection of the phages' different strategies to infect various bacterial and assure the same biological function, i.e. to disrupt the PG. As mentioned before, specific patterns could be identified. For instance the glycoside hydrolases are heavily present in G^- infecting phages. Another example is the predominant domain AMI-2 that is mostly found in *Mycobacterium*-like and *Staphylococcus* phages.

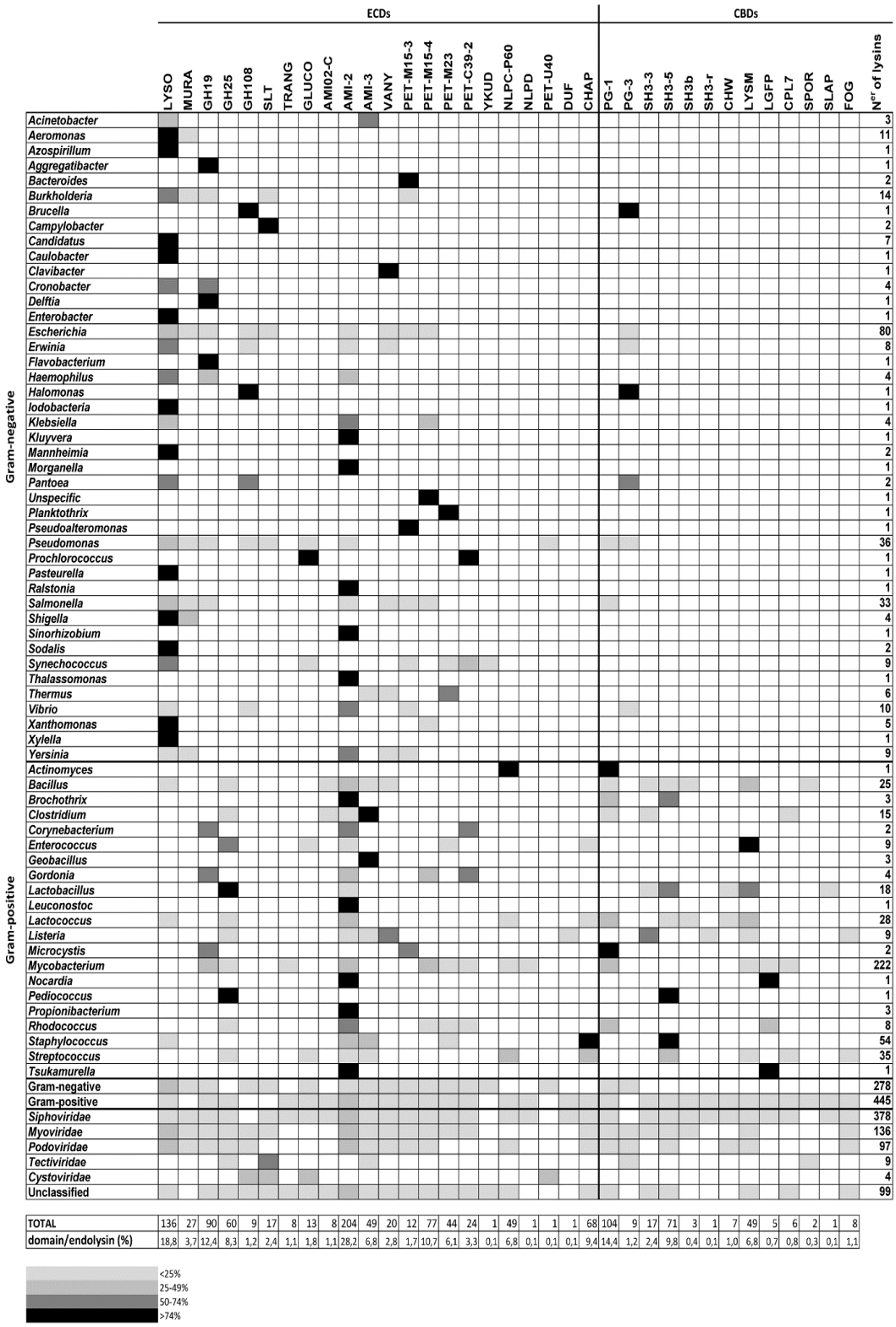

Figure 3.2. Nature and repartition of peptidoglycan hydrolase domains encoded by derived from 727 endolysins.

3.3.4 Cladogram bacteriophage-host-endolysin relationship

To comprehend the possible evolutionary position of phage endolysins, a maximum likelihood tree was constructed. By analyzing the cladogram (**Figure 3.3**) we were able to perceive the great variety of endolysin domain structures, generally with conserved ECDs and little homology within the CBDs.

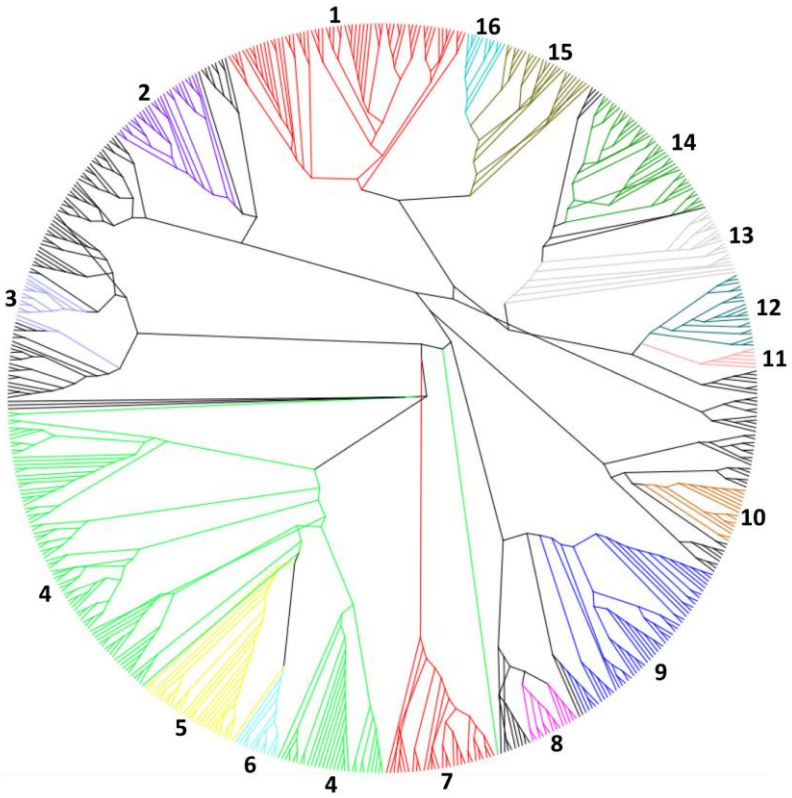

Figure 3.3. Radial cladogram of endolysins of all characterized phages. The cladogram was constructed using PHYLIP v3.68, with Neighbor-Joining algorithm. The resulting cladogram was represented and arranged, without being altered, using the FigTree software (version 1.3.1). Highlighted areas are numbered and correspond to the more conserved clades. 1 - *Mycobacterium*/*Siphoviridae*/AMI-2; 2 - G^+/GH25; 3 - *Lactococcus*/*Siphoviridae*/AMI-2; 4 - G^-/LYSO; 5 - G^-/MURA; 6 - *Streptococcus*/*Siphoviridae*/NLPC-P60; 7 - G^-/*Podoviridae*/AMI-2; 8 - G^-/*Myoviridae*/VANY; 9 - *Staphylococcus*/*Siphoviridae*; 10 - G^-/GH19; 11 - *Escherichia*/*Tectiviridae*/SLT; 12 - *Mycobacterium*/*Siphoviridae*/NLPC-P60/GH25; 13 - *Mycobacterium*/*Siphoviridae*/PET-M15-4/PG1; 14 - *Mycobacterium*/*Siphoviridae*/PETM-15-4/GH19; 15 - *Mycobacterium*/*Siphoviridae*/PET-M23/AMI-2; 16 - *Mycobacterium*/*Siphoviridae*/PET-C39-2/GH19.

Interestingly, there is no distinct clade organization, which shows that the tree is not conceived by just one factor, such as phage family, host or ECD. For tailed phages, the parameter that is apparently more important for the cladogram organization is endolysins' domain architecture, which is visible on the highlighted clades - the more robust clades. Regarding non-tailed phage endolysins, *Escherichia*-like endolysins from *Tectiviridae* contain an SLT catalytic domain and, as expected, they are in the same evolutionary clade. However, it was reported that, despite the amount of similar *Tectiviridae* genomes, one of the major differences was observed when comparing their lytic enzymes (Saren et al, 2005). Oppositely, *Cystoviridae Pseudomonas*-like endolysins appear not to be conserved as they are dispersed over the tree.

3.4 Discussion

3.4.1 The enzymatic catalytic domains - Evolutionary claims

The acquirement of specific ECDs from a large pool of potential candidates may be influenced by three factors:

(*i*) Specific ECD substrate may be restricted to a few bacteria

For instance, because *Staphylococcus*, *Streptococcus* and *Lactococcus* have unique 3→4 glycine pentaglycine (Gly)5, dialanine (L-Ala-L-Ala) or L-Lys-D-Asp interpeptide bridges within the PG, their specific phages have acquired a CHAP domain that exclusively cleave these links (Vollmer & Born, 2009). LYSO activity is dominant in phages infecting G^- species. This can be explained by the ability of many G^+ pathogens to modify their glycan strands by N-glycosylation, de-N-acetylations and/or O-acetylations that contribute to high levels of resistance to lysozyme (Vollmer & Born, 2009).

(*ii*) PG composition and length varies with growth phase and conditions

As a result of generation of the cellular shape, its maintenance and bacterial adaptation, PG structure and composition is continuously changing (incorporation of new and removal of old material) (Glauner et al, 1988). This would drive phages to a careful selection of a capable endolysin that efficiently digests all PG variants (always with available substrate to digest). *E. coli*, *Mycobacteria* and *S. pneumoniae* are known microorganisms in which muropeptides undergo several changes (Pisabarro et al, 1985; Glauner et al, 1988; Lavollay et al, 2008). Interestingly, their infecting phages represent the niche with lytic cassettes that spans the greatest ECD diversity and multiplicity. Especially, Mycobacteriophage endolysins have an impressive number of 127 multi-functional ECD combinations

with preferred combinations of PEP-M13/AMI-2/PG-1, NLPC-P60/GH25 and PET-M15-4/GH19 modules. In some cases, ECDs within the same endolysin may act synergistically, cooperatively or even alone.

(*iii*) Distinct ECDs guarantee a similar biological function

Cleavage of a specific bacterial PG is not restricted to a single ECD, but can be ensured by several ECDs with different cleavage sites. For instance, the MurNAc-N-GlcNAc glycosidase activity is performed exclusively by the LYSO-containing endolysins in the *Xanthomonas* phages, whereas at least four distinct domains (LYSO, MURA, GH108 and SLT) are responsible for this activity in *Escherichia* phage endolysins. The amidase cleavage of the D-lactyl moieties of MurNAc and L-alanine of the short stem peptide (NAM-amidase) is carried out by AMI-2 in *Vibrio* phage endolysins, while in *Bacillus*-like endolysins it is performed by distinct AMI02-C, AMI-2 and AMI-3 domains. In general, ECDs are not global, but are rather found in a restrictive number of bacterial genera. ECDs variety among endolysins resulted from the historical battle between phage and bacterium attaining a wealth of possible PGHs sequences to reach the same final outcome: bacteriolysis.

3.4.2 The cell binding domains - Evolutionary claims

An evolutionary relationship between *S. pneumoniae* autolysins and some streptococcal phage endolysins was originally proposed, based on their significant nucleotide sequence similarities (Garcia et al, 1988). It was suggested that modular endolysins may have evolved by the interchange of phage and bacterial genes encoding individual modules (Garcia et al, 1988), gaining strong support after the creation of functional chimeric phage-bacterial enzymes, which consisted of one phage- and one bacterial-derived exolysin domain (Diaz et al,

1990; Diaz et al, 1991). The recruitment and distribution of CBD through phages genomes (**Figure 3.2**) can be correlated by different facts:

(*i*) Specific CBD receptors may be restricted to a few bacteria

As the major role of endolysins is to enable progeny virions to be released from the host cell, to ensure the effective release of phages the CBDs may have evolved to target a unique and essential component of the host cell wall (Fischetti, 2003). This would explain the variability of this module and the highly selective lytic activity of endolysins. Therefore, in some cases, CBDs can confer highly specific ligand recognition to endolysins, resulting in a very narrow substrate spectrum of the full-length endolysin, often limited to the host species or strain (Perez-Dorado et al, 2007), or to a lesser extent, genus-specific (Loessner et al, 1997; Loessner et al, 2002). Well-studied examples of ligand recognition are the pneumococcal endolysins derived from phages Cp-1 (Cpl-1 endolysin), Dp-1 (PAL endolysin) and Ej-1 (Ej-1 endolysin). Their corresponding CBDs specifically bind choline, which is only present in teichoic acids of the pneumococcal cell wall and which is essential for bacterial viability (Garcia et al, 1988; Sheehan et al, 1997; Saiz et al, 2002). Also, the CBDs of the *L. monocytogenes* phage endolysins Ply118 and Ply500 can bind to different *Listeria* serovar groups as visualized by fusions with green fluorescent protein (GFP), showing that they are correlated with the occurrence of somatic antigens related to these serovars (Loessner et al, 2002).

(*ii*) Minimal disruption of normal flora

The reason for the presence of a CBD typically seen in G^+-like endolysins, lies in the absence of an OM in G^+ bacteria. After external bacterial lysis, CBD keeps the endolysin tethered to the PG, making them unavailable for degrading any adjacent G^+ PG from forthcoming potential hosts (bacterial threshold), thereby

not compromising phage survival (Fischetti, 2008). The strong substrate specificity of *L. monocytogenes* phage endolysins Ply118 and Ply500 of nanomolar affinities is in favour of this hypothesis, suggesting that they have evolved to bind irreversibly to their cell wall ligand (Loessner et al, 2002). On the other hand, the presence of an OM in G^- bacteria that impairs direct external endolysin contact eliminates the need for a CBD in endolysins from phages infecting these bacteria. In this *in silico* analysis, a predominant CBD distribution among G^+ infecting phages was observed (**Figure 3.2**). *Lactobacillus* and *Lactococcus* together with *Bacillus* genera represent the phage niche with the most diverse CBD collection (PG-1, SH3-3, SH3-5, SH3b, CHW, LYSM and SPOR). Excellent examples are phage endolysins with 3 CBDs, only observed in *Lactobacillus* phage A2 (AMI-2/CHW/CHW/CHW) and *Lactobacillus* phage Lb338-1 (GH25/LYSM/LYSM/LYSM), or endolysins containing different types of CBDs, as is the case for the *Lactobacillus* phage phiAT3 endolysin (GH25/SH3-5/LYSM).

(*iii*) Catalytic activity regulator

Rather than binding to the cell wall, CBD-associated domains sometimes can play determining roles in the enzymatic efficiency by allowing enough substrate to reach the catalytic site. Other carbohydrate hydrolases, such as xylanases and cellulases that cleave insoluble carbohydrate polymers, share a similar modular architecture (Khosla & Harbury, 2001) and their CBDs act by increasing enzyme-substrate proximity (Bolam et al, 1998). Equilibrium association constants of CBDs of *Listeria* phage endolysins Ply118 and Ply500 place them in the same range as affinity-matured antibodies against bacterial cell surface antigens. Interestingly, the deletion of their CBDs rendered enzymes with no muralytic activity (Loessner et al, 2002). Also, the activity of a C-terminally truncated *Clostridium* phage phi3626 endolysin was entirely abolished, emphasizing the important role that CBDs play in the enzyme´s activity (Zimmer et al, 2002). As opposed to previous

observations, structural analysis of PlyL indicates that the C-terminal CBD not only targets the endolysin to a specific ligand, but also inhibits the catalytic activity in the absence of the cognate substrate. It has been hypothesized that substrate recognition by the CBD of PlyL disrupts interactions between the CBD and the ECD, relieving the inhibitory effect on the latter (Low et al, 2005). These inter-domain interactions are absent in the C-terminal truncated variant, converting the catalytic domain into a constitutively active domain. Therefore, *B. subtilis*, which is lacking the cognate target, is hydrolyzed more efficiently by the truncated form compared to the full-length version. Consequently, the role of the CBD is variable and therefore each case must be examined individually.

(*iv*) Is it possible to lose non-essential domains?

Though a multi-domain architecture is indicative of a modular enzyme, it does not guarantee its functionality as a modular protein. An analogy comparison can be made for phage endolysins, in which the presence of a CBD does not often constitute a prerequisite for enzyme activity. Deletion of the CBD of *L. monocytogenes* endolysin PlyPSA only reduces the lytic activity (Korndorfer et al, 2006). Also the C-terminal domain of *Lactobacillus delbrueckii* subsp. *lactis* phage LL-H endolysin can be removed without destroying the lytic activity (Vasala et al, 1995). C-terminal deletions of *S. aureus* phage endolysins PlyTW and Ply187, *L. monocytogenes* phage endolysin Ply511, *B. amyloliquefaciens* phage endolysin Morita2001, *B. anthracis* prophage endolysin PlyL and *Bacillus* cereus phage endolysin Ply21 even increase the muralytic activity (Loessner et al, 1998; Loessner et al, 1999; Gaeng et al, 2000; Morita et al, 2001; Low et al, 2005). This pattern is also present in endolysins with dual lytic domains, where in theory both should be equally active. Indeed, silent ECDs (almost devoid of activity) have been observed in several multi-ECDs endolysins studied (streptococcal phage lambdaSa2 and B30 and staphylococcal phage phi11 endolysins) (Donovan et al,

2006a; Donovan & Foster-Frey, 2008; Horgan et al, 2009). Interestingly, in all these cases the N-terminal ECD encodes the active domain with the highest activity.

In conclusion, the ubiquity and huge genetic diversity found in phages is considered to be a result of both vertical and horizontal evolution. Through these processes, phages have acquired different lytic systems employing PG-degrading enzymes to fight a diversified and changeable bacterial cell wall. Although modular enzymes are not common in nature, a number of multicomponent endolysins have been found able to digest the bacterial PG. Therefore, endolysins can be seen as an important result of phage evolution to permit rapid adaptation to new environmental conditions. With the structural and predicted mechanistic basis for phage endolysins now being elucidated, their utility can be further examined exploring novel uncharacterized domains and by tailoring modular endolysins to acquire new functions.

Chapter 4

A highly thermostable Salmonella phage endolysin, Lys68, with broad anti-Gram-negative activity in presence of weak acids

4.1 Introduction

G^- bacterial pathogens are common causes of foodborne (e.g. *Salmonella*, *Escherichia coli* O157:H7) and hospital-acquired (e.g. *Pseudomonas*, *Acinetobacter*) infectious diseases (Chopra et al, 2008; Scallan et al, 2011). In an era in which the threat of antibiotic and multi-resistant bacteria is increasing and solutions are becoming scarce, it is important to search for alternative antimicrobials. One promising alternative approach to prevent or destroy pathogenic bacteria is the use of bacterial cell wall hydrolases. Among them, increasing interest has been given to lysozymes (e.g. hen egg white lysozyme - HEWL) and phage endolysins. HEWL is a marketed protein, largely studied and widely used in food and pharmaceutical industry products. Endolysins are specialized PG-degrading enzymes, part of a universal lytic cassette system encoded by all dsNA phages. In contrast to the obvious potential of endolysins in fighting G^+ pathogens, strategies to overcome the OM need to be developed in order to extend their use to attack G^- bacteria.

This chapter describes a novel *Salmonella* phage endolysin (further abbreviated as Lys68). After an *in silico* analysis, its lytic spectrum, muralytic activity and stability under different pH values and temperatures were analyzed, enlarging the pool of the few characterized G^- phage endolysins described so far. Its antibacterial action against G^- pathogens was also studied and compared to HEWL, an enzyme comparable in size and catalytic activity, in combination with selected OMP agents: EDTA (at 0.5 mM), citric (at 2 mM) and malic acid (at 5 mM), concentrations described in literature as adequate for permeabilization (Doores, 1993; Alakomi, 2007; Walmagh et al, 2012). Finally, the endolysin PG digestion and the OM permeabilizing mechanisms were discussed. As far as we know, this is the first study that exploits the possibilities of combining a phage-encoded endolysin with several weak acids as potential OMP agents, for an efficient killing of several G^- pathogens.

4.2 Materials and methods

4.2.1 Bacterial strains, bacteriophage and chemicals

Bacterial strains used in the work described in this chapter are listed in **Table 4.1** and belong to the Centre of Biological Engineering (CEB) bacterial collection. All strains were grown in Lysogeny broth (LB, Liofilchem) at 37°C, 120 rpm, with the exception of *Pseudomonas fluorescens*, grown at 25°C, and *Campylobacter jenuni,* grown in Columbia Blood agar (Oxoid) in a microaerobic atmosphere (5% O_2 and 10% CO_2) at 42°C and further incubated in NZCYM broth (BD Biosciences) at 55°C.

Table 4.1. Overview of bacterial pathogens strains, references and sources used in chapter 4.

Bacterial strain	Reference(s)	Sources
Salmonella Typhimurium	ATCC 19585 (further designated as LT2)	NA
Salmonella Enteritidis	ATCC 13076 / 932*	NA
Salmonella bongori	SGSC 31001	Frog
Campylobacter jejuni	12662* / New M1*	Poultry
Cronobacter sakazakii	CECT 8581	Child's throat
Cronobacter muytjensii	ATCC 51329	NA
Pseudomonas fluorescens	7A*	Dairy industry
Pseudomonas aeruginosa	ATCC 15692 (further designated as PAO1)	Infected burn/wounds
Acinetobacter baumannii	2*	Infected burn/wounds
Yersinia enterocolitica	SA54291	NA
Klebsiella oxytoca	ATCC 131821	Pharyngeal tonsil
Pantoea agglomerans	SA56341	NA
Enterobacter amnigenus	CECT 48781	Soil
Proteus mirabilis	SA54451	NA
Citrobacter freundii	SA5345	NA
Escherichia coli O157:H7	CECT 47821	Human stool
Shigella sonnei	ATCC 259311	Human faeces

NA - Not available; * strains belonging to the CEB bacterial collection

E. coli cloning and expression strains (Invitrogen) are given in **Table 4.2**. *Salmonella* phage phi68 (encoding the Lys68 endolysin) was isolated from waste effluents and belongs to the CEB phage collection. For other chemicals used, EDTA was acquired from Pronalab while isopropyl-β-D-thiogalactopyranoside (IPTG), HEPES, citric acid and malic acid were purchased from Sigma-Aldrich. HEWL was obtained from Fisher Scientific.

Table 4.2. Gynotypes of *E. coli* cloning and expression strains and vector used in chapter 4.

Bacterial strains	Genotype
TOP10	F^- mcrA Δ(mcrCB-hsdSMR-mrr) Φ80*lac*ZΔ*M15* Δ*lac*X74 *recA1 araD139* Δ(*ara-leu*)7697 *galU galK rpsL*(Str^r) *endA1* λ^-
BL21(DE3)	F^- *ompT* $hsdS_B(r_B^- m_B^-)$ *gal dcm (DE3)*

For transformation of Lys68 constructs (described in the *4.2.3.1 Cloning methodology* section) chemically competent *E. coli* TOP10 and *E. coli* BL21 cells were prepared for cloning and protein recombinant expression, respectively. The procedure to make competent started to grow each colony overnight in 10 mL of LB medium and diluted (1:100) to 50 mL fresh LB medium the following day. After growing at 37°C and 120 rpm and reaching a OD of about 0.3, cell were pelleted (10 min, 4°C, 5000 rpm) and resuspended in 25 mL ice-cold 0.1 M $CaCl_2$ and incubated for 30 min. Next, following a second centrifuge step, cells were resuspended in 1.5 mL of 0.1 M $CaCl_2$ in the presence of 10% glycerol. Competent cells were stored at -80°C prior to use in 100 µL aliquots. Transformation of foreign DNA was accomplished by the heat shock procedure. First, ≈ 200 ng of plasmid was incubated with 100 µL of thawed competent cells on ice for 30 min, after which a heat shock of 42°C for 45 s was carried out. For a proper selection, cells were allowed to grow in liquid LB and plated onto LB agar plates containing the proper antibiotic for each transformant.

4.2.2 *In silico* analysis

Lys68 endolysin was screened by the HHpred webserver (URL http://toolkit.tuebingen.mpg.de/hhpred) using Pfam, InterProScan and COG; with an E-value cut-off of $1x10^{-5}$ and at least 80% of query coverage. The MSA generation method used was HHblits (Remmert et al, 2012).

To identify putative catalytic residues within Lys68 sequence, BlastP searches were conducted. Blasting the endolysin sequence, high homology residues, indicated as probable catalytic residues can be found. To experimentally prove their *in silico* prediction, point mutations (described in the next section) were made using a QuickChange II XL Site-Directed Mutagenesis Kit (Agilent Technologies). Mutagenic primers were designed using a web-based QuickChange Primer Design Program (www.agilent.com/genomics/qcpd).

4.2.3 Cloning, recombinant protein expression and purification

Primers used to clone the Lys68 endolysin were purchased from Invitrogen. The vector pET28a (Novagen) was used to clone and express Lys68, and has a resistant marker for kanamycin (50 µg/mL). Restriction enzymes were purchased from NEB.

4.2.3.1 Cloning methodology

Standard PCR

The isolated *Salmonella* phage phi68 was partially sequenced showing resemblance to the sequenced *S.* Enteritidis typing phage SETP3 (data not shown). Based on phage SETP3 genomic sequence available at NCBI database (reference sequence: NC_009232.2), primers were designed to amplify the putative endolysin gene by PCR. Lys68 open reading frame was amplified using the following PCR amplification mixture and end concentrations given: KAPA HiFi

Buffer Fidelity (1x); 10 mM dNTP Mix (0.3 mM); forward (AGATATCATATGTCAAACCGAAACATTAGC) and revere primers (GTGGTGCTCGAGCTACTTAG) (0.3 µM each), with introduced *Nde*I and *Xho*I restriction sites are underlined; template *Salmonella* phage phi68 DNA (1 to 10 ng); KAPA HiFi DNA Polymerase from KaPaBioSystems (1 U) (Grisp) and PCR-grade water up to 50 µL. The DNA thermal cycler (MJ Mini™ Gradient Thermal Cycler, Biorad) was programmed for a standard PCR reaction of 35 cycles, including: an initial DNA denaturation step (5 min at 98°C), DNA denaturation step (30 s at 98°C), primer annealing step (30 s at a 55°C), and extension step (2 min at 72°C), followed by a final extension step (5 min at 72°C) to allow proper PCR product elongation. After PCR reaction, samples were separated on a 1% agarose gel in TAE electrophoresis buffer (40 mM Tris-HCl pH 7.2, 500 mM sodium acetate and 50 mM EDTA), stained with SYBR® Safe (Invitrogen), visualized by UV illumination (BioRad) and cleaned (DNA Clean & ConcentratorTM-5k, Zymo Research). To clone the amplified Lys68 gene (insert) in the pET28 expression vector selected, both plasmid and insert were double-digested using the same *Nde*I/*Xho*I sticky end endonucleases in the following reaction: 1 µL of DNA (approx. 300 ng), 1 µL of both restriction enzymes (10 U), 1 µL of 10x CutSmart buffer (NEB), and PCR-grade water up to 10 µL. After 2 h incubation, insert/vector digested products were cleaned (DNA Clean & ConcentratorTM-5k, Zymo Research) and ligated (overnight, 16°C) using a T4 ligase (New England Biolabs) and a 3:1 (insert/vector) molar ratio. *E. coli* Top10 cells were transformed with the ligation mixture.

Colony PCR

Colony PCR was carried out to screen for the correct construct before being confirmed by sequencing. *E. coli* TOP10 transformants were transferred by toothpick to a 96-well microtiter plate. Colonies were grown individually in each well containing 100 µL of LB supplemented with antibiotic (50 µg/mL kanamycin)

for 1.5 h at 37°C and in static conditions. Next, the following PCR mixture was made: forward and reverse primers (insert-specific combined with vector-specific primers at 0.4 µM); dNTPs mix (0.2 mM each nucleotide); buffer Dream *Taq* (10x); Dream *Taq* polymerase (2.5 U) (Fermentas); 2.5 µL of cell culture grown in each well and PCR-grade water up to 25 µL total volume. Then, a PCR reaction was conducted: initial denaturation step of 5 min at 95°C followed by 35 cycles consisting of 30 s at 98°C/30 sec at 50°C/2 min at 72°C, ending with a final extension period of 10 min at 72°C. PCR product was loaded onto agarose gels for confirmation. Finally, plasmid of positive constructs was extracted and verified by sequencing (Macrogen).

Mutagenesis

To substitute the putative catalytic residues within the Lys68 sequence, two active site mutations (Glu18Ala and Thr35Ala) were introduced. Two sets of overlapping mutagenic primers (5'-CGCGGCATTCGCGGGGTTCCGGG, forward, 5'-CCCGGAACCCCGCGAATGCCGCG, reverse, for Glu18Ala, and 5'-AGAATGAGAAGTACCTTGCTATTGGCTACGGCCAC, forward 5'-GTGGCCGTAGCCAATAGCAAGGTACTTCTCATTCT, reverse, for Thr35Ala, with mutation basepairs underlined), were applied using the QuickChange II XL Site-Directed Mutagenesis Kit (Agilent Technologies), following the manufacturer's instructions. Briefly, 10 ng of pET28-Lys68 template, 125 ng of the two mutagenic primers, a dNTP mix (1x), a reaction buffer, a Quick Solution reagent 2.5 U of *PfuUltra* HF DNA polymerase and PCR-grade water up to 50 µL (total volume) was added together. After the recommended mutagenic PCR reaction, the product was digested with *Dpn*I for 1 h at 37°C, to allow degradation of parental methylated DNA. After transformation into XL10-Gold ultracompetent cells provided, positive transformants were grown, their plasmid extracted and sent for sequencing (Macrogen).

4.2.3.2 Protein overexpression and purification

After sequencing, all vectors were introduced and expressed in *E. coli* BL21(DE3). Cells were grown in 200 mL LB supplemented with the specific antibiotic (50 µg/mL of kanamycin) to an OD_{600nm} of 0.6 (4 h, 120 rpm at 37°C), and recombinant protein expression was induced with IPTG to a final concentration of 0.5 mM. After optimization, *E. coli* expression temperature (16°C) and temperatures (18 h) were chosen to maximize soluble expression yields. The culture was then centrifuged (9500x*g*, 30 min) and cells were disrupted by resuspending the pellet in 1/25 volumes of lysis buffer (20 mM NaH_2PO_4, 0.5 M NaCl/NaOH, pH 7.4), followed by three cycles of freeze-thawing (-80°C to room temperature). Maintaining the sample on ice, cells were further disrupted by sonication (Cole-Parmer, Ultrasonic Processors) for 8-10 cycles (30 s pulse, 30 s pause). Insoluble cell debris were removed by centrifugation (9500x*g*, 30 min, 4°C). The supernatant was collected and filtered (0.22 µm filters) and applied to Ni^{2+}-NTA resin stacked in HisTrapTM HP 1 ml columns (GE Healthcare) for purification, using protein-dependent imidazole concentrations optimized for and evolving four steps:

1. Equilibrium step - 10 mL of lysis buffer (65 mM imidazole concentration).

2. Loading step - Loading of total soluble expressed *E. coli* extract that was resuspended in lysis buffer (65 mM imidazole concentration).

3. Washing step - 10 mL of lysis buffer (65 mM imidazole concentration).

4. Elution step - 2 mL of lysis buffer with 300 mM imidazole.

Eluted protein fractions were then visualized by standard denaturation SDS-PAGE (sodium dodecyl sulfate polyacrylamide gel electrophoresis) gels using the Bio-Rad system under denaturation conditions. To perform the electrophoresis, a 5% of upper and a 12% lower stacking and separating acrylamide gels were assembled. From the eluted fractions, 10 µL were added to 10 µL of Laemmli buffer (2x)

(Sigma), boiled at 95°C for 5 min and loaded onto the gels together with a Low Molecular Weight ladder (GE Healthcare). Protein bands were routinely separated for 2 h, at 120 volts. Gels were rinsed with water and stained with 0.05% of Commassie brilliant blue R-250 (Sigma) solution for 2 h. Background destaining was performed with several washing steps with water. Only protein samples with purities equal to or higher than 90% were considered pure and used to perform additional studies. Proteins were dialyzed in 10 mM phosphate buffered saline (PBS) at pH 7.2 (using Maxi GeBAflex-tube Dialysis Kit - Gene Bio-Application L.T.D). The Protein concentrations were then determined by the BCA™ Protein Assay Kit with bovine serum albumin as standard (Thermo Scientific).

4.2.4 Biochemical characterization

4.2.4.1 Endolysin lytic spectrum

To determine lytic spectrum of Lys68, a range of different strains was tested (**Table 4.1**). G^- and G^+ overnight grown cultures were overnight grown and diluted 1:100 diluted in the following day in fresh 5 mL LB and allowed grow until reaching the mid-exponential phase (OD_{600nm} of 0.6). Cells were then plated (100 µL) onto LB agar Petri dishes for lawn formations. After 8 h incubation, a 30-µL drop of 2 µM of purified Lys68 was added to visualize lysis halos. In the case of G^- cells a step involving treatment with chloroform vapours was included to permeabilize the OM (Raymond Schuch, 2009). After lawn formations, in a chemical fume hood, 10 mL of chloroform were added to an inverted lid glass plate. Bacterial lawns were inverted on top of the chloroform and incubated for 1 h to allow chloroform evaporation. Finally, a 30-µL drop of 2 µM of Lys68 protein was added to visualize lysis halos. In both cases, halo spots commonly appeared after 30 min up to 1 h after the start of the incubation period.

4.2.4.2 Muralytic activity

The PG lytic (or muralytic) activity was quantified on *P. aeruginosa* PAO1 cells with the OM permeabilized (exposed PG), as a substrate (Lavigne et al, 2004). This substrate was prepared by growing *P. aeruginosa* cells to an OD_{600nm} (optical density at 600 nm) of 0.6, centrifuging them (4000xg, 15 min, 4°C) and resuspending them in a chloroform-saturated 0.05 M Tris buffer (pH 7.7). After gently shaking for 45 min at room temperature, protoplasts were collected (4000xg, 15 min, 4°C), washed and resuspended in 80 mM phosphate buffer (pH 7.2) at an OD_{600nm} of 1.0. Substrate was then stored at -20°C prior to use. To perform the muralytic activity, 30 µL of serial dilutions of enzyme were added to 270 µL of OM permeabilized cells (prepared substrate). The endolysin activity was measured over a period of 30 s or up to 30 min, through the decrease in OD_{600nm} using a BIO-TEK®, Synergy HT Microplate Reader. Obtained values for the negative control (30 µL of PBS pH 7.2) were subtracted from the sample values. The muralytic activity was calculated according to a standardized calculation method optimized and extensively described elsewhere (Briers et al, 2007a). Enzymatic activity was defined as follows: Activity (units/µM) = ((slope (OD_{600nm}/min)/µM))/0.001), where the activity of 1 unit is defined as the concentration of enzyme (in µM) necessary to create a drop in OD_{600nm} of 0.001 per minute. Averages ± standard deviations are given for n = 3 repeats.

<u>pH dependence</u>

The pH dependence on the muralytic activity was assessed using the same 30 µL of serial dilutions of enzyme on 270 µL of OM permeabilized cells, but now resuspended in a universal pH buffer (150 mM KCl, 10 mM KH_2PO_4, 10 mM Na-citrate and 10 mM H_3BO_4) adjusted to different pH values within the range of 3.0 and 10.0. Averages ± standard deviations are given for n = 3 repeats.

Cryo/Thermal stability

For cryostability tests, the same muralytic activity described was performed with Lys68 samples stored during 2 months at cold temperatures (4°C and -20°C). Thermostability was evaluated by incubating the endolysin at several temperatures 40°C, 60°C, 80°C and 100°C for 30 min and in addition at 100°C during different time intervals (5, 10, 20, 25, 30 and 45 min) in a MJ MiniTM BIO-RAD Thermocycler. Following a 30-min cooling step on ice, the (residual) activity was measured using 30 µL of 2 µM Lys68 on 270 µL of OM permeabilized cells resuspended in 80 mM phosphate buffer pH 7.2. The residual muralytic activity of each sample relative to the activity of unheated reference sample at time 0 (= 100% activity) was determined. Averages ± standard deviations are given for n = 3 repeats.

4.2.4.3 Circular dichroism

To analyse the Lys68 endolysin secondary structure, circular dichroism (CD) experiments were performed in the far- and near-UV region, using a Jasco J-815 CD spectrometer equipped with a water-cooled Peltier unit. These experiments were carried out at the INL, the International Iberian Nanotechnology Laboratory in Portugal. The spectra were recorded in a cell width of 0.1-mm path length (110.QS, Hellma) from 185 to 360 nm for all proteins with 1 nm steps, scan speed of 20 nm/min, high sensitivity and a 16 s response time. Three consecutive scans from each sample and its respective buffer baseline were obtained. The averaged baseline spectrum was subtracted from the averaged sample spectrum measured under the same conditions. Secondary structure estimates were derived from the spectra using the CDSSTR (Compton & Johnson, 1986) and CONTINLL (Provencher & Glockner, 1981; van Stokkum et al, 1990) routine of the DICHROWEB (Whitmore & Wallace, 2004; Whitmore & Wallace, 2008) server run on the Set 4 optimized for a wavelength of 190-240 nm. Thermal denaturation/renaturation of the

proteins was measured by monitoring the change in ellipticity in a cell width of 0.1 cm path- length at 222 nm over the range of 20°C to 75°C, in increments of 1°C. The experimental denaturation/renaturation profiles were analyzed by a nonlinear least squares fit assuming a two-state transition and used to calculate the melting temperature (T_m). For CD measurements, a concentration of 8 µM of protein was prepared in the presence of a universal buffer (10 mM KH_2PO_4, 10 mM Na-citrate and 10 mM H_3BO_4) adjusted to different pH values within the range of 3 and 10 (for pH dependence tests) and in 80 mM phosphate buffer pH 7.2 (for thermostability tests). The same conditions were used for the analysis of the pH and temperature on the muralytic activity described above.

4.2.3.4 Fluorescence binding assay

To visualize the OMP effect, *S.* Typhimurium LT2 cells were incubated with 2 mM citric acid and 2 µM KZ-EGFP protein. KZ-EGFP is a previously described PG binding domain from a *Pseudomonas* phage endolysin KZ144 coupled with a green fluorescent protein that has strong G^- PG affinity (Briers et al, 2009). After 30 min incubation period, the sample was washed twice in 10 mM HEPES/NaOH (pH 7.2). Afterwards, a 30-µL drop was spotted onto a microscope slide and images were recorded using a confocal laser scanning microscopy (FluoView FV1000 microscope, Olympus) in search for fluorescent *Salmonella*. Cells treated with water (instead of citric acid) and EFGP were used as negative control.

4.2.5 Antibacterial assays

4.2.5.1 In vitro assays on planktonic exponential cells

An overnight culture of G^- cells was diluted (1:100) in fresh 5 mL LB and incubated at 37°C at 120 rpm. When reaching the mid-exponential phase with an OD_{600nm} of 0.6, cells were resuspended in 10 mM HEPES/NaOH (pH 7.2), and then 100-fold diluted to a final density of 10^6 colony forming units (CFU)/mL. Each culture (50 µL) was incubated for up to 2 h at room temperature with 25 µL of Lys68 (2 µM final concentration) together with 25 µL of water or 25 µL of OMPs (EDTA, citric acid and malic acid) dissolved in water. The final concentrations used were 0.5 mM, 2 mM and 5 mM, respectively, concentrations retrieved from literature (Alakomi, 2007; Briers et al, 2011b). Following the same protocol, HEWL was assessed at a final concentration of 2 µM to compare with the Lys68 results. As a negative control, 50 µL of cells were incubated with 25 µL water and 25 µL of PBS (pH 7.2) (culture control), with 25 µL of OMP and 25 µL of PBS (pH 7.2) (OMP control) or with 25 µL water and 25 µL of endolysin dialyzed in PBS (pH 7.2) (endolysin control). After a 30 min incubation period, cell suspensions were serially diluted and colonies were counted after overnight incubation at 37°C in LB agar plates. The antibacterial activity was quantified as the relative inactivation in logarithmic units (= $\log_{10}$ (N_0/N_i) with N_0 = number of untreated cells (in the negative control) and N_i = number of treated cells counted after incubation). Averages ± standard deviations are given for n = 4 repeats.

4.2.5.2 In vitro assays on different bacterial physiological states

To study the influence against different bacterial physiological states, Lys68/OMPs mixture was tested against planktonic *S.* Typhimurium LT2 under exponential and stationary phase and also against biofilms. *S*. Typhimurium LT2 cells, grown overnight at 37°C, were diluted 1:100 in fresh LB and grown for 3 h (planktonic

exponential phase), 12 h (stationary phase) and 24 h (in this case, 200 µL volume on 96-microplate wells - biofilm cells). In the planktonic and stationary assay, 50 µL cells resuspended in 10 mM HEPES/NaOH (pH 7.2) to a final 10^6 CFU/mL were incubated with 25 µL Lys68 (2 µM final concentration) together with 25 µL of citric and malic acid (2 mM and 5 mM final concentrations, respectively) for 2 h. For biofilm assays, overnight cultures of S. Typhimurium cells were normalized (OD adjusted to 1.0 in LB medium) after which 2 µL of the cell suspension was transferred to 96-well polystyrene plates (Orange Scientific) containing 198 µL of LB. To establish mature biofilms the plate was incubated for 24 h at 37°C and 120 rpms. Afterwards, the culture medium was removed and non-adherent cells were also removed by washing the biofilms twice with 200 µL of 10 mM HEPES/NaOH (pH 7.2). Cells were then incubated with 100 µL of HEPES together with 50 µL Lys68 (2 µM final concentration) and 50 µL of citric and malic acid (2 mM and 5 mM final concentrations, respectively) for 2 h. For all experiments, cells incubated with water (instead of citric/malic acid) or PBS (instead of Lys68) were used as negative control. After incubation, the effect of the Lys68 and OMP mixtures on G^- cells (planktonic and biofilms) was assessed by quantification of the number of CFUs. Again, the antibacterial activity was expressed as the relative inactivation in logarithmic units described above. Averages ± standard deviations are given for n = 4 repeats.

4.3 Results

4.3.1 *In silico* analysis

The 489-bps endolysin gene from *Salmonella* phage phi68, encoding a 162-amino acid protein with a deduced molecular mass of 19.6 kDa, was amplified and sequenced (GenBank accession number for Lys68 nucleotide sequence, KJ475444). Based on data from HHpred output (an E-value of $2.3x10^{-47}$ and 100% of query coverage) Lys68 is predicted to be a globular protein with a conserved domain between amino acids 1-151 and belongs to the glycoside hydrolase family GH24 (CAZY, 2014). This catalytic domain is predicted to degrade cell walls by catalyzing the hydrolysis of 1,4-linkages between N-acetylmuramic acid and N-acetyl-D-glucosamine residues. BlastP comparison revealed high homology (>90%) to six other endolysin proteins from *Salmonella* phages, namely SETP3, ST4, SE2, vB_SenS-Ent1, SS3e and wksl3, that have not yet been characterized *in vitro*. A BlastP analysis also indicates conservation in both presumed catalytic residues Glutamic acid (Glu18) and Threonine (Thr35) for the glycosylase reaction.

4.3.2 Recombinant purification and substrate specificity

Overexpression of Lys68 in *E. coli* BL21(DE3) yielded a soluble protein of 14.3 mg/L. To confirm the predicted catalytic activity and to determine the bacterial host spectrum, Lys68 endolysin (2 µM) drops was spotted on several OM-permeabilized G^- cell substrates and several intact G^+ strain lawns (listed in **Table 4.3** and **Figure 4.1**) with different structural types of PG. All OM permeabilized G^- cell substrates together with *L. monocytogenes* were efficiently lysed. Conversely, the remaining tested G^+ bacteria all survived the treatment of Lys68.

Table 4.3. Lytic activity of Lys68 against Gram-negative or Gram-positive strains.

Bacterial strain		**Relative lysis activity**	
G^-		30 min	1 h
Escherichia coli	BL21(DE3)	Susceptible	
Escherichia coli O157:H7	CECT 4782[1]	Susceptible	
Salmonella Typhimurium	LT2[1]	Intermediate	susceptible
Salmonella Enteritidis	ATCC 13076	Susceptible	
	932*	Susceptible	
Salmonella bongori	SGSC 3100[1]	Susceptible	
Campylobacter jejuni	12662*	Susceptible	
	New M1*	Susceptible	
Cronobacter sakazakii	CECT 858[1]	Susceptible	
Cronobacter muytjensii	ATCC 51329	Susceptible	
Pseudomonas fluorescens	7A[1]*	Susceptible	
Pseudomonas aeruginosa	PAO1[1]	Susceptible	
Acinetobacter Baumannii	2[1]*	Susceptible	
Yersinia enterocolitica	SA5429[1]	Susceptible	
Klebsiella oxytoca	ATCC 13182[1]	Susceptible	
Pantoea agglomerans	SA5634[1]	Intermediate	susceptible
Enterobacter amnigenus	CECT 4878[1]	Susceptible	susceptible
Proteus mirabilis	SA5445[1]	Intermediate	Intermediate
Citrobacter freundii	SA5345	Intermediate	susceptible
Shigella sonne	ATCC 25931[1]	Susceptible	
G^+			
Listeria monocytogenes	CECT 5725	Intermediate	Intermediate
Staphylococcus epidermidis	9142*	Resistant	Resistant
Staphylococcus aureus	CECT 976	Resistant	Resistant
Paenibacillus larvae	H23*	Resistant	Resistant

[1]strains tested with enzymes/OMPs;

*strains from the CEB bacterial collection;

Susceptible (clear lysis halo); Intermediate (turbid lysis halo); Resistant (absence of lysis halo)

Figure 4.1. Visualization of the Lys68 lytic activity on chloroform S. Typhimurium LT2 permeabilized lawn. Six 10 µL-radial endolysin (2 µM) drops resulted in lysis halos. PBS added to the center served as negative control (no lysis halo observed).

4.3.3 Biochemical characterization

4.3.3.1 pH dependence and muralytic activity

Muralytic activity

Biochemical characterization of Lys68 started exploring the muralytic activity under different conditions. Regarding pH dependence, Lys68 remains active over a pH range from 4.0 to 10.0 (maintaining 41.17%±4.81 and 46.31%±0.96 of its activity, respectively) (**Figure 4.2 a**), with a pH optimum around 7.0 (pH of the bacterial cytoplasm). When kept at optimal pH, Lys68 has a muralytic activity of 400 Units/µM that decreases to 310 Units/µM (23.3% less) and 100 Units/µM (74.9% less) when the protein is stored for two months at 4°C and -20°C, respectively (**Figure 4.2 b**).

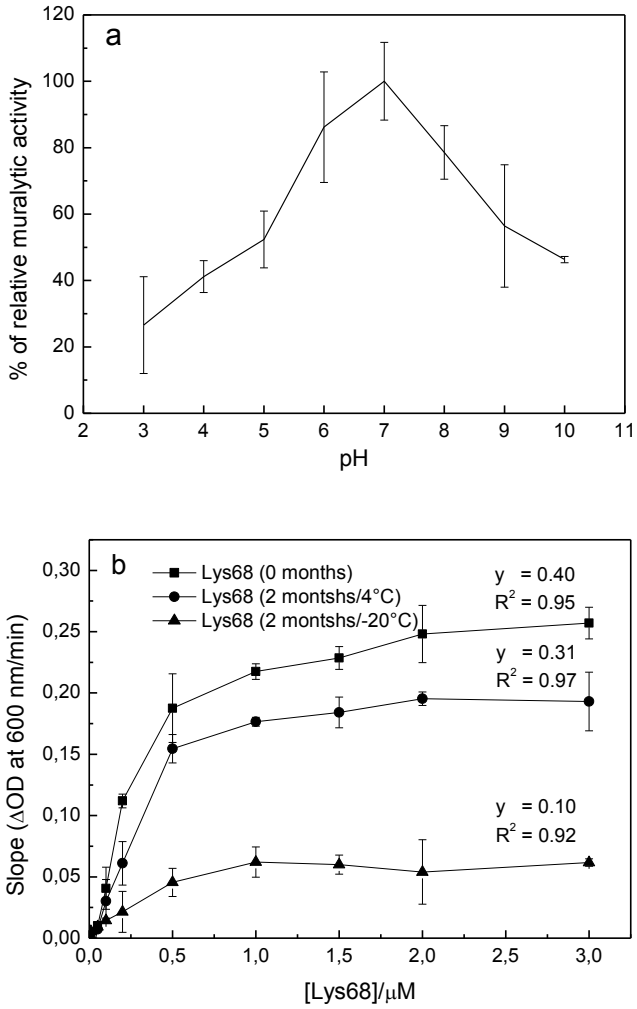

Figure 4.2. Muralytic activity of Lys68. a) pH optimum for enzymatic activity of Lys68. Relative muralytic activity is measured as the slope of the OD_{600nm}/min curve, given in percentage by comparing to the activity at pH 7.0 (the highest measured value) (Y-axis) on OM-permeabilized *P. aeruginosa* PAO1 substrate and is shown for a pH range between 3.0 and 10.0 (X-axis). b) Saturation curves for Lys68 muralytic activity under optimal pH (7.2). The activity in $OD_{600\ nm}$/min (Y-axis) for incremental amounts of Lys68 (0 months - squares; 2 months at 4°C - circles; 2 months at -20°C - triangles) is depicted. Muralytic activity reaches saturation at 2 to 3 μM.

Circular dichroism analysis

To elucidate the major structural features of Lys68, CD studies were employed using a universal buffer at different pH values (**Figure 4.3**). The Lys68 CD profile exhibited two negative dichroic minima at 222 nm and 208 nm and a positive dichroic maximum at 192 nm, which is characteristic of a protein with a high α-helix content.

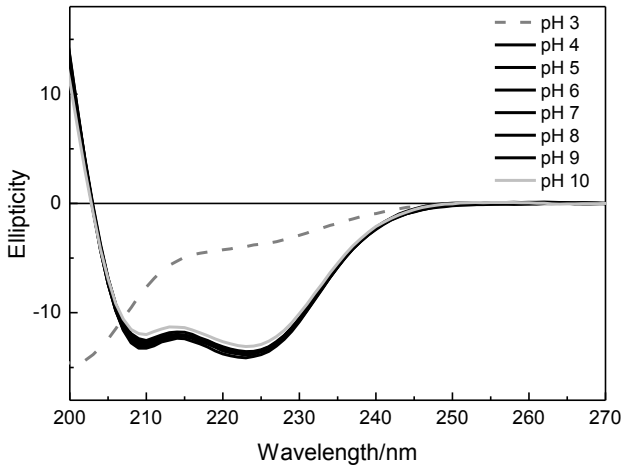

Figure 4.3. Circular dichroism spectra of Lys68 as a function of pH using a universal buffer with adjusted pH (3.0-10.0).

Deconvolution of the CD spectra, using a dataset as specified in materials and methods, allowed us to determine that 37% of Lys68 folds as α-helices, 17% as β-sheet, and 18% as turns, while 27% was unordered. Interestingly, when the pH was between 4.0 and 10.0, the obtained spectra were almost identical and the predicted secondary structures content remained essentially unchanged. These data shows that the secondary structure content of Lys68, at various pH conditions, is highly conserved, even at pH 4.0, similar to the trend observed for HEWL after analysis its CD spectrum (**Supplementary Figure S4.1**). Conformational changes occurred around pH 3.0 with loss of secondary structure.

4.3.3.2 Thermostability

Muralytic activity

Thermal stress of Lys68 was investigated and is depicted in **Figure 4.4**. Thermostability tests showed no reduction on the enzymatic activity after 30 min incubation of the enzyme at 40°C, and only minor loss of activity was observed when incubated at 60 and 80°C during the same time. At 100°C, the muralytic activity dropped to 25.8%, 10.2% and 0.27% of the initial activity after 20, 30 and 45 min incubation, respectively.

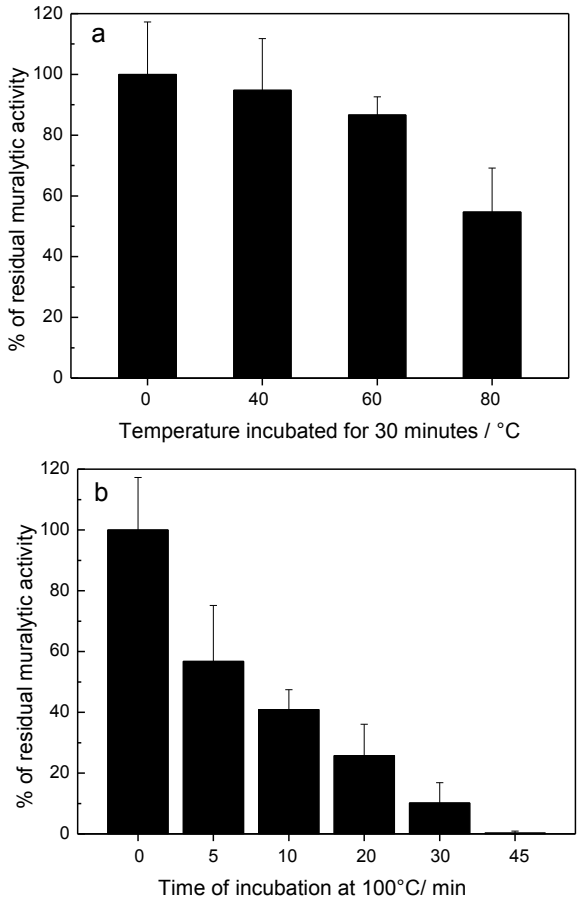

Figure 4.4. Lys68 muralytic activity after thermal stress. a) Residual Lys68 activity (2 µM) on OM permeabilized *P. aeruginosa* PAO1 cell substrate after incubation at 40, 60 and 80°C for 30 min and b) after heat treatment at 100°C for 0, 5, 10, 20, 30 and 45 min, followed by a 30-min cooling step on ice.

Circular dichroism analysis

Related to the muralytic studies, CD studies were performed to evaluate the Lys68 thermostability by following the loss of CD signal (ellipticity) at 222 nm (dichroic band characteristic for α-helical proteins) when increasing the temperature of the sample from 20 to 75°C. Lys68 demonstrated a sigmoidal thermal denaturation profile, reflecting protein unfolding (**Figure 4.5**).

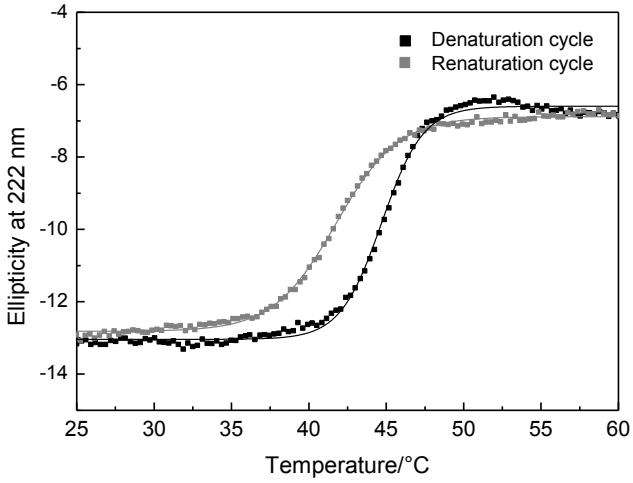

Figure 4.5. Melting curves for Lys68, measured by monitoring the absorbance at 222 nm against increasing (denaturation) and decreasing temperatures (renaturation) at pH 7.0.

The T_m was found to be around 44°C according to a two-state model. Interestingly, the renaturation experiments showed a maximum recovery of the native features after the protein was heated up to 75°C under the same experimental conditions, and a loss in ellipticity of only 1.3%. Employing the thermal denaturation at eight different pH values from 3.0 to 10.0, the T_m of Lys68 increases from 38.1°C (for pH 3.0) to 44.7°C and 43.4°C (optimal pH 6.0-7.0, respectively), after which it decreases again to 36.1°C (for pH 10.0) (**Table 4.4**). This indicates that the protein is more stable at neutral pH and the stability

decreases at acidic or basic pH values, which is positively correlated with the observed optimal pH from the Lys68 muralytic activity.

Table 4.4. Apparent melting temperatures (T_m) of Lys68 as a function of pH (3.0-10.0) as determined by circular dichroism signal at 222 nm in thermal denaturation and renaturation experiments.

pH	T_m (Denaturation cycle)	T_m (Renaturation cycle)
3	-	-
4	38.1°C	35.0°C
5	43.0°C	40.7°C
6	44.7°C	41.8°C
7	43.4°C	40.8°C
8	41.5°C	38.5°C
9	39.4°C	34.6°C
10	36.1°C	-

Afterwards, Lys68 was subjected to thermal stress under different temperatures (40, 60, 80 and 100°C) and protein ellipticity was monitored (**Figures 4.6 a, b**). It was observed that from 4°C to 40°C, Lys68 remained very stable and kept its activity for longer periods. As the incubation temperature increased from 40°C to 60°C, 80°C and 100°C, evident changes in secondary structures occurred, with a continuous decrease in the ellipticity of the 208 nm and 220 nm bands. In accordance, CD thermal stability showed that the loss of muralytic activity upon thermal stress is accompanied with gradual loss of endolysin secondary structure.

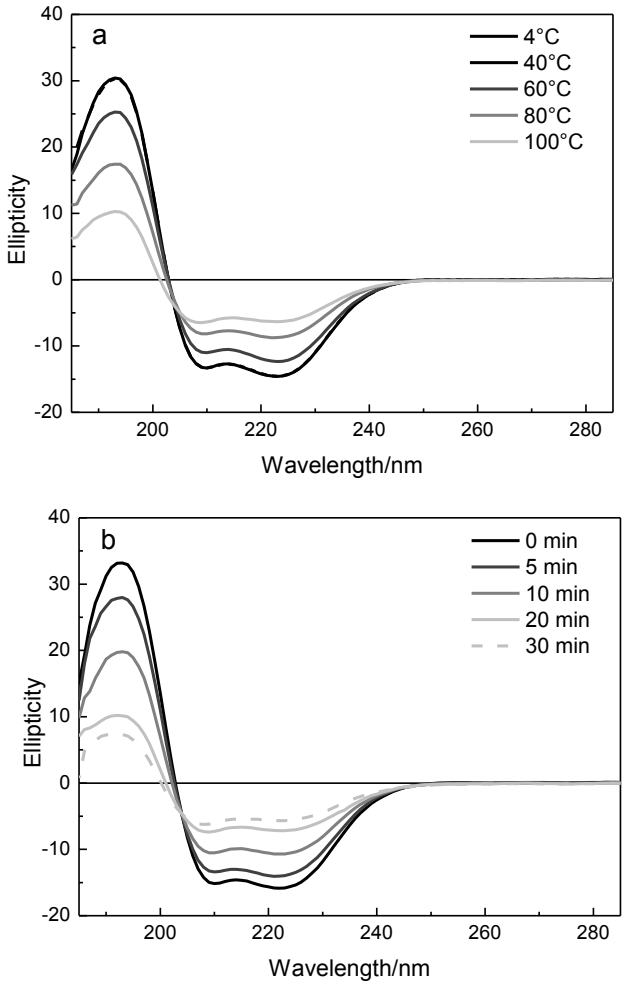

Figure 4.6. Circular dichroism spectra of Lys68 after thermal stress. a) Lys68 (2 µM) incubated at 40, 60 and 80°C for 30 min followed by 30 min incubation on ice, and b) after heat treatment at 100°C for 0, 5, 10, 20, 25 and 30 followed by 30 min incubation on ice.

4.3.4 *In vitro* antibacterial activity

4.3.4.1 Enzymes/OMPs effect on Gram-negative cells

The *in vitro* antibacterial activity of Lys68/OMP and HEWL/OMP was investigated on a wide panel of G^- bacteria (**Table 4.5**). As is depicted, a stronger antibacterial activity was observed against *S.* Typhimurium LT2, *A. baumannii* 2 and *P. aeruginosa* PAO1, compared to the other tested species.

Table 4.5. Combinatorial antibacterial activity of outer membrane permeabilizers with (A and B) or without (C) HEWL/Lys68 on Gram-negative bacterial pathogens. Marked in bold are significant log reduction units observed (≥ 1 log).

A	Bacterial Species	HEWL/Water	HEWL/EDTA	HEWL/Citric	HEWL/Malic
	***Salmonella* Typhimurium LT2**	0.03 ± 0.07	0.14 ± 0.23	0.08 ± 0.15	0.07 ± 0.09
	***Acinetobacter baumannii* 2**	0.01 ± 0.09	0.04 ± 0.06	0.10 ± 0.06	0.17 ± 0.15
	***Pseudomonas aeruginosa* PAO1**	0.02 ± 0.10	**0.89 ± 0.17**	0.24 ± 0.02	**2.44 ± 0.52**
	***Pseudomonas fluorescens* 7A**	0.04 ± 0.04	0.30 ± 0.38	0.28 ± 0.13	**3.77 ± 0.45**
	***Shigella sonnei* ATCC 25931**	0.22 ± 0.29	0.01 ± 0.11	0.02 ± 0.07	0.06 ± 0.12
	***E. coli* O157:H7 CECT 4782**	0.04 ± 0.15	0.11 ± 0.12	0.10 ± 0.05	0.09 ± 0.04
	***Cronobacter sakazakii* CECT 858**	0.11 ± 0.18	0.15 ± 0.20	0.30 ± 0.16	0.20 ± 0.13
	***Pantoea agglomerans* SA5634**	0.04 ± 0.10	0.08 ± 0.15	0.20 ± 0.19	0.22 ± 0.29
	***Enterobacter amnigenus* CECT 4878**	0.04 ± 0.07	0.07 ± 0.13	0.18 ± 0.17	0.26 ± 0.04
	***Proteus mirabilis* SA5445**	0.08 ± 0.03	0.09 ± 0.14	0.03 ± 0.25	0.17 ± 0.14
	***Salmonella bongori* SGSC 3100**	0.02 ± 0.10	0.10 ± 0.09	0.09 ± 0.13	0.47 ± 0.19
	***Klebsiella oxytoca* ATCC 13182**	0.01 ± 0.02	0.10 ± 0.05	0.13 ± 0.08	0.26 ± 0.06
	***Yersinia enterocolitica* SA5429**	0.06 ± 0.05	0.18 ± 0.11	0.11 ± 0.12	0.34 ± 0.11

B	Bacterial Species	Lys68/Water	Lys68/EDTA	Lys68/Citric	Lys68/Malic
	***Salmonella* Typhimurium LT2**	0.14 ± 0.16	0.16 ± 0.12	**2.93 ± 0.45**	**2.65 ± 0.40**
	***Acinetobacter baumannii* 2**	0.04 ± 0.12	0.14 ± 0.22	**1.01 ± 0.33**	**2.93 ± 0.59**
	***Pseudomonas aeruginosa* PAO1**	0.04 ± 0.34	**2.46 ± 0.48**	**1.48 ± 0.35**	**3.31 ± 0.21**
	***Pseudomonas fluorescens* 7A**	0.02 ± 0.10	**1.44 ± 0.67**	**1.40 ± 0.23**	**5.91 ± 0.43**
	***Shigella sonnei* ATCC 25931**	0.13 ± 0.28	0.35 ± 0.44	**1.40 ± 0.33**	**2.42 ± 0.43**
	***E. coli* O157:H7 CECT 4782**	0.02 ± 0.02	0.21 ± 0.14	**1.18 ± 0.12**	**2.37 ± 0.35**
	***Cronobacter sakazakii* CECT 858**	0.16 ± 0.06	0.30 ± 0.09	**1.09 ± 0.19**	**1.40 ± 0.30**
	***Pantoea agglomerans* SA5634**	0.03 ± 0.18	0.13 ± 0.12	0.32 ± 0.18	**1.26 ± 0.18**
	***Enterobacter amnigenus* CECT 4878**	0.04 ± 0.11	0.28 ± 0.18	0.68 ± 0.36	**1.21 ± 0.27**
	***Proteus mirabilis* SA5445**	0.03 ± 0.12	0.09 ± 0.04	0.41 ± 0.29	**0.97 ± 0.25**
	***Salmonella bongori* SGSC 3100**	0.06 ± 0.10	0.08 ± 0.16	0.13 ± 0.09	**0.94 ± 0.05**
	***Klebsiella oxytoca* ATCC 13182**	0.07 ± 0.13	0.12 ± 0.17	0.24 ± 0.14	0.30 ± 0.22
	***Yersinia enterocolitica* SA5429**	0.11 ± 0.10	0.03 ± 0.06	0.18 ± 0.08	0.22 ± 0.07

C	Bacterial Species	------	Water/EDTA	Water/Citric	Water/Malic
	***Salmonella* Typhimurium LT2**		0.09 ± 0.10	0.07 ± 0.05	0.06 ± 0.09
	***Acinetobacter baumannii* 2**		0.04 ± 0.03	0.07 ± 0.05	0.07 ± 0.04
	***Pseudomonas aeruginosa* PAO1**		0.05 ± 0.06	0.60 ± 0.14	**1.54 ± 0.47**
	***Pseudomonas fluorescens* 7A**		0.42 ± 0.31	0.70 ± 0.14	**2.70 ± 0.51**
	***Shigella sonnei* ATCC 25931**		0.01 ± 0.14	0.02 ± 0.14	0.14 ± 0.03
	***E. coli* O157:H7 CECT 4782**		0.06 ± 0.04	0.01 ± 0.09	0.18 ± 0.18
	***Cronobacter sakazakii* CECT 858**		0.17 ± 0.12	0.06 ± 0.14	0.28 ± 0.10
	***Pantoea agglomerans* SA5634**		0.07 ± 0.10	0.03 ± 0.18	0.10 ± 0.18
	***Enterobacter amnigenus* CECT 4878**		0.08 ± 0.08	0.15 ± 0.15	0.16 ± 0.18
	***Proteus mirabilis* SA5445**		0.02 ± 0.10	0.01 ± 0.23	0.03 ± 0.12
	***Salmonella bongori* SGSC 3100**		0.07 ± 0.12	0.05 ± 0.14	0.16 ± 0.03
	***Klebsiella oxytoca* ATCC 13182**		0.12 ± 0.12	0.01 ± 0.09	0.18 ± 0.09
	***Yersinia enterocolitica* SA5429**		0.01 ± 0.06	0.30 ± 0.23	0.06 ± 0.07

The activity of both Lys68 and HEWL alone against exponentially growing cells was insignificant. However, following permeabilization with OMPs a different outcome was observed. Despite being both able to inactivate *Pseudomonas* cells, Lys68/EDTA had a more pronounced killing effect than HEWL/EDTA. Both citric and malic acid were significantly better than EDTA in enhancing the access of Lys68 to the PG, however this advantageous effect was not observed in combination with HEWL. Lys68/citric acid was not only able to kill *Pseudomonas* cells, but also caused a significant reduction of *S.* Typhimurium LT2 (2.93±0.45 log reduction) and *A. baumannii* (1.01±0.33 log reduction) as well of *Shigella sonnei* (1.40±0.33 log reduction), *E. coli* O157:H7 (1.18±0.12 log reduction) and *Cronobacter sakazakii* (1.09±0.19 log reduction).

Interestingly, the effect of Lys68/malic acid was even higher in all strains compared to Lys68/EDTA and Lys68/citric acid. Reductions of 2-3 logs units were observed on *P. aeruginosa* (3.31±0.21), *S.* Typhimurium LT2 (2.65±0.40) and *A. baumannii* (2.93±0.59). Overall, the best log reduction values were consistently obtained with malic acid in combination with Lys68 after 30 min of incubation,

killing 11 different G^- bacterial species**.** In contrast to the other strains, none of the OMPs could sensitize Lys68 to *Klebsiella oxytoca* and *Yersinia enterocolitica* strains.

When incubated for longer periods (2 h), the combinatory effect of citric acid and Lys68 on *S.* Typhimurium LT2 increased remarkably, resulting in a 5.05±0.48 log reduction of viable cells and was also efficient against stationary cells (1.45±0.15 log units of viable cells) and biofilms (1.26±0.10 log units of viable cells) (**Table 4.6**).

Table 4.6. Influence of different *S.* Typhimurium LT2 physiological states (planktonic/biofilm) on the combinatorial effect of Lys68 and outer membrane permeabilizers (citric and malic acid). Marked in bold are significant log reduction units observed (≥ 1 log).

***S.* Tyhpimurium LT2**	**Planktonic**		**Biofilm**
	Exponential phase	**Stationary phase**	
Lys68 + Water	0.11 ± 0.14	0.14 ± 0.07	0.15 ± 0.11
PBS + Citric acid	0.10 ± 0.11	0.08 ± 0.11	0.09 ± 0.19
PBS + Malic acid	0.08 ± 0.20	0.19 ± 0.18	0.15 ± 0.25
Lys68 + Citric acid	**5.05 ± 0.48**	**1.45 ± 0.15**	**1.26 ± 0.10**
Lys68 + Malic acid	**3.19 ± 0.53**	0.55 ± 0.28	**1.31 ± 0.13**

4.3.4.2 OM permeabilization mechanism

To further investigate whether the permeabilizing effect of citric and malic acid is compound- or pH-related, *S.* Typhimurium LT2 cells were incubated with Lys68 in the presence of HCl (to drop the pH to 4.2 and 3.8, similar to citric and malic acid, respectively) for a 30 min period (**Table 4.7**).

Table 4.7. *S.* Typhimurium LT2 log reduction units after incubation with enzymes and acids. Marked at bold are significant log reduction units observed (≥ 1 log).

	Water	HEWL	Lys68	Lys68 + $MgCl_2$
HCl, pH 4.2	0.14 ± 0.18	0.12 ± 0.05	**2.44 ± 0.56**	0.10 ± 0.18
HCl, pH 3.8	0.01 ± 0.17	0.11 ± 0.10	**2.66 ± 0.42**	0.20 ± 0.13
Citric acid, pH 4.2	0.21 ± 0.14	0.09 ± 0.08	**3.08 ± 035**	0.24 ± 0.10
Malic acid, pH 3.8	0.11 ± 0.09	0.13 ± 0.06	**2.63 ± 0.47**	0.18 ± 0.16

The results summarized in **Table 4.7** show that the log reduction units of viable cells are mostly due to the acidity. In the presence of HCl, Lys68 is able to kill 2.44±0.56 log of viable cells at pH 4.2 (3.08±0.35 for citric acid) and a 2.66±0.42 log reduction of viable cells was obtained at pH 3.8 (2.63±0.47 for malic acid). In the case of HEWL, both organic acids and HCl were inactive towards *S*. Typhimurium LT2.

It has been described that $MgCl_2$ can interact with the LPS layer via divalent cations (Mg^{2+}), contributing to the stability of the OM (Alakomi et al, 2000). Subsequently, this results in a decrease in permeability of the OM to external agents. Consequently, the addition of 5 mM of $MgCl_2$ abolished the Lys68 antibacterial activity in all tested conditions (**Table 4.7**).

To visualise the effect of organic acids as G^- OMPs, an experiment was conducted incubating *S.* Typhimurium LT2 cells with citric acid in the presence of a fluorescent probe. This fluorescent probe was constructed earlier and consists of a *Pseudomonas* phage KZ144 endolysin binding domain fused with an enhanced green fluorescent protein (KZ-EGPF) that has high affinity to G^- PG (Briers et al, 2009). When incubating the cells for a 30-min period, green fluorescent *Salmonella* cells could be observed by epifluorescence microscopy (**Figure 4.7**), indicative of cell permeablization.

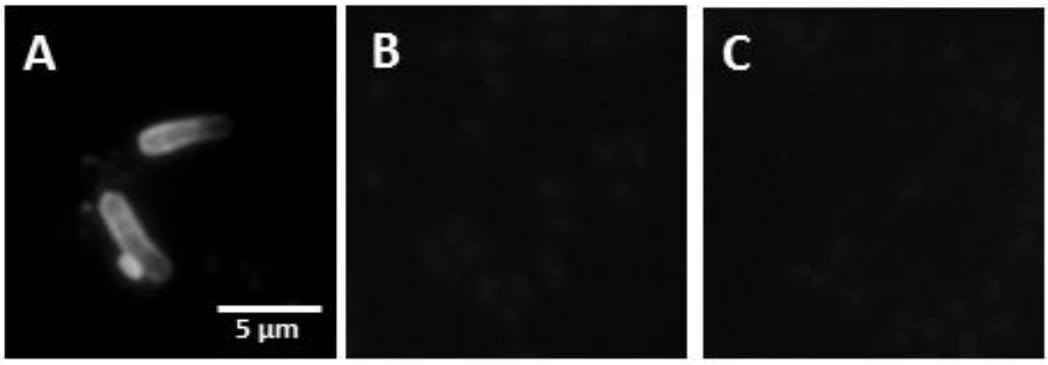

Figure 4.7. Epifluorescence microscopy of the *S.* Typhimurium LT2 cells permeabilized with citric acid. a) Cells incubated with 2 mM citric acid and 2 µM of KZ-EGFP protein; b) Cells incubated with 2 mM citric acid and 2 µM of wild-type EGFP protein; and c) Cells incubated with water and 2 µM of wild-type EGFP protein for 30 min. Cell pellets were then washed twice and visualized using epifluorescence microscopy with a 1500 magnification. This image has been converted to black and white.

4.3.4.3 Lys68 PG digestion mechanism

To assess the Lys68 PG digestion mechanism and explain the activity of the endolysin at low pH, an analysis of its presumed essential catalytic residues was made. Lys68 is classified as a member of the GH24 family (CAZY, 2014), which has a glutamine (Glu) residue as the proton donor. The catalytic nucleophile however is yet unknown. To identify a putative nucleophile, BlastP searches were conducted. Results showed that, besides Glu-18, a second amino acid residue, Thr-35, was highly conserved, which could indicate a role as a putative catalytic residue of Lys68. Mutagenesis of both presumably essential catalytic residues resulted in one inactive enzyme (Glu18Ala) and one enzyme with similar activity (Thr35Ala) compared to the Lys68 wild-type (**Figure 4.8 a**). Analysis of mutated proteins by CD did not provide any evidence for significant structural alterations due to the amino acid replacements (**Figure 4.8 b**). Therefore, the absence of activity was entirely attributed to the Glu18Ala substitution.

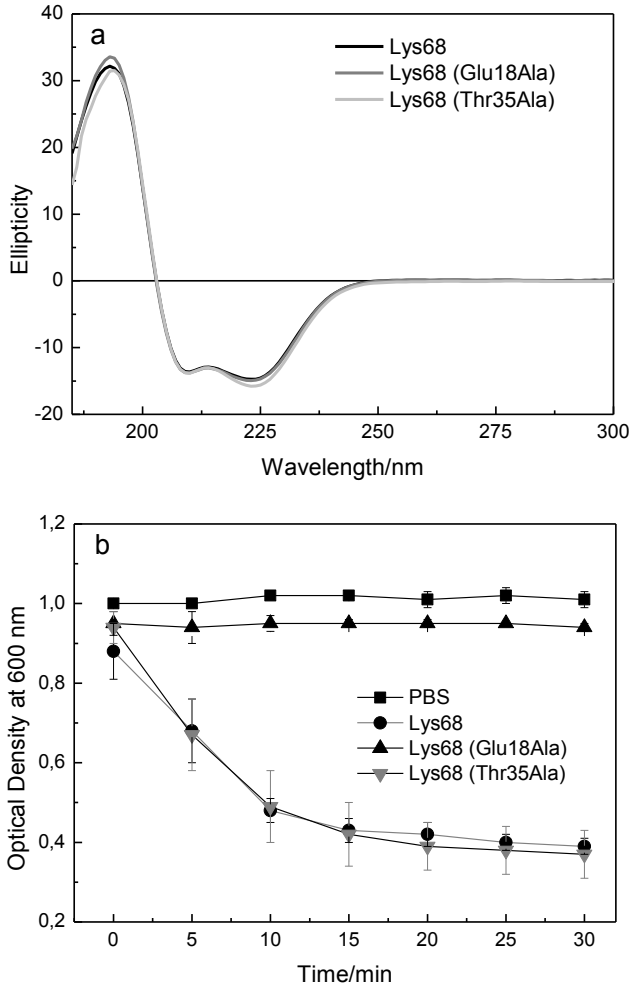

Figure 4.8. Muralytic activity and secondary structure comparisons between Lys68 wild-type and mutant variants. a) Circular dichroism spectra of Lys68 wild-type and the two mutants (Glu18Ala and Thr35Ala). b) Muralytic activity of same proteins on *P. aeruginosa* OM permeabilized cells measured as optical density decrease.

Based on the experimental data, the BlastP results, and the fact that there is no available 3D structure of a Lys68 homolog, a possible second catalytic residue could not be identified. Recently, Wohlkönig and coworkers described the existence of two subgroups within the GH24 family; one that has a Glu-Asp-Thr catalytic triad and another that only consists of Glu as the catalytic residue (Wohlkonig et al, 2010). The amino acid Glu has been shown in a the goose egg-

white lysozyme as the single responsible catalytic residue for the digestion of PG bonds (Weaver et al, 1995). Therefore, it is proposed that Lys68 operates through a two-step mechanism involving Glu-18 (**Figure 4.9**).

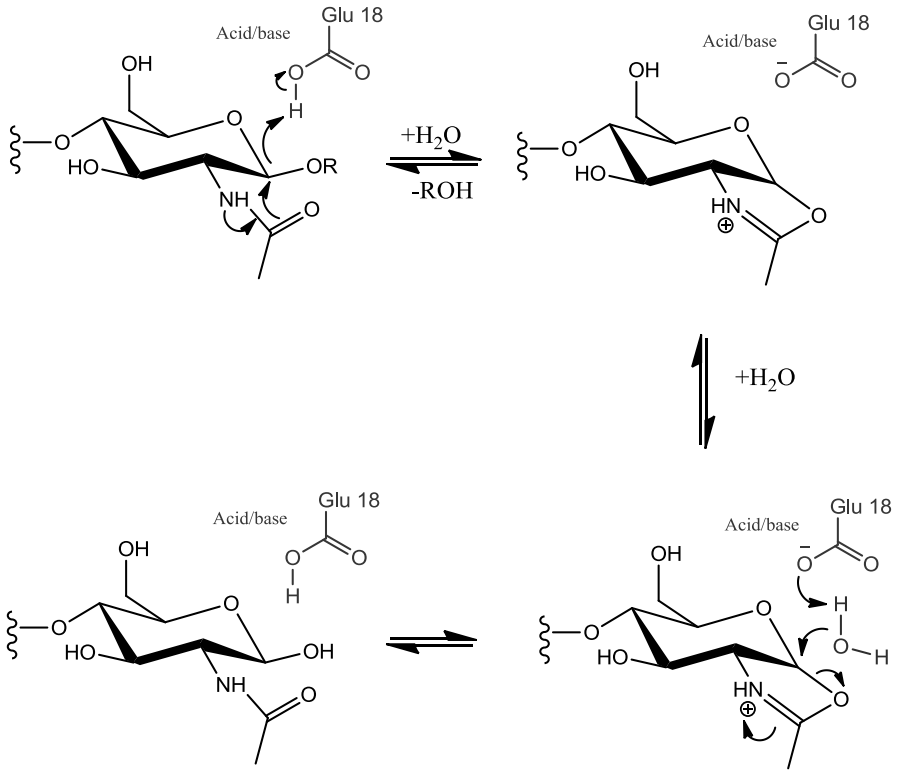

Figure 4.9. Proposed Lys68 mechanism of action. Lys68 hydrolyse the 1,4-linkages between N-acetylmuramic acid and N-acetyl-D-glucosamine, through a two-step mechanism involving Glu-18 catalytic residue to cleave the peptidoglycan.

In the first step N-acetylhexosaminidases, which have an acetamido group, are capable of neighboring group participation to form an intermediate oxazolinium ion, with acidic assistance provided by the Glu-18 carboxylate. In the second step, the now deprotonated acidic carboxylate acts as a base and assists a nucleophilic water to hydrolyze the oxazolinium ion intermediate, giving the hydrolyzed product (through individual inversions that lead to a net retention of configuration).

4.4 Discussion

In recent years, endolysins of phages infecting G^+ bacteria have been extensively studied (Fischetti, 2010). In contrast, G^- phage endolysins have been poorly explored, because the impermeable bacterial OM protects the underlying PG layer from enzymatic hydrolysis by the exogenous endolysin. In this work, a novel endolysin from a G^- infecting phage is described. *In silico* characterization of Lys68 from the *Salmonella* phage phi68 shows elevated protein similarity (>90% identity) to other *Salmonella* phage endolysins belonging to the same lysozyme-like superfamily. The observed globular structure (ECD alone) is also shared by most other G^- phage endolysins, contrary to modular archetypes (ECD and CBD) typically seen in endolysins from a G^+ background (Oliveira et al, 2013).

A biochemical characterization showed that Lys68 displays some interesting characteristics. Regarding substrate specificity, Lys68 degrades the PG of all 20 G^- organisms tested, however it was ineffective against all included G^+ strains, with the exception of *L. monocytogenes*. Consequently, Lys68 displays a broader lytic spectrum than the phage from which was derived from, whose spectrum is limited to *S.* Enteritidis strains (Sillankorva et al, 2010). This broader spectrum is explained by the common PG A1γ chemotype shared by the sensitive G^- species and also *L. monocytogenes*, whereas the remaining insensitive G^+ strains like *Staphylococcus epidermidis* 9142 and *Staphylococcus aureus* 976 presumably have an A3α PG chemotype (Schleifer & Kandler, 1972). This chemotype was previously shown to be resistant to other muralytic enzymes, like HEWL (Archibald AR, 1993). The observed muralytic activity of the globular Lys68 (400 Units/µM) is lower compared to other described modular G^--like endolysins (e.g. KZ144 and EL188 with 2058 and 4735 U/µM, respectively, calculated using the same method) (Walmagh et al, 2012). This can be explained by the fact that the latter two enzymes contain cell wall binding domains that direct the enzymes to the PG substrate, increasing the muralytic activity. Nevertheless, when compared to the

globular HEWL (35 Units/µM, reported elsewhere), Lys68 is 12 times more active (Briers et al, 2007a). In addition to adequate profiles of activity and specificity, antimicrobial enzymes require good structural stability. Therefore the pH effect on the Lys68's conformational stability was characterized. The endolysin's secondary structure showed to be highly conserved between pH values of 4.0 to 10.0. At pH 3.0, more turns and unordered/random coils are formed in Lys68 than at higher pH values. Stability tests showed that Lys68 was more stable around pH 6.0-7.0 (with melting temperatures of 44.7°C and 43.4°C), matching the pH where optimal muralytic activity is observed.

Once subjected to thermostability tests, some endolysins surprisingly maintain their activity after long heating periods. Within endolysins from a G^- background, *Pseudomonas* phage endolysins KZ144 and EL188 activity still remains high after being exposed at 50°C for 10 min (Briers et al, 2007b). In contrast, the phage T4 lysozyme only retains a minor fraction of its activity after a 5 min treatment at 65°C (Nakagawa et al, 1985). Recently, a highly thermostable modular endolysin (PVPSE1gp146) with resistance to temperatures up to 100°C was described (Walmagh et al, 2012). Lys68 is a globular protein where the muralytic activity is only completely inactivated after 30 min at 100°C. Because the melting temperature of the endolysin at pH 7.0 is 44°C, it seems that under the stress caused by higher temperatures, the endolysin is able to gradually regain its secondary structure to a point where, at high temperatures and prolonged exposures, it cannot refold. Recently, a similar folding/refolding mechanism was suggested by Schmelcher and coworkers to explain the high thermostability of the G^+ *L. monocytogenes* phage endolysins, HPL118 and HPL511 (Schmelcher et al, 2012b). In their study, HPL118 and HPL511 retained 35% of activity after 30 min at 90°C.

To allow a better passage of endolysins through the OM, a combinatorial approach was used on G^- bacteria, combining the bacterial cell wall-degrading

enzyme Lys68 or HEWL with an OMP. Both proteins combined with EDTA could reduce *P. aeruginosa* to some extent. A similar effect has been previously described with endolysin EL188 from *Pseudomonas* infecting phage EL only on *P. aeruginosa* strain PAOI (Briers et al, 2011b). The positive effect of EDTA on the antibacterial activity is caused by the powerful OM permeabilization capacity of EDTA through binding and withdrawal of the stabilizing divalent cations Mg^{2+} and Ca^{2+}, present in the LPS layer of the G^- OM (Vaara, 1992). As a result, the bacterial PG becomes more prone to the muralytic activity of the externally added endolysins. However, the sensitivity of other bacterial species to the destabilizing effect of EDTA was much lower, even when EDTA was increased to 5 mM (see **Supplementary Table S4.1**). In seems that the type and structure of the OM plays a key role for the antibacterial efficacy of the enzyme/EDTA combinatorial effect. Possibly, due to the low number of phosphate groups per LPS molecule and the corresponding amount of stabilizing divalent cations in the OM of *Enterobacteriaceae* compared to the *Pseudomonadaceae*, EDTA turns out to be ineffective to the former group. The observed synergetic effects of citric acid and malic acid, has never been described for phage endolysins. In this respect, both citric acid and malic acid had a better permeabilizing effect than EDTA, and were able to permeabilize several G^- strains tested enhancing the activity of Lys68. In particular against exponential *S.* Typhimurium LT2 cells, an even more profound effect was observed when extending the reaction from 30 minutes to 2 hours, although proving to be less efficient against stationary cells and biofilms. The lower efficiency in killing stationary cells can be a result of two aspects; *i)* structural changes in the OM (e.g. LPS biosynthesis), compromising the endolysin entry or LPS permeabilization through the organic acids, or *ii)* chemical modifications in the PG (e.g. glycosylations or acetylations) known to contribute to high levels of resistance to glycosyl hydrolases (Vollmer & Born, 2009; Rolfe et al, 2012). As for biofilms, beside the presence of several bacterial physiological states that can give rise to similar problems, additional diffusion limitations due to

the high density matrix content can hinder the efficacy of endolysins and antimicrobials in general (Mah & O'Toole, 2001). Although the permeabilizing capacity of citric acid by chelating divalent cations from the OM associated with its protonated form has been reported, additional acidity can contribute to OM damage. It has been proposed that the LPS disintegration is accomplished by the ability of undissociated acid groups to interact/pass through the negatively charged LPS (where negatively charged acids are repulsed) and migrate inside the cell to cause sublethal damages (e.g. leading to OM membrane disruption) (Alakomi et al, 2000; Theron & Lues, 2011). The 2 mM of citric acid (pKa 3.13 at 25°C) and 5 mM of malic acid (pKa 3.4 at 25°C) used, caused a drop of pH to 4.2 and 3.8, respectively. Because similar log reduction units were obtained using HCl instead of citric or malic acid combined with Lys68, the acidity effect seems to play a key role in the OM permeabilization. Because millimolar concentrations of these organic acids by themselves did not have antibacterial effect on the cells (with exception of *Pseudomonas*), they seem to be enough to compromise the cell wall to a level that allows Lys68 to act on the PG, causing bacterial death. Recently, a combined treatment with different organic acids to induce cell permeability in *E. coli* O157:H7 was reported (Kim & Rhee, 2013). Transmission electron microscopy images showed clear membrane disintegration that potentiated the bactericidal action of medium-chain fatty acids. When bacterial suspensions were supplemented with 5 mM of $MgCl_2$, the effect of Lys68 combined with organic acids was completely abolished. $MgCl_2$ has the ability to protect the bacterial OM damaged from the acid challenge, an effect already observed in the presence of lactic acid (Alakomi et al, 2000).

Based on the carbohydrate-active enzymes classification, several amino acids have been identified within lysozyme-like proteins to play a key role in the glycosidase reaction (CAZY, 2014). HEWL's (belonging to the GH22 class) active site, which cleaves polysaccharide chains in bacterial cell walls, is constituted essentially by the two amino acids Glu-35 (pKa, 6.1-6.2) and Asp-52 (pKa, 3.4-4.5),

which are only functional if the former is non-ionized and the latter is ionized (Webb et al, 2010). Hence, the absence of enzymatic activity in the presence of malic and citric acid is related to the deionization of Asp52 in an acidic pH. Lys68 has a different catalytic system. Since the Thr-35 mutation did not affect Lys68 antimicrobial activities, it can be concluded that Thr-35 is not involved in the catalysis of PG. Therefore, it is tempting to speculate that Lys68 operates through a two-step mechanism involving Glu-18, capable of digesting the 1,4-linkages between N-acetylmuramic acid and N-acetyl-D-glucosamine residues of the PG in a low pH environment (pH around 4.0) through a retaining mechanism. The catalytic activity of amino acid Glu-73 in the goose egg-white lysozyme has been proved by Weaver and co-workers to be enough to digest the PG bonds (Weaver et al, 1995).

To summarize, G^- bacterial pathogens prevail in various surroundings and their resilience is aided by the presence of an OM that prevents toxic substances from entering the cell. Lys68 demonstrates very good stability properties and its efficient combination with EDTA, citric acid and malic acid could be greatly explored in many fields to combat G^- pathogens. Lys68/EDTA could be used as a therapeutic product to control *P. aeroginosa*, typically present in burn wound infections or as food preservative against *P. fluorescents*. The broad antimicrobial effect of Lys68/citric acid and Lys68/malic acid could be explored in food and clinical settings as an effective sanitizer to prevent food spoilage and nosocomial bacterial infections. Additionally, the powerful effect of Lys68 with the organic acids can be used therapeutically to treat for example topical infections as chronic wounds, when applied in a cream or ointment. Altogether, this study proposes the combination of a bacterial cell wall hydrolase from phage origin (Lys68) with EDTA, citric and malic acid for biotechnological and medical applications to fight G^- pathogens in the agricultural, food and medical industry.

Chapter 5

Activity of an Acinetobacter phage endolysin, ABgp46, against Gram-negative pathogens in planktonic and biofilm cultures

5.1 Introduction

Although chapter 4 demonstrated the efficacy of endolysin/organic acid mixtures to control G^- pathogens, it is important to validate this technology for other endolysins and prove their transversal application. Multidrug-resistant bacteria and biofilms are also important factors that need to be addressed in depth, as most G^- bacteria, like *Pseudomonas* and *Acinetobacter*, are naturally resistant to antibiotics (e.g. low outer membrane permeability) or able to quickly acquire new resistance mechanisms (e.g. horizontal transfer of resistance genes) (Bonomo & Szabo, 2006). Their ability to form biofilms is another important aspect that makes them more tolerant to varied antimicrobial agents (e.g. related to the limited diffusion transport and the presence of different bacterial physiological states) (Mah & O'Toole, 2001).

This chapter describes the isolation of a novel phage-encoded endolysin (ABgp46) and a depolymerase (ABgp42) (part of the tail-fiber), originating from an *Acinetobacter baumannii* phage. Depolymerases are polysaccharide-degrading enzymes encoded by phages that act against the extracellular polymeric substances found in biofilms, increasing their anti-biofilm efficiency (Lu & Collins, 2007; Cornelissen et al, 2011). ABgp46 was first analyzed for its stability under different pH values and then tested against planktonic G^- (antibiotic resistant) bacteria in the presence and absence of OMPs agents. In this chapter, several organic acids were tested (citric, malic, lactic, benzoic and acetic acid) to widen novel synergies with substantial biotechnological interest, and compared with EDTA, as it is the only agent described so far able to act synergistically with endolysins (Walmagh et al, 2012). In the end, it was intended to explore the anti-biofilm endolysin-organic acid-depolymerase activity formula. Endolysin anti-biofilm activity is a field that still remains scarcely explored, with only few successes reported against G^+ *Staphyloccocus* and *Streptococcus* biofilms (Sass & Bierbaum, 2007; Shen et al, 2013).

5.2 Materials and methods

5.2.1 Bacterial strains, bacteriophage and chemicals

Bacterial strains used are listed in **Table 5.1**. Without exceptions, all strains were grown in LB (Liofilchem) at 37°C and 120 rpm. *E. coli* cloning and expression strains (Agilent Technologies, Invitrogen and Merck4Biosciences) are shown in **Table 5.2**. *E. coli* strains BL21-CodonPlus-(DE3)-RIL (30 µg/mL chloramphenicol), BL21-CodonPlus-(DE3)-RP, (30 µg/mL chloramphenicol) and Origami™ 2(DE3) (12.5 µg/mL tetracycline and 50 µg/mL streptomycin) were grown under the specified conditions. *E. coli* Top10 was used for cloning purposes while the remaining strains were used for recombinant expression. *E. coli* strains were transformed as described in chapter 4. *A. baumannii* phage vb_AbaP_CEB1 (encoding the ABgp46 endolysin and the ABgp42 depolymerase part of the tail-fiber) was isolated from waste effluents and belongs to the CEB phage collection.

Table 5.1. Overview of bacterial pathogens strains, references and sources used in chapter 5.

Bacterial strain	Reference(s)	Sources
Salmonella Typhimurium	ATCC 19585 (further designated as LT2)	NA
Pseudomonas aeruginosa	ATCC 15692 (further designated as PAO1)	Infected burn/wounds
Klebsiella oxytoca	ATCC 131821	Pharyngeal tonsil
Acinetobacter baumannii	1*/ 2* / 3* / 4* / 5* / 6* / 7* / 8* / 10*	Infected burn/wounds
Escherichia coli O157:H7	CECT 47821	Human stool

NA - Not available; * strains kindly provided by Hospital de Braga

Table 5.2. Genotypes of *E. coli* cloning and expression strains used in chapter 5.

Bacterial strains	Genotype
TOP10	F$^-$ mcrA Δ(mcrCB-hsdSMR-mrr) Φ80*lacZΔM15* Δ*lac*X74 *recA1 araD139* Δ(*ara-leu*)7697 *galU galK rpsL*(Str^r) *endA1* λ$^-$
BL21(DE3)	F$^-$ *ompT hsdS$_B$(r$_B^-$ m$_B^-$) gal dcm (DE3)*
BL21-CodonPlus-(DE3)-RIL	F$^-$ ompT *hsdS*(r$_B^-$m$_B^-$) *dcm* + Tet^r *gal* λ(DE3) *endA* Hte (*argU ileY leuW Cam^r*)
BL21-CodonPlus-(DE3)-Rp	F$^-$ ompT *hsdS*(r$_B^-$m$_B^-$) *dcm* + Tet^r *gal* λ(DE3) *endA* Hte ([*argU proL Cam^r*)
Origami™ 2(DE3)	Δ *(ara-leu)7697* Δ *lacX74* Δ *phoA PvuII phoR araD139 ahpC galE galK rpsL F'[lac$^+$ lacI^q pro]* (DE3) *gor522::*Tn*10 trxB* (Str^R, Tet^R)

EDTA was acquired from Pronalab while IPTG, HEPES, citric, malic, lactic, benzoic and acetic acid were purchased from Sigma-Aldrich.

5.2.2 *In silico* analysis of endolysins

The endolysin sequence used was screened by the HHpred webserver (URL http://toolkit.tuebingen.mpg.de/hhpred) using Pfam, InterProScan and COG; with an E-value cut-off of 1x10^{-5} and at least 80% of query coverage. The MSA generation method used was HHblits (Remmert et al, 2012). Multiple sequence alignments were generated through ClustalW online (URL http://www.genome.jp/tools/clustalw/).

5.2.3 Cloning, recombinant protein expression and purification

All primers used to clone the ABgp46 endolysin and ABgp42 depolymerase were purchased from Invitrogen. The vector pET15b (Novagen) was used to clone and express both proteins, and has the resistant marker gene for ampicillin (100 µg/mL). Restriction enzymes were purchased from NEB and all DNA cleaning steps were performed using DNA Clean & ConcentratorTM-5k (Zymo Research). All final constructs were verified by sequencing (Macrogen).

5.2.3.1 Cloning methodology

The standard PCR cloning procedure for the ABgp46 endolysin and the ABgp42 depolymerase ORFs into pET15b was carried out as explained in chapter 4. For ABgp46, specific set of primer 5-GGCAGCCATATGATTCTGACTAAAGACGGGTTTAG (forward) and 5- GCAGCCGGATCCCTATAAGCTCCGTAGAGCGC (reverse), with the *Nde*I/*Bam*HI restriction endonuclease sites underlined, and annealing temperature of 55°C, were used in a PCR reaction. As for ABgp42, the primers 5-GGCAGCCATATGATGCACGCTGACCCATGTTGG (forward) and 5-CAGCTGTAAACGTTATCCGTTGCTAAGGATCCGGCTGC (reverse), with the *Nde*I/*Bam*HI restriction endonuclease sites underlined and an annealing temperature of 56°C were chosen.

5.2.3.2 Protein overexpression and purification

Both proteins were cloned in pET15b, making use of the present N-terminal His6 for fused expression. The *E. coli* expression system, purification using Ni^{2+}-NTA chromatography, band purification visualization, dialysis in 10 mM PBS pH 7.2 and protein quantification were carried out as explained previously in chapter 4. Only proteins with a purity higher than 90%, as judged by SDS-PAGE analysis, were considered for *in vitro* studies. *E. coli* BL21(DE3) expression strain and 25 mM imidazole purification stringency were chosen for ABgp46 endolysin expression and purification. For the ABgp42 depolymerase, a set of different optimization parameters (*E. coli* expression strains listed in **Table 5.2**), inducer concentration (from 0.5 to 1.5 mM), expression time (from 4 to 18 h) and temperatures (from 16°C to 37°C) were conducted, however without being able to express the protein.

5.2.4 Biochemical characterization

5.2.4.1 Fluorescence measurements

Intrinsic fluorescence emission spectra of the ABgp46 endolysin were recorded over the 300-400 nm range with a Jasco FP-750 spectrofluorimeter equipped with a Peltier thermostat. An excitation wavelength of 295 nm was used to minimize the mission arising from tyrosine residues. Two µM of protein was used in a universal buffer with pH adjusted from 4.0 to 8.0 and thermal denaturation on monitor heating the sample from 20 to 70°C. The variation of the tertiary structure was analyzed based on parameter a defined as: (IF_{325}/IF_{360}) protein, IF is intensity of fluorescence. These experiments were carried out at the ICRM, the Istituto di chimica del riconoscimento molecolare, in Italy.

5.2.4.2 Circular dicrhoism

Endolysin circular dichroism (CD) spectra were recorded in the Far-UV region (195-260 nm) with a Jasco 600. Thermal denaturation was recorded with 5°C increment steps from 20 to 75°C, using a universal buffer (pH 4.0-8.0). All CD signals were baseline corrected and smoothed with the Spectra Analysis JASCO software. In all cases, a concentration of 8 µM (0.18 mg/mL) was used in an optical path of 0.1 cm. These experiments were carried out at the ICRM, the Istituto di chimica del riconoscimento molecolare, in Italy.

5.2.5 Antibacterial assays

5.2.5.1 In vitro assays on planktonic cells

In vitro assays on planktonic cells were performed as described in chapter 4 with some minor modifications. Mid-exponential phase cells (OD_{600nm} of 0.6),

resuspended and 100-fold diluted in 10 mM HEPES/NaOH (pH 7.2), were prepared. Each culture (50 µL) was incubated for 2 h at room temperature with 25 µL of ABgp46 endolysin (final concentration of 2 µM) together with 25 µL of water or 25 µL or OMPs (EDTA, citric, malic, lactic, benzoic and acetic acid) dissolved in water. The final concentrations used were optimized during this work (see concentrations in **Table 5.5**). As a negative control, 50 µL of cells were incubated with 25 µL of PBS (pH 7.2) (instead of ABgp46) or with 25 µL water (instead or OMPs). Cell counting and antibacterial activity quantification was done as previously described. Averages ± standard deviations are given for n = 4 repeats.

5.2.5.2 In vitro assays on biofilm cells

Overnight bacterial cells were normalized (OD adjusted to 1.0 in LB medium) after which 2 µL of the cell suspension was transferred to 96-well polystyrene plates (Orange Scientific) containing 198 µL of LB. To establish mature biofilms the plate was incubated for 24 h at 37°C and 120 rpms. Afterwards, the culture medium was removed and non-adherent cells were also removed by washing the biofilms twice with 200 µL of 10 mM HEPES/NaOH (pH 7.2). Cells were then incubated for 2 h with 100 µL of HEPES together with 50 µL of ABgp46 endolysin (2 µM final concentration) and 50 µL of the best OMP agent selected (EDTA, citric and malic acid). Optimized final concentrations used were: 0.5 mM, 3.55 mM and 4.55 mM, respectively. As negative controls, cells were incubated with water (instead of OMPs) or incubated with PBS (instead of endolysin). After incubation CFUs were counted in LB agar plates. Again, the antibacterial activity was quantified as the relative inactivation in logarithmic units, as described previously. Averages ± standard deviations are given for n = 4 repeats.

5.3 Results

5.3.1 *In silico* analysis

The *A. baumannii* phage vb_AbaP_CEB1 was previously isolated and sequenced (unpublished data). ORF 46 (referred to as ABgp46), encoding a 185-amino acid protein with a deduced molecular mass of 23.1 kDa, is predicted to act as a peptidoglycan hydrolase. HHpred output shows that ABgp46 belongs to the GH19 of the glycosidase family, a class of enzymes that cleaves the O-glycosidic bond of the bacterial PG. *In silico* analysis through BlastP showed close resemblance to five other endolysins from *Acinetobacter* phages (phiAB2, phiAB3, ABP-01 and ABP-04), with high homology (95%) (**Supplementary Figure S5.1**). ORF 42 encodes the tail-fiber gene and a depolymerase that is part of this gene (referred to as ABgp42). Through HHpred, the depolymerase domain is predicted to consist of 208 amino acids, resulting in a molecular mass of 22.6 KDa, (**Supplementary Figure S5.2**) and resembles a pectate lyase 3 (PF12708) from the Pec lyase clan (CLO268). BlastP analysis did not identify other close related phage proteins.

5.3.2 Recombinant expression and purification

Recombinant expression of ABgp46 endolysin in *E. coli* BL21(DE3) yielded a soluble protein of 20.5 mg/L. The ABgp42 depolymerase encoding domain was expressed under several conditions. However, despite numerous attempts to express the protein in several *E. coli* expression strains (derived from both BL21 and K12 strains) and different induction temperatures (from 37 to 16°C), times (4 to 16 h) and concentrations (1.5 to 0.5 mM IPTG), no protein was expressed. Therefore, the following sections only describe the biochemical characterization and *in vitro* antibacterial assays of the endolysin protein.

5.3.3 Biochemical characterization

An analysis of the ABgp46 secondary and tertiary structure was performed under different pH values, using CD and protein intrinsic fluorescence, respectively. This exploratory characterization was used to understand the prospect of a hurdle approach using ABgpL46 and OMPs, especially at low pH. Finding a stable endolysin under these conditions would enable possible combinations with organic acids, as an antibacterial formula for clinical or food application against G^- bacterial pathogens.

5.3.3.1 Circular dicrhoism analysis

With CD measurements, the ABgp46 secondary structure was monitored. The CD spectra of ABgp46 was analyzed as a function of pH with a universal buffer with a pH adjusted from 4.0 to 8.0 (**Figure 5.1**).

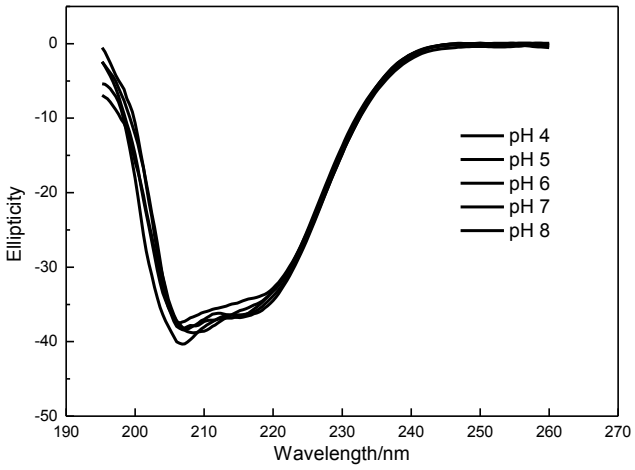

Figure 5.1. Far-UV Circular dichroism spectra of ABgp46 under different pH values (4.0-8.0).

The signal minima around 208 and at 220 nm that prevail in the far-UV CD spectra, is indicative of α-helices in this protein. Unfortunately, due to signal noise generated in far-UV, CD spectra could only be recorded from 260 to 200 nm and, subsequently, it was not possible to estimate the content of the α-helice, β-sheet, turns and unordered structures and compare these results with the data obtained for the Lys68 endolysin. Ellipticity overlapping signatures indicate an unchanged protein secondary structure. To determine more in depth the enzyme's conformational stability, a thermal treatment was employed by increasing temperature (5°C steps between 20 to 70°C) of the protein solution at different pH values. Secondary structure changes were analyzed by monitoring CD intensity at 222 nm where α-helix structures show a negative peak and the melting temperatures (T_m) at which the enzyme underwent a secondary structure are shown in **Table 5.3**.

Table 5.3. Apparent melting temperatures (T_m) of ABgp46 as a function of pH (4.0-8.0) and temperature monitored by Circular dichroism intensity at 222 nm. Possible renaturation cycles were not monitored due to protein aggregation above T_m.

pH	T_m (Denaturation cycle)	T_m Observations
4	40-45°C	Not aggregated
5	45-50°C	Aggregated
6	45-50°C	Aggregated
7	45-50°C	Aggregated
8	45-50°C	Aggregated

No differences were observed in the pH range 5.0-8.0, where all T_m were recorded as being between 45-50°C. Unfortunately, it was not possible to determine the precise value of T_m because the spectropolarimeter employed was not equipped with a thermostat that allows a variation of the temperature with a constant rate. At temperatures above T_m secondary structure changes caused protein aggregation. At pH 4.0, a clear shift of T_m, between 40-45°C, was observed

indicating a less favourable condition to maintain the secondary structure integrity. Interestingly, this was the only pH where protein aggregation did not occur.

5.3.3.2 Fluorescence measurements

Similarly to CD, the fluorescence spectra of ABgp46 were obtained at different pH values and temperatures in order to analyse changes in tertiary structure. Taking advantage of the two Tryptophans (Trp-95 and Trp-135) present in the sequence, an excitation wavelength of 295 nm was used, minimizing the contribution of tyrosine fluorescence. As an indication of significant tertiary structure changes, Trp fluorescence shifts were analyzed using the Parameter A defined as the IF_{325}/IF_{360} ratio (where IF equals to the intensity of fluorescence) (**Figure 5.2**).

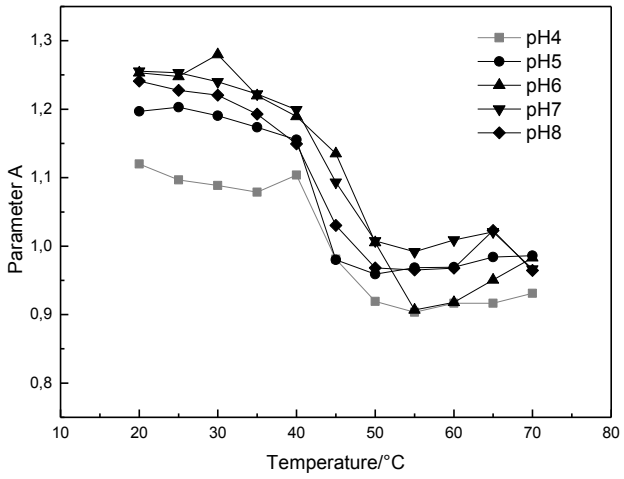

Figure 5.2. Correlation between fluorescence spectra and conformational changes deduced by plotting Parameter A as a function of temperature.

Increasing the temperature from 20 to 70°C, parameter A showed an analogous trend for all pH values, where a sudden signal shift was identified between 40 to 50°C. Such spectral variations are typically observed when the medium that

surrounds the fluorophore differs in polarity and/or as a consequence of conformational changes. Based on CD and parameter A data, it is likely that secondary and tertiary structure changes are happening when the protein is heated from 40°C to higher temperatures, resulting in an unfolded and denatured protein.

5.3.4 *In vitro* antibacterial activity

5.3.4.1 ABgp46 against planktonic cells

The *in vitro* antibacterial activity of the recombinant Abgp46 was investigated on a wide set of G^- strains (**Table 5.4**).

Table 5.4. Antibacterial activity of ABgp46 against several Gram-negative bacterial pathogens. Marked in bold are significant log reduction units observed (≥ 1 log).

Bacterial Species	ABgp46/Water	Patterns of antibiotic resistance*
***Pseudomonas aeruginosa* PAOI**	0.03 ± 0.02	NA
***Salmonella* Typhimurium LT2**	0.14 ± 0.05	NA
***E. coli* O157:H7 CECT 4782**	0.17 ± 0.12	NA
***Cronobacter sakazakii* CECT 858**	0.23 ± 0.26	NA
***Klebsiella oxytoca* ATCC 13182**	0.18 ± 0.13	NA
Acinetobacter baumannii 1	**1.77 ± 0.06**	Resistant to 13 out of 18 tested antibiotics
Acinetobacter baumannii 2	**0.93 ± 0.25**	NA
Acinetobacter baumannii 3	0.43 ± 0.61	Resistant to 14 out of 18 tested antibiotics
Acinetobacter baumannii 4	**1.00 ± 0.32**	NA
Acinetobacter baumannii 5	0.81 ± 0.21	NA
Acinetobacter baumannii 6	0.51 ± 0.68	NA
Acinetobacter baumannii 7	0.18 ± 0.11	Resistant to 14 out of 18 tested antibiotics
Acinetobacter baumannii 8	0.37 ± 0.39	Resistant to 11 out of 18 tested antibiotics
Acinetobacter baumannii 10	**1.20 ± 0.46**	Resistant to 11 out of 18 tested antibiotics

*Patterns of antibiotic resistance was provided by Hospital de Braga and were based on susceptibility tests performed according to the NCCLS for antibiotic resistance; NA - not available

The activity of 2 µM Abgp46 alone on tested cells was insignificant as expected, with the exception of *A. baumannii* strains. Interestingly, some *Acinetobacter* strains were sensitive to the endolysin, causing a log reduction units of viable cells, from 0.18±0.11 (lowest effect) to 1.77±0.06 (highest effect), including strains resistant to several antibiotics.

5.3.4.2 ABgp46/OMP formula against planktonic cells

To broaden and enhance the antimicrobial effect of the Abgp46 to other G^- pathogens, the previous unsensitized *E. coli* O157:H7 CECT 4782 was chosen as a model strain, to test and optimize an ABgp46/OMP formula. In addition to the previously characterized OMPs citric and malic acid, other organic agents were used (lactic, benzoic and acetic acid) to sensitize the G^- OM to the endolysin. Each OMP was used in different concentrations (to achieve three distinct reaction pH values of 7.0, 5.5 and pH 4.0) and combined with ABgp46 to assess the best antibacterial condition after 2 h incubation (illustrated in **Table 5.5**). At pH 7.0, only the ABgp46/citric acid was able to reduce *E. coli* cells (0.86±0.38 logs). At pH 5.5, the effect was broadened to ABgp46/citric acid, ABgp46/malic acid and ABgp46/lactic acid mixtures reducing approx. 1 log of *E. coli* cells. Consistently, the effect was more pronounced at pH of 4.0. The combinatorial effects of ABgp46/citric acid, ABgp46/malic acid and ABgp46/lactic acid mixtures resulted in 2.98±0.77, 2.18±0.82 and 0.98±0.58 log reductions. In this condition, the antibacterial effect was also extended to ABgp46/benzoic acid inactivating approx. 1 log of *E. coli* cells. The ABgp46/acetic acid combination only had a moderate effect (0.42±0.29).

Taken into account the most efficient conditions tested, ABgp46/OMPs mixtures (OMPs concentrations used to achieve a pH of 4.0) were tested in the presence of 5mM $MgCl_2$. $MgCl_2$ provides an extra source of available divalent cations (Mg^{2+}) that can link to the LPS negatively charged phosphate groups, strengthening the

LPS monolayer. Therefore, as expected, the addition of 5 mM of $MgCl_2$ abolished the activity of all ABgp46/OMP combinations.

Table 5.5. Combinatorial antibacterial activity of ABgp46 with outer membrane permeabilizers under different concentrations against *E. coli* O157:H7. For a specific pH, different concentrations (given in mM) of EDTA, citric, malic, lactic, benzoic and acetic acid are used in combination with 2 µM of ABgp46 to reduce *E. coli* O157:H7 cells in presence or absence of 5 mM of $MgCl_2$. Marked in bold are significant log reduction units observed (≥ 1 log).

pH	OMPs	Molarity (mM)	PBS/OMPs	ABgp46/OMPs	ABgp46/OMPs + 5mM $MgCl_2$
7.0 ± 0.1	EDTA	0.50	0.27 ± 0.11	0.32 ± 0.15	-
	Citric	0.36	0.21 ± 0.14	**0.86 ± 0.38**	
	Malic	0.60	0.24 ± 0.11	0.53 ± 0.28	
	Lactic	1.20	0.24 ± 0.14	0.55 ± 0.31	
	Benzoic	1.20	0.26 ± 0.15	0.49 ± 0.34	
	Acetic	1.20	0.25 ± 0.14	0.53 ± 0.30	
5.5 ± 0.1	Citric	1.50	0.20 ± 0.13	**1.55 ± 0.45**	-
	Malic	3.30	0.17 ± 0.14	**1.13 ± 0.39**	
	Lactic	3.45	0.31 ± 0.07	**0.95 ± 0.14**	
	Benzoic	3.55	0.27 ± 0.13	0.44 ± 0.33	
	Acetic	4.35	0.26 ± 0.12	0.21 ± 0.22	
4.0 ± 0.1	Citric	3.65	0.28 ± 0.06	**2.98 ± 0.77**	0.15 ± 0.04
	Malic	4.55	0.24 ± 0.18	**2.18 ± 0.82**	0.10 ± 0.03
	Lactic	8.00	0.27 ± 0.18	**0.98 ± 0.58**	0.15 ± 0.04
	Benzoic	10.00	0.57 ± 0.58	**1.08 ± 0.57**	0.02 ± 0.03
	Acetic	20.00	0.22 ± 0.08	0.42 ± 0.29	0.11 ± 0.10

After optimizing, citric acid (at 3.65 mM) and malic acid (at 4.55 mM) were selected as the best OMPs to be combined with ABgp46. Therefore, their synergistic effect was further tested on the remaining unsensitized G^- strains tested earlier and compared with the gold standard EDTA (at 0.5 mM) (**Table 5.6**).

Table 5.6. Combinatorial antibacterial activity of the best ABgp46/outer membrane permeabilizers (EDTA, citric and malic acid) formula against broad range of planktonic Gram-negative pathogens. Marked in bold are significant log reduction units observed (≥ 1 log). * the detection level of 10 CFU/mL has been reached.

Bacterial Species	ABgp46/EDTA	ABgp46/Citric	ABgp46/Malic
***Acinetobacter baumannii* 2**	**>5.50***	**>5.50***	**>5.50***
***Pseudomonas aeruginosa* PAOI**	**>5.50***	**>5.50***	**>5.50***
***Salmonella* Typhimurium LT2**	0.57 ± 0.20	**4.94 ± 0.39**	**4.27 ± 0.69**
Cronobacter sakazakii CECT 858	**1.21 ± 0.38**	**2.10 ± 0.59**	**0.98 ± 0.53**
***Klebsiella oxytoca* ATCC 13182**	0.26 ± 0.48	**0.96 ± 0.35**	0.81 ± 0.12

No surviving *P. aeruginosa* and *A. baumannii* cells could be detected after coincubation with the ABgp46 in the presence of all OMPs. In addition, *S.* Typhimurium (up to 4.94±0.38 log) was almost completely eradicated when citric or malic acid was used. Lower, but still significant reductions, ranging from 1 to 3 logs, were observed against *Cronobacter sakazakii*. In case of *Klebsiella oxytoca*, only the ABgp46/citric acid and ABgp46/malic acid combinations showed a bactericidal effect with log reductions of 0.96±0.35 and 0.81±0.12 viable cells, respectively. Overall, a powerful antibacterial effect was observed when ABgp46 is combined with selected OMPs, and its effect was found to be even more pronounced in the presence of citric or malic acid than when the chelating agent EDTA was used.

5.3.4.3 ABgp46/OMP formula against biofilms

Given the high synergetic antibacterial effect observed with the ABgp46/OMP optimized formula, experiments were conducted to test its efficiency against biofilms (**Table 5.5**). Diffusion limitations are known to arise readily in biofilm systems because fluid flow is reduced. Additionally, several types of bacterial physiological state are found in the biofilms. Both diffusion limitations and

different physiological states are well-known aspects that reduce the effectiveness of antimicrobials against biofilms. To anticipate these circumstances and improve the antimicrobial efficiency, a depolymerase, encoded by the same *Acinetobacter* phage vb_AbaP_CEB1, was intended to be used. As no protein was expressed, as was mentioned before, biofilms antibacterial studies were conducted by incubating ABgp46/OMP mixtures against *A. baumannii* 2 and *P. aeruginosa* PAOI biofilms for 2 hours (**Table 5.7**).

Table 5.7. Combinatorial antibacterial activity of the best outer membrane permeabilizers in absence (A) and presence (B) of ABgp46 against *A. baumannii* 2 and *P. aeruginosa* PAOI biofilms.

A	Bacterial Species	PBS/EDTA	PBS/Citric	PBS/Malic
	***Acinetobacter baumannii* 2**	0.05 ± 0.01	0.08 ± 0.11	0.24 ± 0.19
	***Pseudomonas aeruginosa* PAOI**	0.14 ± 0.01	0.20 ± 0.10	0.21 ± 0.13

B	Bacterial Species	ABgp46/EDTA	ABgp46/Citric	ABgp46/Malic
	***Acinetobacter baumannii* 2**	0.48 ± 0.28	0.20 ± 0.11	0.19 ± 0.05
	***Pseudomonas aeruginosa* PAOI**	0.32 ± 0.26	0.10 ± 0.14	0.54 ± 0.06

The results demonstrate an absence of killing effect when OMPs were added alone to both bacteria. When ABgp46 was combined with OMPs, a slight improvement was observed, although still with an insignificant effect. No major differences were observed when ABgp46 was combined with citric or malic acid that on average, were only able to reduce 0.3 to 0.5 log of both *A. baumannii* and *P. aeruginosa* cells.

5.4 Discussion

G^- bacterial infections have always been a threat to human health. In particular, infections caused by antibiotic resistant bacteria are problematic and their incidence is constantly reported worldwide. Phage-encoded endolysins represent one promising avenue of investigation to fight all these pathogens. After cloning the ABgp46 endolysin, this protein was easily overexpressed in the *E. coli* BL21(DE3) strain. For the heterologous production of the anti-biofilm-degrading depolymerase, production efforts remained unsuccessful in several *E. coli* expression strains. As no obvious solubility issues, hydrophobic regions or low *E. coli* codon usage were detected, other expression systems rather than *E. coli* should be considered in the future.

A biochemical characterization of ABgp46 was carried out in order to evaluate its potential applications with organic acids to overcome the most obvious limitation - the presence of a bacterial OM diffusion barrier. CD and fluorescent analysis showed that pH changes from 4.0 to 8.0 do not have much influence on the structure of ABgp46. As for the absence of aggregation only observed at pH 4.0, it is possible that positively charged amino acids are repulsing protein interactions avoiding aggregation.

Regarding the potential use of ABgp46 as an antimicrobial compound, the enzyme was first tested without the help of any permeabilizer. Interestingly, despite the present of the OM protecting the PG layer, externally added ABgp46 was active against several *Acinetobacter* strains, including antibiotic-resistant phenotypes, suggesting that the protein can intrinsically destabilize its OM. This is a rare event reported for endolysins. The T4 lysozyme (from the T4 phage), was the first endolysin described to naturally kill G^- cells. It was proved that its C-terminal positively charged amphipathic α-helix (named α-4) is responsible to cause OM disruption, having a stronger bactericidal effect than the enzymatic PG hydrolysis (During et al, 1999). Later, endolysins Lys1521 (from a *B. amyloliquefaciens* phage)

and LysAB2 (from *A. baumanni* phage) were also reported to spontaneously inactivate G^- cells. In these cases, it is assumed that their C-terminal side, rich in positively charged amino acids surrounded with hydrophobic residues, interact with the bacterial LPS. However, in opposite synthetic α-4 of the T4 lysozyme bactericidal effect observed, studies conducted showed that Lys1521 and LysAB2 C-terminal region does not have an antibacterial effect themselves, but rather mediate the N-terminal enzymatic domain to enter the cells, allowing them to digest the PG and cause bacteriolysis (Morita et al, 2001; Lai et al, 2011). More recently, the endolysin OBPgp279 (from *A. baumanni* and *P. fluorescens* phages, respectively), was shown to lyse *Pseudomonas* cells (Walmagh et al, 2012), although no predicted mechanism was identified. In all cases, it seems that when endolysins are able to spontaneously kill G^- bacteria (without any OMP), they only have a moderate effect, reducing an approximately 1 log of viable cells. This effect was also observed for ABgp46, able to reduce on average 1 log of *Acinetobacter* strains. Because this enzyme has 96% identity to the previously characterized LysAB2 (see the **Supplemental Figure S5.1**), the same C-terminal amphipathic region (amino acid sequence between 112 and 145) identified can explain its spontaneous activity against *Acinetobacter* cells.

To improve the antibacterial activity, ABgp46 was combined with different OMP agents and concentrations (citric, malic, lactic, benzoic and acetic acid). Consistently, an increasing antibacterial effect was observed using OMPs at higher concentrations, reaching a maximum at low pH (4.0). Interestingly, besides CD and fluorescence analyses predicting low structural stability at pH 4.0, the endolysin muralytic activity is not compromised at the same pH, when combined to the organic acids. As for the OM permeabilization mechanism, the relation between low pH and an antibacterial effect suggests an acidity promoted killing effect. However, different Abgp46/OMP outcomes, under the same condition (at pH 4.0), were observed. Several aspects can individually potentiate the OM-destabilizing effect: *i*) pKa of each acid, which will determine the percentage of deprotonated

(undissociated) and protonated (dissociated) acid groups available outside de cells. Only the undissociated forms are able to migrate inside the cells. Intracellularly, acids dissociate (intracellular pH (≈7.2) is more alkaline than the extracellular pH) and high anion and proton concentrations will compromise/inhibit several cellular reactions, among which, the OM stabilization/maintenance; *ii*) the level of hydrophobicity of the undissociated groups, that will also influence their translocation through LPS hydrophobic interactions to become toxic; *iii*) the different accumulation of the anions groups that will inhibit specific types of cellular reactions, compromising the cells in a different extent (Roe et al, 1998; Alakomi et al, 2000; Breidt et al, 2004). Because the following bactericidal decreasing effect was observed: citric acid (pKa 3.13) > malic acid (pKa 3.4) > lactic acid (pKa 3.86) ≈ benzoic acid (pKa 4.19) > acetic acid (pKa 4.76) when combined with the endolysin, we speculate that this is a reflection of acid dissociation constant (pK_a) increase. This is somehow unexpected, as increasing the pKa favours undissociated groups that could penetrate into the cytoplasmic membrane potentiating cell damage. In opposite, acids with low pKa values would produce more hydrogen ions (not able to internalize) when exposed to an aqueous environment. Nevertheless, a similar trend was observed when organic acids (with lower pKa values) were incubated with medium-chain fatty acids (Kim & Rhee, 2013). These authors speculated that the medium-chain fatty acid action, suggested to interact with the bacterial cell membranes, results in sublethal injuries allowing hydrogen ions to pass into the cell and achieve a marked bactericidal effect. Maybe a similar mechanism is happening in the presence of ABgp46, explaining why ABgp46/citric acid and ABgp46/malic acid are better combinations than when ABgp46 is combined with lactic, benzoic or acetic acid. Additionally, the chelating properties only observed in citric and malic acid will likely empower the LPS destabilization compared to the remaining non-chelating acids. Indeed, the entire antibacterial effect was abolished when the ABgp46/OMP formula was applied in presence of 5 mM of

$MgCl_2$. Addition of an extra source of the divalent cation Mg^{2+} will strengthen the electrostatic interactions between neighbouring LPS components, that seem to avoid acid entry and sequential sublethal damage, and protects the LPS network from the putative chelation effect.

After narrowing down an initial large list of OMP candidates, EDTA, citric acid and malic acid were selected for further testing against a larger group of G^- cells. ABgp46/EDTA revealed to be only efficient to *Pseudomonas and Acinetobacter* cells, although eradicating the cultures within 2 hours. Compared with EDTA, the combinations of citric acid and malic acid with ABgp46 had a more powerful and broaden effect, with an antibacterial effect on all tested strains. The same pattern was previously observed with Lys68 in chapter 4. As mentioned before, while EDTA acts as a chelating agent, sequestering LPS-stabilizing divalent cations, organic acids are predicted to destabilize the bacterial OM by an acidic effect, probably by lowering the bacterial internal pH and the accumulation of toxic substances (sublethal injury) (Alakomi et al, 2000; Theron & Lues, 2011). *P. aeruginosa* is known to have an LPS with a high phosphate content and consequently a higher concentration of stabilizing divalent cations, increasing the electrostatic interaction that contributes to LPS stability (Nikaido, 2003). Cation-binding sites are therefore both the strength and the weakness of the *P. aeruginosa* LPS layer. On the other hand, *Enterobacteriaceae*, such as *E. coli* and *S.* Typhimurium, are known to have a lower phosphorylation degree in LPS, compensated by increased hydrophobic packing of the lipid A moiety (Nikaido, 2003). Therefore one could speculate that this variation might explain the specific EDTA action against *Pseudomonas* and *Acinetobacter* cell wall, which seems to be more prone to a chelation effect.

Regarding biofilm control, diffusion limitations represent one of the major hurdles to commonly applied antimicrobials. No antibacterial activity could be detected against *A. baumanni* and *P. aeruginosa* biofilms when ABgp46 was combined with

EDTA, citric acid or malic acid. As mentioned before, besides the obvious diffusion problems, several types of bacterial physiological states are found in biofilms (Mah & O'Toole, 2001). This physiological heterogeneity can contribute to higher resistance to the endolysin/OMP mixtures. For instance, if a higher amount of stationary cells is found, they will possess different OM composition (LPS and PG chemical modifications), compromising the endolysin entry or LPS permeabilization through the OMPs (Rolfe et al, 2012). Also the wide range of physiological states found in biofilms can favour phenotypes known to activate acid tolerance systems (e.g. consuming or removing excess of protons by decarboxylation reactions and ion transporters, changing membrane composition), protecting themselves from the organic acids OM-destabilization (Warnecke & Gill, 2005). Altogether, these results indicate that ABgp46 is an effective endolysin against several planktonic G^- bacteria, including multiple drug-resistant bacteria, in presence of weak acids. Achieving better performance against biofilms, by completing the formulation with an efficient anti-biofilm compound (using polysaccharides-degrading compounds such as a phage-encoded-depolymerases or synthetic sodium periodate), will turn this technology even more appealing as a therapeutic/disinfectant agent to control these pathogens.

Chapter 6

Chimeric endolysins for better antibacterial performance

6.1 Introduction

Endolysins, when externally administered to G^- bacterial cells, are hampered in their function to degrade the PG due to the presence of a protective OM. The LPS, the major component of the OM, is the most important structure that provides diffusion limitations for many external agents, like endolysins (Delcour, 2009). Apart from the use of OMPs (described elsewhere in this thesis) or high hydrostatic pressure treatments (Nakimbugwe et al, 2006; Briers et al, 2008) to permeabilize the OM to endolysins, the covalent modification of endolysins with LPS-destabilizing peptides could be an alternative approach. As mentioned before, ionic and hydrophobic interactions represent the major LPS-stabilizing forces (Vaara, 1999; Nikaido, 2003). Consequently, tagging peptides of polycationic, hydrophobic or amphipathic nature, known to interfere with these stabilizing forces, could assist endolysins to spontaneously penetrate this barrier and become active antimicrobials.

In parallel, using G^--like endolysins to attack G^+ bacteria has received less attention. In theory, endolysins are also able lyse G^+ bacteria that share the same A1γ PG chemotype as their G^- counterparts. *L. monocytogenes,* an important foodborne pathogen, is an example that contains this PG (Schleifer & Kandler, 1972). *Listeria* phage endolysins, known for their modular structure, have CBDs described to be essential for their muralytic activity and specificity towards *Listeria* PG (Loessner et al, 2002; Schmelcher et al, 2011; Eugster & Loessner, 2012). It is expected that G^--like endolysins will also be active against *Listeria* cells and their activity improved by inserting these specific CBDs.

This chapter describes an engineered-class of endolysins (PVP-SE1gp146 and Lys68) fused to LPS-destabilizing peptides (chimeric PVP-SE1gp146) or to CBDs (chimeric Lys68) to fight G^- or G^+ (*L. monocytogenes*), respectively. The list of LPS-destabilizing and CBD peptides used in the work reported herein is listed in **Table 6.1**.

Table 6.1. **List of selected LPS-destabilizing/Cell binding domain fusion peptides**. For each peptide, their amino acid sequence and literature reference are depicted. LPS-destabilizing peptides can either have a polycationic, hydrophobic, amphipathic nature. Cell binding domains (CBDs) here described recognize specific *Listeria* serovars and come from different *Listeria* phage endolysin sequences.

Peptide	Physiochemical property	Amino acid sequence	Reference
LPS-destabilizing			
α 4-helix of T4 lysozyme	Amphipathic	PNRAKRVITTFRT	(Matthews & Remington, 1974)
Lycotoxin1	Amphipathic	IWLTALKFLGKHAAKKLAKQQLSKL	(Yan & Adams, 1998)
Parasin1	Amphipathic	KGRGKQGGKVRAKAKTRSS	(Park et al, 1998)
PP	Hydrophobic	FFVAP	(Ibrahim et al, 1994)
PK*	Polycationic	KRKKRKKRK	Patent WO/2010/149792
ArtiMW1*	Hydrophobic	GFFIPAVILPSIAFLIVP	Walmagh, unpubllshed
ArtiMW2*	Amphipathic	GKPGWLIKVALKFKKLIRRPLKRLA	Walmagh, unpubllshed

	Serogroups that recognize	From endolysin (protein ID)	Reference
Cell binding domain			
CBDP35	1/2, 3, 4, 5 and 6	YP_001468812.1	(Schmelcher et al, 2010)
CBDP40	1/2, 3, 4, 5 and 6	YP_002261442.1	(Schmelcher et al, 2010)
CBD500	4, 5 and 6	YP_001468411.1	(Schmelcher et al, 2010)

*randomly designed peptides at the Artilysins™ company;

Abbreviations: PP, pentapeptide; PK, polycationic peptide.

PVP-SE1gp146 is a previously characterized modular *Salmonella* phage endolysin (Walmagh et al, 2012). This domain configuration is rare among G^--like endolysins and is associated with a high enzymatic activity. Addition of 0.5 mM EDTA turns this enzyme active against multi-drug resistant G^- bacteria. Due to these features, PVP-SE1gp146 is an optimal candidate for covalent modification tests to further improve its activity. To construct chimeric PVP-SE1gp146 proteins with enhanced activity, several fusion patterns with (putative) LPS-destabilizing peptides were chosen based on their: *i*) peptide length; *ii*) anti-G^- activity and *iii*) cationic, hydrophobic and amphipathic nature. Based on this rational, the cationic peptide

(PK) was designed to permeabilize G^- OM by competing with/displacement of the LPS stabilizing cation-binding sites. The hydrophobic peptides (PP and ArtiMW1) are able to increase OM permeabilization by destabilizing the lipid A acyl chain-phospholipid hydrophobic stacking (Nikaido, 2003). The PP peptide was previously fused to HEWL, enhancing its activity towards G^- cells (Ibrahim et al, 1994). Finally, anti-G^- active peptides (Lycotoxin1, Parasin1 and α4) and the newly designed ArtiMW2, are small, linear amphipathic peptides that tend to promote the formation of membrane pores. Lyxotoxin1 is a strong haemolytic, membrane pore forming peptide, isolated from the venom of the Wolf Spider *Lycosa carolinensis* (Yan & Adams, 1998). Parasin1 is a peptide with a wide antimicrobial spectrum and low haemolytic activity, isolated from a catfish *Parasilurus asotu* (Park et al, 1998). The α4-helix of T4 lysozyme has a strong membrane disruption mechanism that seems to be more active than the PG degradation bactericidal effect of the T4 lysozyme (During et al, 1999).

For chimeric Lys68 proteins, CBDs belonging to listerial phage full-length endolysins (PlyP35, PlyP40 and Ply500) were selected as fusion patterns (**Table 6.1**) to direct and increase endolysin activity towards *Listeria* cells. These CBD are known to confer species- and serovar-specificity to their corresponding endolysins. While CBDP35 and CBDP40 are able to recognize a larger group of *Listeria* cells, the CBD500 only confers ligands recognition of serovars belonging to groups 4, 5 and 6 (Schmelcher et al, 2010). As mentioned before the presence of a CBD can lower, maintain or increase the full-length endolysin activity and this effect is protein-dependent (Oliveira et al, 2012). Therefore, besides conferring specificity towards *Listeria*, it was intended to evaluate if the presence of an extra CBD would increase the Lys68 muralytic activity (i.e. achieve a steeper slope of a resulting lysis curve that measures optical density in function of time - translated in a higher killing capacity), as observed with modular G^--like endolysins (Walmagh et al, 2012).

6.2 Materials and methods

6.2.1 Bacterial strains, bacteriophage and chemicals

All bacterial strains used in the work described in this chapter are listed in **Table 6.2**. With no exceptions, all strains were grown in LB (Liofilchem) at 37°C and 120 rpm. *E. coli* cloning and expression strains (Invitrogen, Stratagene or Novagen) are listed in **Table 6.3**. BL21-CodonPlus-(DE3)-RIL and XL1-Blue MRF' were both grown in 30 µg/mL chloramphenicol. *Salmonella* phage phi68 (encoding the Lys68 endolysin) and the *Salmonella* phage PVP-SE1 (encoding the PVP-SE1gp146 endolysin) were isolated from waste effluents and belong to the CEB phage collection. EDTA was acquired from Pronalab while IPTG and HEPES were purchased from Sigma-Aldrich.

Table 6.2. Overview of bacterial pathogens strains, references and sources used in chapter 6.

Bacterial strain	Reference(s)	Sources
Salmonella Typhimurium	ATCC 19585 (further designated as LT2)	NA
Pseudomonas aeruginosa	ATCC 15692 (further designated as PAO1)	Infected burn/wounds
Escherichia coli	XL1-Blue MRF’	Agilent commercial stain
Listeria inocua	CECT 4030	NA
Listeria ivanovii	CECT 5375	Goat
Listeria seeligeri	CECT 5339	Animal faeces
Listeria welshimeri	CECT 5371	NA
Listeria monocytogenes	CECT 5725 / CECT 5873 / CECT 938 / CECT 911 / CECT 933 / CECT 934 / CECT 937 7 CECT 936 / CECT 4031 / 923* / 994*	Chicken; 4c / NA / NA / Spinal fluid of man with cerebrospinal meningitis / Human / Brain of sheep with circling disease / 15 day old child / NA / Rabbit / Canning / Goat Milk

NA - Not available; * strains belonging to the CEB bacterial collection

Table 6.3. Genotypes of *E. coli* cloning and expression strains used in chapter 6.

Bacterial strains	Genotype
TOP10	F$^-$ mcrA Δ(mcrCB-hsdSMR-mrr) Φ80*lac*ZΔ*M15* Δ*lac*X74 *recA1 araD139* Δ(*ara-leu*)7697 *galU galK rpsL*(Str^r) *endA1* λ$^-$
JM109	endA1 glnV44 thi-1 relA1 gyrA96 recA1 mcrB$^+$ Δ(lac-proAB) e14- [F' traD36 proAB$^+$ lacI^q lacZΔM15] hsdR17($r_K^-m_K^+$)
BL21(DE3)	F$^-$ *ompT hsdS$_B$*(r_B^- m_B^-) *gal dcm (DE3)*
BL21-CodonPlus-(DE3)-RIL	F$^-$ ompT *hsdS*($r_B^-m_B^-$) *dcm* + Tet^r *gal* λ(DE3) *endA* Hte (*argU ileY leuW Cam^r*)
XL1-Blue MRF'	Δ(*mcrA*)*183* Δ(*mcrCB-hsdSMR-mrr*)*173 endA1 supE44 thi-1 recA1* gyrA96 relA1 lac *[F'* proAB lacI^{q}ZΔM15 *Tn*10 *(Tet^r)]*

E. coli Top10 and JM109 were used for cloning purposes. All strains, except *E. coli* TOP10, were used for recombinant protein expression. *E. coli* strains were transformed as described in chapter 4.

Table 6.4. Overview of cloning and expression vectors used in chapter 6. Vector name, resistance marker and function are given. Amp^r=ampicillin-resistant; kan^r=kanamycin resistant

Vector	Resistance marker	Function
pEXP5CT/Topo®	Amp^r	Cloning and recombinant expression of PVP-SE1gp146 wt and PVP-SE1gp146 variants
pET28a	Kan^r	Recombinant expression of Lys68
pQE-30	Amp^r	Cloning and recombinant expression of Lys68 variants

6.2.2 Cloning, recombinant protein expression and purification

A summary of all constructs, expression and purification methodology is given in **Table 6.5**. All primers used were purchased from Invitrogen. The vectors pET28a and pEXP5CT/Topo® were purchased from Novagen and Invitrogen, respectively. *E. coli* strains harbouring pET28a (50 µg/mL kanamycin) or pEXP5CT/Topo® (100 µg/mL ampicillin) were grown in the presence of the indicated antibiotic concentrations.

6.2.2.1 Cloning methodology

Cloning procedures for Lys68 wt are described in chapter 4. Lys68 variants were cloned in pQE-30 vector using similar standard PCR cloning procedure. DNA templates, specific primers, restriction enzymes, and the CBD containing vectors (pQE-30-P35, pQE-30-P40 and pQE-30-500) are listed in **Table 6.5**.

N-terminal peptide tags (α4 and PP) were fused to PVP-SE1gp146 using a TA cloning technique (thymine(T)/adenine(A) complementary base pairs cloning technique that avoids the use of restriction enzymes). A tail PCR was first carried out using phage PVP-SE1 genomic purified DNA, a *Pfu* polymerase (1.25 U, Thermo Fisher Scientific) and two primers, of which the forward primer is harbouring the peptide-coding sequence (α4 and PP). After a PCR reaction and product confirmation by agarose gel electroforesis, a second independent extension (15 min at 72°C) was done by adding to the mixture 1 µL of Dream *Taq* polymerase (5 U) (Thermo Fisher Scientific), compatible with the previous buffer reaction used. This *Taq* polymerase has a non-template-dependent terminal transferase activity and will add a single deoxyadenosine (A) to the 3' ends of the PCR. After this, the insert is cloned into the commercial pEXP5CT-TOPO® expression vector (Life Technologies) following manufacturer's procedures. This vector is provided linearized with single 3'-thymidine (T) overhangs for TA cloning and a Topoisomerase I covalently bound to the vector. Briefly, the amplified and extended PCR product is added to the commercial vector and allowed to incubate for 5 min at room temperature. To finalize the process competent *E. coli* cells were transformed with the ligation mixture.

Table 6.5. Overview of all expression constructs used in chapter 6. Plasmid names, cloning primers and amplification methodology used ("standard PCR", T/A cloning or Ligation independent cloning), as well as expression and purification conditions optimized for each construct (temperature, inducer concentration, induction time, expression strain and purification stringency) are depicted. For standard PCR cloning, restriction digestion sites are underlined in the primers.

CONSTRUCT NAME	PRIMER SEQUENCES (5' → 3')	CLONING METHODOLOGY (TEMPLATE AND VECTOR)	EXPRESSION CONDITIONS	PURIFICATION STRINGENCY
PVP-SE1gp146	PREPARATION CONSTRUCT PROVIDED [1]	-	-	-
*Ecl*136II-PVP-SE1gp146	PREPARATION CONSTRUCT PROVIDED [1]	-	-	-
α4-PVP-SE1gp146	TTGGAATGGGGAGCCCGAACCGTGCAAAACGTGTAATCA CATTGGAGGAGCCGGTACGGAAGGTGGTGATTACACGTT	Phage PVP-SE1 genomic DNA T/A cloning in pEXP5CT	16°C-18h BL21(DE3)-RIL	60 mM Imidazole
PP-PVP-SE1gp146	ATGGGATCCTTCTTCGTAGCACCGGGCTCCTCCAATGCTGCAAT CGAGGTTAGAACAGATTTTGCCT	Phage PVP-SE1 genomic DNA T/A cloning in pEXP5CT	16°C-18h BL21(DE3)-RIL	70 mM Imidazole
Lycotoxin1-PVP-SE1gp146	GGAATGGGGAGCATCTGGCTGACCGCACTGAAATTCCTCGGCAAACACGCCGCAA CATTGGAGGAGCCCAGTTTGGATAATTGCTGTTTTGCCAGTTTCTTTGCGGCGTGTT	pEXP5CT/*Ecl*136II-PVP-SE1gp146 template Ligation independent cloning	16°C-18h BL21(DE3)-RIL	60 mM Imidazole
Parasin1-PVP-SE1gp146	TTGGAATGGGGAGCAAAGGCCGTGGCAAGCAGGGAGGCAAAGTACGTG CATTGGAGGAGCCTGAGGAACGGGTCTTTGCTTTTGCACGTACTTTGC	pEXP5CT/*Ecl*136II-PVP-SE1gp146 template Ligation independent cloning	16°C-18h BL21(DE3)-RIL	60 mM Imidazole
ArtMW1-PVP-SE1gp146	TTATGGGCTTCTTCATCCCGGCAGTAATCCTGCCCTCCA CATTGGAGGAGCCCGGTACGATCAGGAATGCGATGGAGGGCAGGATT	pEXP5CT/*Ecl*136II-PVP-SE1gp146 template Ligation independent cloning	16°C-18h BL21(DE3)-RIL	65 mM Imidazole
ArtMW2-PVP-SE1gp146	TTATGGGCAAACCGGGCTGGCTGATCAAAGTAGCACTGAAGTTCAAGA CATTGGAGGAGCCTGCCAGTCTCTTCAGCGGACGACGGATCAGTTTCTTGAACTTCAG	pEXP5CT/*Ecl*136II-PVP-SE1gp146 template Ligation independent cloning	16°C-18h BL21(DE3)-RIL	70 mM Imidazole
Lys68	AGATATCATATGTCAAACCGAAACATTAGC GTGGTGCTCGAGCTACTTAG	phi68 genomic DNA Standard PCR, pET28a *Nde*I/*Xho*I	16°C-18h BL21(DE3)	85 mM Imidazole
pQE-30-P35	PREPARATION CONSTRUCT PROVIDED IN JM109 [2]	-	-	-
pQE-30-P40	PREPARATION CONSTRUCT PROVIDED IN XL1-Blue MRF' [2]	-	-	-
pQE-30-500	PREPARATION CONSTRUCT PROVIDED IN JM109	-	-	-
Lys68-CBDP35	GGGGGGGATCCATGTCAAACCGAAACATTAGC GGGGGGAGCTCGGAGGAGCCGGAGGTACCCTTAGCGCCACGGC	pQE-30-P35 template Standard PCR, pQE-30 *BamH*I/*Sac*I	16°C-18h JM109	25 mM Imidazole
Lys68-CBDP40	GGGGGGGATCCATGTCAAACCGAAACATTAGC GGGGGGAGCTCGGAGGAGCCGGAGGTACCCTTAGCGCCACGGC	pQE-30-P40 template Standard PCR, pQE-30 *BamH*I/*Sac*I	16°C-18h JM109	25 mM Imidazole
Lys68-CBD500	GGGGGGGATCCATGTCAAACCGAAACATTAGC GGGGGGAGCTCGGAGGAGCCGGAGGTACCCTTAGCGCCACGGC	pQE-30-500 template Standard PCR, pQE-30 *BamH*I/*Sac*I	16°C-18h JM109	25 mM Imidazole

Abbreviations: α4, PP, Lycotoxin1, Parasin1 are antibacterial peptides; PK, ArtMW1 and ArtMW2 are rationally design peptides; P35, P40 and P500, are different *Listeria* phage modular endolysins. Empty spaces detonate tasks not made.

[1] Plasmids containing PVP-SE1gp146 and pEXP5CT/*Ecl*136II-PVP-SE1gp146 were provided by the Laboratory of Gene Technology from the katholieke universiteit of Leuven

[2] PQ-30 containing three different *Listeria* phage endolysins were kindly provided by the ETH Zurich, Institute of Food, Nutrition and Health

For the remaining constructs, N-terminal peptide tags (ArtMW1, ArtMW2, Lycotoxin1 and Parasin1) were fused to PVP-SE1gp146 endolysin by an adapted version of the Ligation Independent Cloning (LIC) technique (Haun et al, 1992), using pEXP5CT/*Ecl*136II-PVP-SE1gp146 as a template (having a C-terminal His6). First, two complementary peptide-encoding cassettes (20 µM each, **Table 6.5**) were hybridized (heated at 95°C and allowed to gradually cool down to 40°C). In parallel, pEXP5CT/*Ecl*136II-PVP-SE1gp146 (≈200 ng) was linearized by the *Ecl*136II digestion (introduced unique restriction endonuclease site present) for 2 h at 37°C. Both peptide-encoding cassette and linearized pEXP5CT/*Ecl*136II-PVP-SE1gp146 vector were then incubated with a T4 DNA polymerase (Fermentas) with a 3'→5' exonuclease activity, in the presence of a dCTP mixture (Promega). The T4 exonuclease activity stops at the first dCTP present in the sequence, creating LIC-compatible sticky ends. A short 20 min incubation step at room temperature of the LIC-compatible hybridized peptide-encoding cassettes and vectors completes the cloning process, without the necessity of a ligase. As described before, all constructs were first verified by colony PCR. Afterwards, plasmid of positive transformants were extracted and verified by sequencing (Macrogen or using Big Dye polymerase, ABI3130 Sequencer, Life Technologies).

6.2.2.2 Protein overexpression and purification

All expression vectors used contained an N-terminal (pET28a, pQE-30) or C-terminal (pEXP5CT/Topo®) His6 tag for downstream expression. *E. coli* expression system, expression conditions and the purification stringency for Ni^{2+}-NTA affinity chromatography, were individually optimized and are illustrated in **Table 6.5**. Protein recombinant expression, purification and quantification procedures were explained previously in chapter 4. Only proteins with a higher than 90% purity, as judged by SDS-PAGE analysis, were considered for dialysis in 10 mM PBS pH 7.2 and to perform *in vitro* studies.

6.2.3 Antibacterial assays of endolysins with LPS-destabilizing peptides

The antibacterial assay was executed in a similar way as described in chapter 4. Briefly, mid-exponential phase cells (listed in **Table 6.2**) with an $OD6_{00nm}$ of 0.6, were resuspended in 10 mM HEPES/NaOH (pH 7.2) and then 100-fold diluted to a final density of 10^6 CFU/mL. Each culture (50 µL) was incubated for 30 min at room temperature with 25 µL of PVP-SE1gp146 wild-type (wt) and variants dialyzed in PBS pH 7.2 (5 µM final concentration) together with 25 µL of water or 25 µL of EDTA. As a negative control, 50 µL of cells were incubated with 25 µL water or 25 µL of PBS pH 7.2. After a 30 min incubation period, CFUs were counted and the antibacterial activity assessed as previously described in chapter 4. Averages ± standard deviations are given for n = 3 repeats.

6.2.4 Antibacterial assays of endolysins with cell binding domains

Antibacterial assays of endolysins with CBDs were measured in terms of relative activity. *Listeria* cells (listed in **Table 6.2**) were grown to mid-exponential phase with an OD_{600nm} of 0.6, resuspended in 10 mM HEPES/NaOH (pH 7.2) to achieve a final OD_{600nm} of 1.0. Turbidity measurements were then performed through the decrease in OD by adding a 20-µL drop of each protein (2 µM) onto 180 µL of different *Listeria* serovar cells (with an initial OD_{600nm} of 1.0) for 2 h. As a negative control 20 µL of PBS (pH 7.2) was used. Final OD values were categorized to indicate the sensitivity of the reaction: -, non-sensitive (OD from 1.0 to 0.8); +, sensitive (OD from 0.8 to 0.3) and ++, very sensitive (OD from 0.3 to 0.0).

6.3 Results

6.3.1 Modified endolysins recombinant expression

A range of LPS-destabilizing peptides and CBDs were tagged to PVP-SE1gp146 and Lys68, respectively. After optimization of different expression parameters, as described in materials and methods, each construct was expressed differently, as demonstrated in **Table 6.6**.

Table 6.6. Recombinant purification yields of Lys68 and PVP-SE1 wild-type proteins and their C- or N-terminal modified variants. The total yield for each protein is indicated in amount of purified protein (in mg) per liter of E. *coli* expression culture. For a given yield, a reduction percentage (%) of soluble protein is given compared to the wild-type protein.

Fusion	Fusion side	PVP-SE1gp146		Lys68	
		Yield (mg/L)	Reduction percentage	Yield (mg/L)	Reduction percentage
Wild-type protein		38.2	--	11.2	--
LPS-destabilizing peptide					
α4	N-terminal	1.5	96 %	NC	
Lycotoxin1	N-terminal	4.3	89 %	NC	
Parasin1	N-terminal	5.1	87 %	NC	
PK	N-terminal	65.2	(70%)*		
ArtiMW1	N-terminal	3.2	92 %	NC	
ArtiMW2	N-terminal	2.4	94 %	NC	
Cell binding domain					
CBDP35	C-terminal	NC		6.5	42 %
CBDP40	C-terminal	NC		9.1	19 %
CBD500	C-terminal	NC		5.8	48 %

NC – Not constructed; * Increased (not reduction) of expression yield

N-terminal LPS-destabilizing peptides were inserted to give a final construct type of **peptide**-**PVP-SE1gp146-His6**. In most of the cases, recombinant expressions yields of modified proteins drastically decreased compared to the wt (reductions

of more than 87%). The amount of soluble protein however, was still sufficient to perform the antibacterial assays (results presented in the 6.3.2 Antibacterial assays of endolysins with LPS-destabilizing peptides section). Interestingly, the PK-SE1gp146-His6 construct was the only fusion, for which a higher expression yield (70% more compared to the wt) was obtained.

Lys68 was C-terminally tagged with different CBDs to give the construct type of **His6-Lys68-CBD**. While the introduction of LPS-destabilizing peptides (AMPs or newly design) significantly reduced the expression yields, Lys68-CBD fusions expression levels were influenced to a much lesser extent (with only 19% to 48% reductions), albeit still lower than the protein wt. For all chimeras tested no insoluble proteins were obtained (data not shown).

6.3.2 Antibacterial assays of endolysins with LPS-destabilizing peptides

After cloning and recombinant expression, PVP-SE1gp146 wt and its N-terminal variants were incubated with mid-exponentially grown cells (*P. aeruginosa* PAO1, *S.* Typhimurium LT2 and *E. coli* XL1-Blue MRF`) in the presence and absence of 0.5 mM of EDTA for 30 min. To determine the antibacterial activity in log reduction units, cells suspensions were serially diluted and CFUs were counted (**Table 6.7**).

Table 6.7. Antibacterial activity of PVP-SE1gp146 (wt and variants) against *P. aeruginosa* PAO1, *S.* Typhimurium LT2 and *E. coli* XL1-Blue MRF´ in absence (A) and presence (B) of EDTA. For each protein, log reduction units are depicted and significant reductions (≥ 1 log) are marked in bold.

A Peptide	*P. aeroginosa* PAO1	*S.* Typhimurium LT2	*E.coli* XL1-Blue MRF´
Wild-type	0.19 ± 0.01	0.13 ± 0.02	0.14 ± 0.04
PK	**1.56 ± 0.10**	0.30 ± 0.10	0.69 ± 0.09
α4	**1.26 ± 0.12**	0.14 ± 0.12	0.42 ± 0.21
PP	**1.16 ± 0.17**	0.24 ± 0.16	0.26 ± 0.09
ArtiMW1	**1.26 ± 0.07**	0.10 ± 0.07	0.20 ± 0.05
ArtiMW2	0.63 ± 0.11	0.12 ± 0.12	0.10 ± 0.09
Lycotoxin1	**1.00 ± 0.24**	0.20 ± 0.22	0.59 ± 0.39
Parasin1	0.52 ± 0.12	0.04 ± 0.03	0.49 ± 0.15

B	Peptide	*P. aeroginosa* PAO1	*S.* Typhimurium LT2	*E.coli* XL1-Blue MRF´
	EDTA	0.28 ± 0.02	0.05 ± 0.05	0.29 ± 0.11
	Wild-type	**3.68 ± 0.13**	0.14 ± 0.21	0.34 ± 0.02
	PK	**4.92 ± 0.23**	**0.73 ± 0.30**	**0.85 ± 0.17**
	α4	**4.22 ± 0.30**	0.47 ± 0.24	**0.85 ± 0.17**
	PP	**3.69 ± 0.11**	0.47 ± 0.07	0.54 ± 0.10
	ArtiMW1	**3.95 ± 0.09**	0.27 ± 0.15	0.36 ± 0.11
	ArtiMW2	**3.99 ± 0.17**	0.41 ± 0.25	0.16 ± 0.10
	Lycotoxin1	**3.79 ± 0.07**	**0.87 ± 0.28**	0.34 ± 0.15
	Parasin1	**3.85 ± 0.08**	0.59 ± 0.38	0.69 ± 0.24

In the absence of OMP, PVP-SE1gp146 displayed no antibacterial activity on the three tested strains, as was expected. Once equipping the endolysin with different LPS-destabilizing peptides, a bactericidal effect emerged against *P. aeruginosa* and *S.* Typhimurium. The PK peptide proved to be the best fusion, not only able to cause a log reduction of 1.56±0.10 of *P. aeruginosa*, but also inactivating 0.69±0.09 of *E. coli* cells in 30 min. As for α4, PP and ArtiMW2 peptides, they were exclusively active against *P. aeruginosa,* reducing an approximate 1 log of viable cells.

In the presence of EDTA (0.5 mM), all endolysin variants had a much stronger effect. While the wt protein was able to reduce 3.68±0.13 logs of viable *P. aeruginosa* cells, the PK, α4, ArtiMW1 and ArtiMW2 fusion peptides improved the killing effect (log reductions of 4.92±0.23, 4.22±0.30, 3.95±0.09 and 3.99±0.17, respectively). Regarding the antibacterial impact against *S.* Typhimurium and *E. coli,* a much lower effect was observed. The Lycotoxin1 and α4 peptides were shown to be active against two strains. Compared to the wt protein, these peptides were similarly active towards *P. aeruginosa*, but could also reduce *S.* Typhimurium or *E. coli* cells by almost 1 log after 30 min incubation. Remarkably, the PK peptide not only gave the highest log reduction units of all proteins, but was also the only peptide able to kill all three tested strains in combination with EDTA (log reductions of 4.92±0.23, 0.73±0.30 and 0.85±0.17 for *P. aeruginosa*, *S.* Typhimurium and *E. coli*, respectively).

6.3.3 Antibacterial assays of the endolysins with cell binding domains

In order to improve the application potential of the G⁻-like endolysin against *L.* monocytogenes, Lys68 was equipped with three different *Listeria* CBDs. After recombinant expression, all constructed endolysins were evaluated in terms of relative lysis activity (**Table 6.8**, **Figure 6.1**).

Table 6.8. Endolysins relative lysis activity. Turbidity measurements were performed through the decrease in OD by adding a 20-µL drop of each protein (2 µM) onto 180 µL of different *Listeria* serovar cells (with an initial OD_{600nm} of 1.0) for 2 h. As a negative control 20 µL of PBS (pH 7.2) was used. Relative activity is given depending on the final OD value: -, non-sensitive (OD from 1.0 to 0.8); +, sensitive (OD from 0.8 to 0.3) and ++, very sensitive (OD from 0.3 to 0.0). The most sensitive strain is highlighted in bold.

			Relative lysis activity			
Listeria species		**Serotype**	**Lys68**	**Lys68-P35**	**Lys68-P40**	**Lys68-500**
L. monocytogenes	CECT 4031T	1a	++	+	+	+
	CECT 5873	1/2a	++	+	+	+
	CECT 936	1/2b	++	+	+	+
	CECT 911	1/2c	++	+	-	+
	CECT 933	3a	++	+	+	+
	CECT 937	3b	++	+	+	+
	CECT 938	3c	++	+	-	-
	CECT 934	4a	++	+	-	-
	923*	4b	++	+	-	-
	CECT 5725	**4c**	**++**	**++**	**++**	**++**
	994*	4ab	++	+	+	+
Listeria welshimeri	CECT 5371	6a	++	+	-	+
Listeria seeligeri	CECT 5339	6b	++	+	+	+
Listeria inocua	CECT 4030	Unknown	+	-	-	-
Listeria ivanovii	CECT 5375	Unknown	+	-	-	-

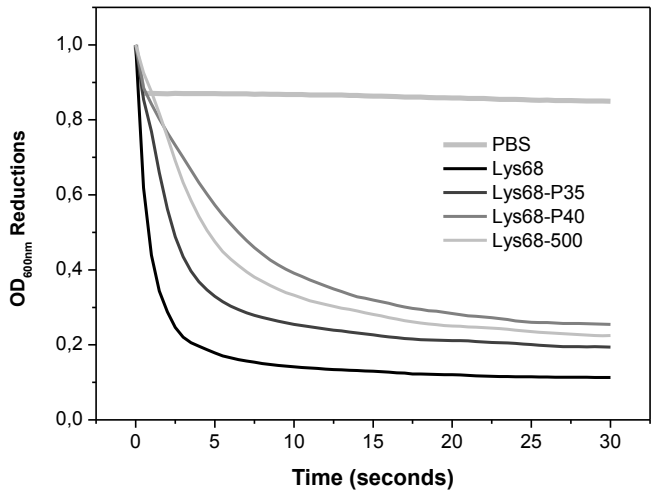

Figure 6.1. Turbidity measurements of Lys68 and CBD variants against *L. monocytogenes* CECT 5725.

Results show that Lys68 was able to digest the cell wall of all *Listeria* cells. As expected, being a globular endolysin displaying a single ECD, Lys68 activity revealed to be unspecific towards *Listeria* cells. While the relative activity of Lys68 demonstrated the ability of killing all 15 strains tested, Lys68-P35, Lys68-P40 and Lys68-500 (containing different Listeria-specific CBDs) could only reduce the OD of 13, 8 and 10 strains, respectively. Lys68 alone consistently remained more active than its variants, and always reached lower OD values after incubation with the different *Listeria* cells for 2 hours. **Figure 6.1** shows the turbidity assay of Lys68 and its fusion variants against the most sensitive *Listeria* strain (CECT 5725). With this strain, OD reductions from OD 1.0 to 0.2-0.3 were obtained within only 30 seconds. Kinetics curves demonstrate that the Lys68 wt displayed the steepest lysis curve (i.e. highest muralytic activity). For all tested serovars a consistent higher muralytic activity of Lys68 wt compared to the CBD variants was observed.

6.4 Discussion

After a careful selection of peptides for the covalent modification of endolysins, their recombinant expression revealed to be, in most cases, critical in obtaining large amounts of soluble proteins to test. Several aspects can interfere with protein *E. coli* recombinant expression (e.g. preferential codon usage, physicochemical properties of its amino acid sequence, including hydrophobicity, electrostatic charge, its toxicity) (Price et al, 2011; Gopal & Kumar, 2013). Generally, it was possible to heterologously produce the endolysins fused to LPS-destabilizing peptides, however the obtained production yield was very low (87% to 96% reductions). Production levels decreased to a lower extent when fused to CBD domains (47% of maximum reductions). This decrease in protein production may indicate that inherent toxicity of the LPS-destabilizing peptides is determinant for the lower recombinant expression levels of these proteins. A unique event happened with the PK fusion, as it was the only protein expressed in higher quantity (more 70% increased than the wt) and therefore seems to favour protein synthesis. Expressed proteins were then tested in two separate parts; PVP-SE1gp146 tagged with LPS-destabilizing peptides was tested against G^- bacteria and CBD-fused Lys68 was tested for enhanced antibacterial performance against G^+ *Listeria* cells.

When PVP-SE1gp146 was fused to different LPS-destabilizing peptides, an increase of activity could be observed for most of the proteins. However, this effect seems to be bacteria- and peptide-related. In general, when fused to PVP-SE1gp146 the intrinsic LPS-destabilizing peptides were only able to inactivate *Pseudomonas* cells. The polycationic peptide PK had the strongest effect (1.56±0.10). When combined with EDTA, the effect could be increased and extended to *Salmonella* and *E. coli*. Peptides such as the PK, α4, PP and Lycotoxin1, could increase PVP-SE1gp146 wt activity towards *Pseudomonas* (max. reductions of 4.92±0.23 logs), but also against *Salmonella* (max. reductions of

0.87±0.28 logs) and *E. coli* (max. reductions of 0.85±0.17 logs). The structure and composition of the different LPS can explain the higher sensitivity of *Pseudomonas* over the *Salmonella* and *E. coli*. *Pseudomonas* LPS is strongly dependent on high phosphate ionic interactions with surrounding divalent cations (Nikaido, 2003). On the other hand, *Salmonella* and *E. coli* LPS is more stabilized by hydrophobic interactions of the Lipid A moieties (and lower phosphorylation degree) (Nikaido, 2003). The combined effect of the polycationic peptide PK and EDTA had the strongest effect against *Pseudomonas*. They both act in a different manner on the cations responsible for *Pseudomonas* LPS integrity, namely by cation displacement (PK) and removal (EDTA). Peptides selected to increase the cationic, hydrophobic and amphipatic strength of the PVP-SE1gp146 proved to be effective against *Salmonella* and *E. coli,* although to a lesser extent. Nevertheless, the results obtained should be taken in careful consideration. The addition of extra amino acids may interfere differently with the chimeric protein folding and influence its function. This could explain the different synergistic, additive and antagonistic effects observed with the different peptides and EDTA combinations. Overall, it was shown that this rational design of phage-encoded endolysins is able to increase the antibacterial activity. However, unless *in silico* analysis could be used to anticipate the chimeric endolysins expression, folding, function and activity, only experimental validations will determine the best peptide fusion partner.

A similar approach was pursued to clone CBD peptides into Lys68. CBDs were tested to turn the Lys68 more specific and active against *Listeria* cells. Lys68 wt demonstrated to have a broader lytic range compared to the Lys68-CBD variants. These results were expected, as Lys68 is a globular protein (only containing an ECD) that should behave unspecifically. For Lys68 tagged with CBPP35 or CBDP40 its lytic spectra still remained high as they also do not confer serovar-specificity. However for Lys68-500, 10 different serovars were sensitive to this protein, including serovars where CBD500 did not recognize in the *Listeria* phage endolysin

Ply500 (e.g. type 1/2 and 3) (Schmelcher et al, 2010). Therefore, this *Listeria* CBD is not displaying the same antibacterial specificity. In terms of activity, with no exceptions, none of the CBDs assisted Lys68 in reducing the OD of the *Listeria* cells worked in a faster way (i.e. higher muralytic activity). One can speculate, as described earlier, that the presence of a CBD is hindering (instead of improving) the muralytic activity of the catalytic domain (Cheng & Fischetti, 2007; Horgan et al, 2009). Another aspect to take into account is that modified proteins might not fold properly, thereby hindering ECD or CBD functionality. Either one of those factors may hamper proper ECD muralytic activity and CBD recognition. Additionally, a shift of ionic strength and pH condition for an optimal activity can also be impairing the enzyme activity, as demonstrated before to different *Listeria* phage modular endolysins (Schmelcher et al, 2012b). Therefore, to exclude previous theories, future tests covering a range of different protein concentrations, pH values and ionic strengths should be carried out to clarify the role of the CBDs on the Lys68 activity.

Taking everything into consideration, (modified) G^--like endolysins can become a new generation of powerful antimicrobials to fight bacterial pathogens either from food to veterinary and medical settings.

Chapter 7

General conclusions and future work

7.1 General conclusions

The main goal of this work was to expand the knowledge of phage-encoded endolysins and explore their bactericidal properties against bacterial pathogens, with particular emphasis on G^- bacteria. Finding strategies to overcome the presence of a highly protective OM that makes G^- bacteria less accessible for externally added antimicrobials, such as endolysins, represented the most important scientific challenge of this study (described in chapter 1).

In silico analysis of all available endolysins sequences, showed an enormous diversity of endolysins with different molecular structures and functions (chapter 3). This diversity is driven by the dynamic adaptation of phages that continuously need to co-evolve with a diverse group of bacterial hosts. Therefore, endolysins represent a varied group of antimicrobials that could be of use in fighting bacterial infections. Additionally, through an ever increasing knowledge on protein design and better available molecular biology tools, tailor-made enzymes can still be developed to achieve the desired or enhanced properties for industrial and medical use.

In vitro, the biochemical characterization of two different G^- phage endolysins (Lys68 and ABgp46) contributed to enlarge the knowledge of a group of enzymes until recently scarcely explored (chapter 4 and 5). It was shown that an endolysin from a G^-- background can have a prolonged shelf-life (up to 2 months with no significant activity lost), be stable and active under a broad range of pH values (from acidic to basic conditions) and also be thermostable (withstanding temperatures up to 100°C). The fact that the characterized Lys68 is able to refold after thermal denaturation ($>T_m$) explains its high thermostability. A PG digestion mechanism was also proposed for Lys68, explaining its muralytic activity in an acidic environment. This biochemical characterization is of great importance to discover new desirable traits that can be used for biotechnological applications.

To overcome the bacterial OM diffusion limitation, both endolysins (Lys68 and ABgp46) were combined with different OMPs against a vast panel of G^- bacterial pathogens (chapter 4 and 5). The observed specific antibacterial bacterial effect is correlated with the bacterial LPS structure and composition. EDTA, which acts by chelation, was able to permeabilize the OM for the penetration of endolysins, but only in a few bacterial species, namely *Pseudomonas* and *Acinetobacter* species. The organic acids citric and malic acids were able to promote a broader OM permeabilization, acting synergistically with our endolysins to kill most of the G^- strains tested. The low pH present was recognized to be important for the OM destabilization and subsequent permeabilization to endolysins. However, we speculate that undissociated acid groups from organic acids tested, can penetrate differently through the bacterial LPS, damaging or inhibiting several OM-stabilizing enzymatic processes, explaining the differences in synergy observed when combining endolysins with different weak acids at the same pH. We further demonstrated that endolysins were not only efficient antimicrobials in the presence of OMPs, but also that they were occasionally able to kill specific groups of bacteria without the aid of any OM permeabilization, including antibiotic resistant phenotypes (chapter 5). Overall, this endolysin-based antimicrobial approach also has its limitations: some bacteria (*K. oxytoca* and *Y. enterocolitica*) remain less sensitised by the endolysin/OMP formula; its efficiency decreased in the presence of different bacterial physiological states and against biofilms; the strategy of using weak acids (that mostly act at low pH) could limit future biotechnological applications in sectors where these substances are prohibited or allowed in very low concentrations. A certain concentration of these weak acids must be present, in order to provide acidity needed to permeabilize the OM to endolysins. Nevertheless, other OMPs, enzymes or combinations can still be searched in order optimize and expand their use.

To boost the previous endolysin/OMP antibacterial efficiency, a rational design of introducing specific LPS-destabilizing peptides (with different cationic,

hydrophobic and amphipathic nature) was performed, to allow a spontaneous endolysin penetration of the OM (chapter 6). This strategy revealed to be in most cases efficient, however proved to be peptide- and bacteria- dependent. In the absence of EDTA, peptide fusions could increase the PVP-SE1gp146 wt antibacterial activity mostly against *P. aeruginosa,* from a minimum of 0.33 (for Parasin1 peptide) to a maximum of 1.37 logs reductions (for PK peptide). When combined with EDTA, the effect was in general more pronounced and broader against all *Pseudomonas*, *Salmonella* and *E. coli* strains. The variation of the primary LPS-stabilizing forces between *Pseudomonas* (mostly based on ionic interactions) and *Salmonella* and *E. coli* (mostly based on hydrophobic packing) appears to be determinant for the sensitivity observed to the different LPS-destabilizing peptides tested (Raetz & Whitfield, 2002). However, this approach implicates covalent modifications of the native protein. This is not only limiting their recombinant expression, but also only small increased bactericidal effects are observed in a few cases, that might limit their future biotechnology application. Since it is likely that conformational changes of the fusion protein by steric hindrance of the tagged peptides are hampering the endolysin`s action, it is desirable to perform a preliminary bioinformatics analysis that might predict upfront the protein folding, before advancing with the construction of the envisaged fusions. Another option is to randomly select OM-destabilizing peptides followed by a high-throughput screening procedure to speed up the process, as rational design is a time-consuming process. This would allow to generate and screen several LSP-destabilizing peptides with good potential before expressing and purifying them at large scale. Despite all the covalent endolysin modifications, this strategy still proved to be efficient in enhancing the endolysins`s antibacterial performance, effect further improved in the presence of an OMP agent.

With a different purpose, endolysin covalent modifications with CBDs intended to improve the activity of a G^--like endolysin against *L. monocytogenes*. Several examples are known in which the CBD is reported to be crucial for the endolysin’s

specificity/activity (Loessner et al, 2002; Schmelcher et al, 2011; Eugster & Loessner, 2012). However, fusing a CBD to Lys68 did not make the endolysin specific or enhance its muralytic activity against *Listeria* cells. Similar folding issues predicted to be happening with the endolysin tagged with different LPS-destabilizing peptides, might explain the results obtained. To be sure of this, changing the experimental conditions should be first considered, like modifying the ionic strength or the pH and buffer composition. In theory, modifying these enzymes can cause a shift in the optical physiological conditions in which they perform the best, compared to the Lys68 wt conditions. Also, other antibacterial specificity tests, such as spotting an endolysin drop into bacterial lawns, could be performed to assess its lytic spectrum and to help establish the CBD functionality in Lys68. Alternatively, CBD fusions can be tagged to other interesting endolysins of G^- origin (e.g. ABgp46 or PVP-SE1gp146) to accomplish the desired objective of efficiently kill *Listeria* cells.

7.2 Future perspectives

With the expertise built up by previous studies that involved phage-encoded endolysins to target G^- pathogens, it is proposed some strategies to further optimize the endolysin-based technology developed so far.

Widen the screening efforts to select better OMPs and endolysins

We have previously seen G^--like endolysins with extraordinary characteristics. For instance, the T4 lysozyme has a dual antibacterial activity; *i)* a bactericidal effect owned by its amphipathic nature in disrupting the bacteria cellular membranes and *ii)* lethal PG enzymatic digestion (During et al, 1999). Other enzymes have also impressed us for their intrinsic ability to enter the OM, becoming active antimicrobials against G^- cells without the aid of OMPs (e.g. LysAB2, OBPgp279

and ABgp46) or for their high thermostability (e.g. Lys68) (Lai et al, 2011; Walmagh et al, 2012). Additionally, novel domains here described *in silico* (within dsNA phages and even identified in *Tectiviridae* and *Cystoviridae* phages) can represent valuable properties worth exploring. Therefore, a continuous search for new phage-encoded endolysins in the enormous reservoir of phages is a recommended strategy, combined with the exploitation of a more "friendly and broad use" of OMPs. Although most of the OMPs here described are naturally occurring compounds, their versatility can be compromised depending on their use, type of bacteria and infection. This endolysin/OMP technology is more efficient to certain groups of bacteria and, in case of organic acids, their use is restricted to situations where low pH can be applied.

Improving anti-biofilm activity

Biofilms are microbial communities responsible for several infectious diseases related to their ubiquitous nature. They are hard-to-treat cell populations that have become highly tolerant to varied antimicrobial agents (Lewis, 2008). In order to efficiently kill biofilms, a cocktail of different polysaccharides-degrading compounds (e.g. cocktail phage-encoded depolymerases, synthethic sodium periodate and dispersin B), DNases (like the Dornase from Pulmozyme®) and proteases can be combined with endolysins to decompose the polysaccharides, extracellular DNA and proteins typically present in biofilms, enhancing the anti-biofilm activity. Dispersin B, an enzyme isolated from *Aggregatibacter actinomycetemcomitans* (Kaplan et al, 2003) that possesses an anti-biofilm activity, seems to be a good candidate. While many phage depolymerases are only able to degrade specific biofilm matrix components, limiting the type of bacterial biofilm (Hughes et al, 1998; Cornelissen et al, 2011), the poly-N-acetylglucosamine-degrading activity of dispersin B is able to digest structural poly-acetyl glucosamines present in both G^+ (e.g. *S. epidermidis*) and G^- bacteria

biofilms (e.g. *E. coli*, *P. fluorescens, Yersinia pestis*,) (Kaplan et al, 2004; Itoh et al, 2005; Lu & Collins, 2007). Therefore, dispersin B is considered to be a broad spectrum anti-biofilm agent and could be combined with the endolysin/OMP formula to overcome the biofilm diffusion limitation problems. Additionally, dispersin B detaches biofilms in a few minutes (<10 min) and has an optimal pH value for activity around 4.0-5.0 (Kaplan et al, 2004). This is the range of pH where the endolysin/OMP mixtures are more efficient.

Tailoring endolysins with LPS-destabilizing peptides

Three alternatives are proposed to the rational LPS-destabilising peptide design addressed here. Rather than using AMPs, endolysins tagged with cell-penetrating peptides (CPPs) could be constructed. CPPs, also known as protein transduction domains, are short peptides (generally not exceeding 30 amino acids) found within proteins that are able to cross cellular membranes (Bechara & Sagan, 2013). TAT (12 residues between the 48-60 region) and Penetratin (16 residues between the 53-58 region) from the Trans-Activator of Transcription (from HIV virus) and Antennapedia homeodomain (from the Drosophilia melanogaster insect) proteins, respectively, were the first CPPs found to be responsible for spontaneous translocation over the cell membrane (Derossi et al, 1994; Vives et al, 1997). Although CPPs, like AMPs, have similar characteristics (physiochemical properties, secondary structure), they are considered to have low toxicity and haemolytic effect (manifested only at higher concentrations) (Zhu & Shin, 2009; Splith & Neundorf, 2011). CPPs (like TAT and penetratin) are well-known peptides able to interact with G^- bacterial membranes (Bourre et al, 2010; Bahnsen et al, 2012; Garro et al, 2013). Their inherent low toxicity should improve the protein recombinant expression (showed to be generally limited for AMPs containing proteins). CPP-endolysin proteins could then be tested in the similar way as was done with the PVP-SE1gp146 chimeras.

A randomized strategy could be used to quickly generate and find novel AMPs or CPPs. The rational design developed here is a time-consuming process that sometimes creates low expression yields and results in enzymes with a moderate antibacterial effect. For this, PVP-SE1gp146 gene for example, could be amplified using a circular PCR approach, in which a forward primer (carrying the putative LPS-destabilizing signal inserted in the protein N-terminal side) contains an N-randomized domain. By linearizing the vector, each PCR cycle would generate a protein with a different peptide. A high-throughput screening process could then be used to identify the protein with the best LPS-destabilizing property.

One of the major hurdles of using LPS-destabilizing peptides in endolysins to target G^- cells is their lack of specificity, which is a crucial aspect when only certain groups of bacteria need to be targeted. To narrow the action of endolysins, understanding and exploring the bacteriocins` mode of action could provide important information. For example, endolysins could be tagged with microcin uptake domains. Microcins are gene-encoded peptides produced by *Enterobacteriaceae.* After synthesis, they occasionally undergo post-translation modifications, thus converting to mature molecules, with the aim to kill closely related competitor strains that threat their survival (Morin et al, 2011). Their narrow activity spectrum is exerted intracellularly, after translocation across the OM through specific TonB-dependent receptors, involved in the energy-dependent iron uptake. Once inside the cell, they can behave as bactericidal (e.g. targeting the mannose permease) or bacteriostatic agents (e.g. inhibiting the bacterial RNA polymerase) (Vincent et al, 2004; Bieler et al, 2006). Some of the microcin uptake domains (e.g. Colicin V), that are responsible for their internalization, have been identified (Azpiroz & Lavina, 2007). These domains could be tagged to endolysins in order to target them to a specific group of bacteria. An excellent example in which this strategy was applied is the creation of a hybrid T4 lysozyme, coupled to a pesticin domain (Lukacik et al, 2012). This engineered endolysin was able to reduce 1 log in 24 hours of TonB dependent

Yersinia and *E. coli* species. This "slow mode of action" however, may lead to the appearance of resistant phenotypes. Nevertheless, other endolysin/microcin combinations must be constructed in order to evaluate their efficiency and resistance development.

Tailoring endolysins with cell binding domains

Once modifying the molecular structure of a certain protein, its function can be altered or shifted to different performance conditions. Lys68 was engineered into a modular protein with three different listerial CBDs, however no improvement in activity was observed. Some listeria endolysins possessing different CBDs are known to acquire specific pH, ionic strength conditions (Schmelcher et al, 2012b). To evaluate this possibility, photometric lysis assays could be performed on the Lys68 mutants to calculate the range of concentration needed to perform additional studies. Afterwards, all proteins could be tested to determine the pH range (e.g. 3.0-10.0) and ionic strength (e.g. 10-1000 mM of NaCl) requirements for optical muralytic activity of each protein. Additionally, the same modifications can be applied to other endolysins (such ABgp46 or PVP-SE1gp146) or even by inserting other CBDs, specific to other G^+ bacteria that harbours similar A1γ PG chemotype (such as *Bacillus* species).

Currently, G^+ phage endolysins are recognized as useful antimicrobial or bacterial specific recognition tools to fight bacterial pathogens, soon expected to make the first R&D transitions into real commercial products. In fact, Micreos already has a commercial endolysin-based product named Staphefekt™ to prevented or control skin infections. In recent years, efforts have been made to fully explore the biotechnological potential of endolysins by also tackling G^- bacteria. This work proves the enormous potential of G^--like endolysins, once selecting proper enzymes, OMPs and covalent modification. With an ever increasing knowledge, it is expected that this endolysin-based technology can soon also make transitions

from the proof-of-principle stage to food, agricultural and medicinal use. Such antimicrobials are gaining particular and intensified interest in an era where policies involving non-synthetic food preservatives and the threat of antibiotic and multi-resistant bacteria are increasing and solutions are becoming scarce.

References

Web references

European Food Safety Authority (EFSA):

www.efsa.europa.eu/EFSA/efsa_locale-1178620753812_1211902031795.htm

Centers for Disease Control and Prevention (CDC):

www.cdc.gov/ncidod/eid/vol5no5/mead.htm

United States Economic Research Service (USDA-ERS):

www.ers.usda.gov/amber-waves/2013-november/recent-estimates-of-the-cost-of-foodborne-illness-are-in-general-agreement

United States Environmental Protection Agency (US EPA):

www.epa.gov/teach/chem_summ/Nitrates_summary.pdf

Carbohydrate-Active enZYmes (CAZY) Database:

www.cazy.org/Glycoside-Hydrolases

Other references

Ackermann HW (2003). Bacteriophage observations and evolution. *Res Microbiol* 154: 245-51.

Ackermann HW (2007). 5500 Phages examined in the electron microscope. *Arch Virol* 152: 227-43.

Alakomi H-L (2007). Weakening of the Gram-negative bacterial outer membrane PhD thesis, University of Helsinki

Alakomi HL, Skytta E, Saarela M, Mattila-Sandholm T, Latva-Kala K, Helander IM (2000). Lactic acid permeabilizes gram-negative bacteria by disrupting the outer membrane. *Appl Environ Microbiol* 66: 2001-5.

Archibald AR HI, Harwood CR (1993). *Bacillus subtilis* and other Gram-positive bacteria, biochemistry, physiology and molecular genetics. In: Sonenshein A. L. HJA, Losick R. (eds.) Cell wall structure, synthesis and turnover, American Society for Microbiology. pp 381–410.

Azpiroz MF, Lavina M (2007). Modular structure of microcin H47 and colicin V. *Antimicrob Agents Chemother* 51: 2412-9.

Bahnsen JS, Franzyk H, Sandberg-Schaal A, Nielsen HM (2012). Antimicrobial and cell-penetrating properties of penetratin analogs: effect of sequence and secondary structure. *Biochim Biophys Acta* 1828: 223-32.

Baker JR, Liu C, Dong S, Pritchard DG (2006). Endopeptidase and glycosidase activities of the bacteriophage B30 lysin. *Appl Environ Microbiol* 72: 6825-8.

Bechara C, Sagan S (2013). Cell-penetrating peptides: 20 years later, where do we stand? *FEBS Lett* 587: 1693-702.

Bieler S, Silva F, Soto C, Belin D (2006). Bactericidal activity of both secreted and nonsecreted microcin E492 requires the mannose permease. *J Bacteriol* 188: 7049-61.

Bolam DN, Ciruela A, McQueen-Mason S, Simpson P, Williamson MP, Rixon JE, Boraston A, Hazlewood GP, Gilbert HJ (1998). *Pseudomonas* cellulose-binding domains mediate their effects by increasing enzyme substrate proximity. *Biochem J* 331 (Pt 3): 775-81.

Bonomo RA, Szabo D (2006). Mechanisms of multidrug resistance in *Acinetobacter* species and *Pseudomonas aeruginosa*. *Clin Infect Dis* 43 Suppl 2: S49-56.

Borysowski J, Weber-Dabrowska B, Gorski A (2006). Bacteriophage endolysins as a novel class of antibacterial agents. *Exp Biol Med (Maywood)* 231: 366-77.

Bourre L, Giuntini F, Eggleston IM, Mosse CA, Macrobert AJ, Wilson M (2010). Effective photoinactivation of Gram-positive and Gram-negative bacterial strains using an HIV-1 Tat peptide-porphyrin conjugate. *Photochem Photobiol Sci* 9: 1613-20.

Boyce JD, Davidson BE, Hillier AJ (1995). Identification of prophage genes expressed in lysogens of the *Lactococcus lactis* bacteriophage BK5-T. *Appl Environ Microbiol* 61: 4099-104.

Breidt F, Jr., Hayes JS, McFeeters RF (2004). Independent effects of acetic acid and pH on survival of *Escherichia coli* in simulated acidified pickle products. *J Food Prot* 67: 12-8.

Briers Y, Cornelissen A, Aertsen A, Hertveldt K, Michiels CW, Volckaert G, Lavigne R (2008). Analysis of outer membrane permeability of *Pseudomonas aeruginosa* and bactericidal activity of endolysins KZ144 and EL188 under high hydrostatic pressure. *FEMS Microbiol Lett* 280: 113-9.

Briers Y, Lavigne R, Volckaert G, Hertveldt K (2007a). A standardized approach for accurate quantification of murein hydrolase activity in high-throughput assays. *J Biochem Biophys Methods* 70: 531-3.

Briers Y, Peeters LM, Volckaert G, Lavigne R (2011a). The lysis cassette of bacteriophage varphiKMV encodes a signal-arrest-release endolysin and a pinholin. *Bacteriophage* 1: 25-30.

Briers Y, Schmelcher M, Loessner MJ, Hendrix J, Engelborghs Y, Volckaert G, Lavigne R (2009). The high-affinity peptidoglycan binding domain of *Pseudomonas* phage endolysin KZ144. *Biochem Biophys Res Commun* 383: 187-91.

Briers Y, Volckaert G, Cornelissen A, Lagaert S, Michiels CW, Hertveldt K, Lavigne R (2007b). Muralytic activity and modular structure of the endolysins of *Pseudomonas aeruginosa* bacteriophages phiKZ and EL. *Mol Microbiol* 65: 1334-44.

Briers Y, Walmagh M, Lavigne R (2011b). Use of bacteriophage endolysin EL188 and outer membrane permeabilizers against *Pseudomonas aeruginosa*. *J Appl Microbiol* 110: 778-85.

Brussow H, Hendrix RW (2002). Phage genomics: small is beautiful. *Cell* 108: 13-6.

Buist G, Steen A, Kok J, Kuipers OP (2008). LysM, a widely distributed protein motif for binding to (peptido)glycans. *Mol Microbiol* 68: 838-47.

Cantarel BL, Coutinho PM, Rancurel C, Bernard T, Lombard V, Henrissat B (2009). The Carbohydrate-Active EnZymes database (CAZy): an expert resource for Glycogenomics. *Nucleic Acids Res* 37: D233-8.

Catalao MJ, Gil F, Moniz-Pereira J, Sao-Jose C, Pimentel M (2012). Diversity in bacterial lysis systems: bacteriophages show the way. *FEMS Microbiol Rev* 37: 554-71.

Celia LK, Nelson D, Kerr DE (2008). Characterization of a bacteriophage lysin (Ply700) from

Streptococcus uberis. *Vet Microbiol* 130: 107-17.

Cheng Q, Fischetti VA (2007). Mutagenesis of a bacteriophage lytic enzyme PlyGBS significantly increases its antibacterial activity against group B streptococci. *Appl Microbiol Biotechnol* 74: 1284-91.

Cheng Q, Nelson D, Zhu S, Fischetti VA (2005). Removal of group B streptococci colonizing the vagina and oropharynx of mice with a bacteriophage lytic enzyme. *Antimicrob Agents Chemother* 49: 111-7.

Cheng X, Zhang X, Pflugrath JW, Studier FW (1994). The structure of bacteriophage T7 lysozyme, a zinc amidase and an inhibitor of T7 RNA polymerase. *Proc Natl Acad Sci U S A* 91: 4034-8.

Chopra I, Schofield C, Everett M, O'Neill A, Miller K, Wilcox M, Frere JM, Dawson M, Czaplewski L, Urleb U, Courvalin P (2008). Treatment of health-care-associated infections caused by Gram-negative bacteria: a consensus statement. *Lancet Infect Dis* 8: 133-9.

Compton LA, Johnson WC, Jr. (1986). Analysis of protein circular dichroism spectra for secondary structure using a simple matrix multiplication. *Anal Biochem* 155: 155-67.

Cornelissen A, Ceyssens PJ, T'Syen J, Van Praet H, Noben JP, Shaburova OV, Krylov VN, Volckaert G, Lavigne R (2011). The T7-related *Pseudomonas putida* phage phi15 displays virion-associated biofilm degradation properties. *PLoS One* 6: e18597.

Delcour AH (2009). Outer membrane permeability and antibiotic resistance. *Biochim Biophys Acta* 1794: 808-16.

Derossi D, Joliot AH, Chassaing G, Prochiantz A (1994). The third helix of the Antennapedia homeodomain translocates through biological membranes. *J Biol Chem* 269: 10444-50.

Diaz E, Lopez R, Garcia JL (1990). Chimeric phage-bacterial enzymes: a clue to the modular evolution of genes. *Proc Natl Acad Sci U S A* 87: 8125-9.

Diaz E, Lopez R, Garcia JL (1991). Chimeric pneumococcal cell wall lytic enzymes reveal important physiological and evolutionary traits. *J Biol Chem* 266: 5464-71.

Djurkovic S, Loeffler JM, Fischetti VA (2005). Synergistic killing of *Streptococcus pneumoniae* with the bacteriophage lytic enzyme Cpl-1 and penicillin or gentamicin depends on the level of penicillin resistance. *Antimicrob Agents Chemother* 49: 1225-8.

Doehn JM, Fischer K, Reppe K, Gutbier B, Tschernig T, Hocke AC, Fischetti VA, Loffler J, Suttorp N, Hippenstiel S, Witzenrath M (2013). Delivery of the endolysin Cpl-1 by inhalation rescues mice with fatal pneumococcal pneumonia. *J Antimicrob Chemother* 68: 2111-7.

Donovan DM, Foster-Frey J (2008). LambdaSa2 prophage endolysin requires Cpl-7-binding domains and amidase-5 domain for antimicrobial lysis of streptococci. *FEMS Microbiol Lett* 287: 22-33.

Donovan DM, Foster-Frey J, Dong S, Rousseau GM, Moineau S, Pritchard DG (2006a). The cell lysis activity of the *Streptococcus agalactiae* bacteriophage B30 endolysin relies on the cysteine, histidine-dependent amidohydrolase/peptidase domain. *Appl Environ Microbiol* 72: 5108-12.

Donovan DM, Lardeo M, Foster-Frey J (2006b). Lysis of staphylococcal *mastitis* pathogens by bacteriophage phi11 endolysin. *FEMS Microbiol Lett* 265: 133-9.

Doores (1993). Organic acids. In: Davidson PMB, A.L. (eds.) Antimicrobials in Food., Marcel Dekker Ltd. pp 95-136.

During K, Porsch P, Mahn A, Brinkmann O, Gieffers W (1999). The non-enzymatic microbicidal

activity of lysozymes. *FEBS Lett* 449: 93-100.

El-Tahawy AT (2004). The crisis of antibiotic-resistance in bacteria. *Saudi Med J* 25: 837-42.

Eugster MR, Loessner MJ (2012). Wall teichoic acids restrict access of bacteriophage endolysin Ply118, Ply511, and PlyP40 cell wall binding domains to the *Listeria monocytogenes* peptidoglycan. *J Bacteriol* 194: 6498-506.

Fernandez-Tornero C, Garcia E, de Pascual-Teresa B, Lopez R, Gimenez-Gallego G, Romero A (2005). Ofloxacin-like antibiotics inhibit pneumococcal cell wall-degrading virulence factors. *J Biol Chem* 280: 19948-57.

Fischetti VA (2003). Novel method to control pathogenic bacteria on human mucous membranes. *Ann N Y Acad Sci* 987: 207-14.

Fischetti VA (2005). Bacteriophage lytic enzymes: novel anti-infectives. *Trends Microbiol* 13: 491-6.

Fischetti VA (2008). Bacteriophage endolysins: a novel anti-infective to control Gram-positive pathogens. *Int J Med Microbiol* 300: 357-62.

Fischetti VA (2010). Bacteriophage endolysins: a novel anti-infective to control Gram-positive pathogens. *Int J Med Microbiol* 300: 357-62.

Gaeng S, Scherer S, Neve H, Loessner MJ (2000). Gene cloning and expression and secretion of *Listeria monocytogenes* bacteriophage-lytic enzymes in *Lactococcus lactis*. *Appl Environ Microbiol* 66: 2951-8.

Gandhi TN, DePestel DD, Collins CD, Nagel J, Washer LL (2010). Managing antimicrobial resistance in intensive care units. *Crit Care Med* 38: S315-23.

Garcia E, Garcia JL, Garcia P, Arraras A, Sanchez-Puelles JM, Lopez R (1988). Molecular evolution of lytic enzymes of *Streptococcus pneumoniae* and its bacteriophages. *Proc Natl Acad Sci U S A* 85: 914-8.

Garcia P, Garcia JL, Garcia E, Sanchez-Puelles JM, Lopez R (1990). Modular organization of the lytic enzymes of *Streptococcus pneumoniae* and its bacteriophages. *Gene* 86: 81-8.

Garcia P, Martinez B, Rodriguez L, Rodriguez A (2010). Synergy between the phage endolysin LysH5 and nisin to kill *Staphylococcus aureus* in pasteurized milk. *Int J Food Microbiol* 141: 151-5.

Garro AD, Olivella MS, Bombasaro JA, Lima B, Tapia A, Feresin G, Perczel A, Somlai C, Penke B, Lopez Cascales J, Rodriguez AM, Enriz RD (2013). Penetratin and derivatives acting as antibacterial agents. *Chem Biol Drug Des* 82: 167-77.

Glauner B, Holtje JV, Schwarz U (1988). The composition of the murein of *Escherichia coli*. *J Biol Chem* 263: 10088-95.

Gopal GJ, Kumar A (2013). Strategies for the production of recombinant protein in *Escherichia coli*. *Protein J* 32: 419-25.

Grundling A, Schneewind O (2006). Cross-linked peptidoglycan mediates lysostaphin binding to the cell wall envelope of *Staphylococcus aureus*. *J Bacteriol* 188: 2463-72.

Gupta R, Prasad Y (2011). P-27/HP endolysin as antibacterial agent for antibiotic resistant *Staphylococcus aureus* of human infections. *Curr Microbiol* 63: 39-45.

Haun RS, Serventi IM, Moss J (1992). Rapid, reliable ligation-independent cloning of PCR products using modified plasmid vectors. *Biotechniques* 13: 515-8.

Hermoso JA, Monterroso B, Albert A, Galan B, Ahrazem O, Garcia P, Martinez-Ripoll M, Garcia JL,

Menendez M (2003). Structural basis for selective recognition of pneumococcal cell wall by modular endolysin from phage Cp-1. *Structure* 11: 1239-49.

Hirshfield IN, Terzulli S, O'Byrne C (2003). Weak organic acids: a panoply of effects on bacteria. *Sci Prog* 86: 245-69.

Holst O, Molinaro A (2009). Core region and lipid A components of lipopolysaccharides. In: Moran AP, Holst O, Brennan P, Itzstein Mv (eds.) Microbial glycobiology - structures, relevance and applications, Elsevier Inc. pp 29–56.

Hoopes JT, Stark CJ, Kim HA, Sussman DJ, Donovan DM, Nelson DC (2009). Use of a bacteriophage lysin, PlyC, as an enzyme disinfectant against *Streptococcus equi*. *Appl Environ Microbiol* 75: 1388-94.

Horgan M, O'Flynn G, Garry J, Cooney J, Coffey A, Fitzgerald GF, Ross RP, McAuliffe O (2009). Phage lysin LysK can be truncated to its CHAP domain and retain lytic activity against live antibiotic-resistant staphylococci. *Appl Environ Microbiol* 75: 872-4.

Hu S, Kong J, Kong W, Guo T, Ji M (2010). Characterization of a novel LysM domain from *Lactobacillus fermentum* bacteriophage endolysin and its use as an anchor to display heterologous proteins on the surfaces of lactic acid bacteria. *Appl Environ Microbiol* 76: 2410-8.

Hughes KA, Sutherland IW, Jones MV (1998). Biofilm susceptibility to bacteriophage attack: the role of phage-borne polysaccharide depolymerase. *Microbiology* 144 (Pt 11): 3039-47.

Ibrahim HR, Yamada M, Matsushita K, Kobayashi K, Kato A (1994). Enhanced bactericidal action of lysozyme to *Escherichia coli* by inserting a hydrophobic pentapeptide into its C terminus. *J Biol Chem* 269: 5059-63.

In YW, Kim JJ, Kim HJ, Oh SW (2013). Antimicrobial Activities of Acetic Acid, Citric Acid and Lactic Acid against *Shigella* Species. *Journal of Food Safety* 33: 79-85.

Itoh Y, Wang X, Hinnebusch BJ, Preston JF, 3rd, Romeo T (2005). Depolymerization of beta-1,6-N-acetyl-D-glucosamine disrupts the integrity of diverse bacterial biofilms. *J Bacteriol* 187: 382-7.

Jado I, Lopez R, Garcia E, Fenoll A, Casal J, Garcia P (2003). Phage lytic enzymes as therapy for antibiotic-resistant *Streptococcus pneumoniae* infection in a murine sepsis model. *J Antimicrob Chemother* 52: 967-73.

Jun SY, Jung GM, Yoon SJ, Oh MD, Choi YJ, Lee WJ, Kong JC, Seol JG, Kang SH (2013). Antibacterial properties of a pre-formulated recombinant phage endolysin, SAL-1. *Int J Antimicrob Agents* 41: 156-61.

Kakikawa M, Yokoi KJ, Kimoto H, Nakano M, Kawasaki K, Taketo A, Kodaira K (2002). Molecular analysis of the lysis protein Lys encoded by *Lactobacillus plantarum* phage phig1e. *Gene* 299: 227-34.

Kaplan JB, Ragunath C, Ramasubbu N, Fine DH (2003). Detachment of *Actinobacillus actinomycetemcomitans* biofilm cells by an endogenous beta-hexosaminidase activity. *J Bacteriol* 185: 4693-8.

Kaplan JB, Ragunath C, Velliyagounder K, Fine DH, Ramasubbu N (2004). Enzymatic detachment of *Staphylococcus epidermidis* biofilms. *Antimicrob Agents Chemother* 48: 2633-6.

Khosla C, Harbury PB (2001). Modular enzymes. *Nature* 409: 247-52.

Kim SA, Rhee MS (2013). Marked Synergistic Bactericidal Effects and Mode of Action of Medium-Chain Fatty Acids in Combination with Organic Acids against *Escherichia coli* O157:H7. *Applied and*

Environmental Microbiology 79: 6552-6560.

Kim WS, Salm H, Geider K (2004). Expression of bacteriophage phiEa1h lysozyme in *Escherichia coli* and its activity in growth inhibition of *Erwinia amylovora*. *Microbiology* 150: 2707-14.

Kirkpatrick C, Maurer LM, Oyelakin NE, Yoncheva YN, Maurer R, Slonczewski JL (2001). Acetate and formate stress: opposite responses in the proteome of *Escherichia coli*. *J Bacteriol* 183: 6466-77.

Klevens RM, Edwards JR, Richards CL, Jr., Horan TC, Gaynes RP, Pollock DA, Cardo DM (2007). Estimating health care-associated infections and deaths in U.S. hospitals, 2002. *Public Health Rep* 122: 160-6.

Knirel YA (2009). O-Specific polysaccharides of Gram-negative bacteria. In: Moran AP, Holst O, Brennan P, Itzstein Mv (eds.) Microbial glycobiology - structures, relevance and applications, Elsevier Inc. pp 57–74.

Korndorfer IP, Danzer J, Schmelcher M, Zimmer M, Skerra A, Loessner MJ (2006). The crystal structure of the bacteriophage PSA endolysin reveals a unique fold responsible for specific recognition of *Listeria* cell walls. *J Mol Biol* 364: 678-89.

Kretzer JW, Lehmann R, Schmelcher M, Banz M, Kim KP, Korn C, Loessner MJ (2007). Use of high-affinity cell wall-binding domains of bacteriophage endolysins for immobilization and separation of bacterial cells. *Appl Environ Microbiol* 73: 1992-2000.

Kung HC, Hoyert DL, Xu J, Murphy SL (2008). Deaths: final data for 2005. *Natl Vital Stat Rep* 56: 1-120.

Labrie SJ, Samson JE, Moineau S (2010). Bacteriophage resistance mechanisms. *Nat Rev Microbiol* 8: 317-27.

Lai MJ, Lin NT, Hu A, Soo PC, Chen LK, Chen LH, Chang KC (2011). Antibacterial activity of *Acinetobacter baumannii* phage varphiAB2 endolysin (LysAB2) against both gram-positive and gram-negative bacteria. *Appl Microbiol Biotechnol* 90: 529-39.

Lavigne R, Briers Y, Hertveldt K, Robben J, Volckaert G (2004). Identification and characterization of a highly thermostable bacteriophage lysozyme. *Cell Mol Life Sci* 61: 2753-9.

Lavollay M, Arthur M, Fourgeaud M, Dubost L, Marie A, Veziris N, Blanot D, Gutmann L, Mainardi JL (2008). The peptidoglycan of stationary-phase *Mycobacterium tuberculosis* predominantly contains cross-links generated by L,D-transpeptidation. *J Bacteriol* 190: 4360-6.

Leive L, Shovlin VK, Mergenhagen SE (1968). Physical, chemical, and immunological properties of lipopolysaccharide released from *Escherichia coli* by ethylenediaminetetraacetate. *J Biol Chem* 243: 6384-91.

Lewis K (2008). Multidrug tolerance of biofilms and persister cells. *Curr Top Microbiol Immunol* 322: 107-31.

Liu B, Wu S, Song Q, Zhang X, Xie L (2006). Two novel bacteriophages of thermophilic bacteria isolated from deep-sea hydrothermal fields. *Curr Microbiol* 53: 163-6.

Loeffler JM, Djurkovic S, Fischetti VA (2003). Phage lytic enzyme Cpl-1 as a novel antimicrobial for pneumococcal bacteremia. *Infect Immun* 71: 6199-204.

Loeffler JM, Fischetti VA (2003). Synergistic lethal effect of a combination of phage lytic enzymes with different activities on penicillin-sensitive and -resistant *Streptococcus pneumoniae* strains. *Antimicrob Agents Chemother* 47: 375-7.

Loeffler JM, Nelson D, Fischetti VA (2001). Rapid killing of *Streptococcus pneumoniae* with a

bacteriophage cell wall hydrolase. *Science* 294: 2170-2.

Loessner MJ, Gaeng S, Scherer S (1999). Evidence for a holin-like protein gene fully embedded out of frame in the endolysin gene of *Staphylococcus aureus* bacteriophage 187. *J Bacteriol* 181: 4452-60.

Loessner MJ, Gaeng S, Wendlinger G, Maier SK, Scherer S (1998). The two-component lysis system of *Staphylococcus aureus* bacteriophage Twort: a large TTG-start holin and an associated amidase endolysin. *FEMS Microbiol Lett* 162: 265-74.

Loessner MJ, Kramer K, Ebel F, Scherer S (2002). C-terminal domains of *Listeria monocytogenes* bacteriophage murein hydrolases determine specific recognition and high-affinity binding to bacterial cell wall carbohydrates. *Mol Microbiol* 44: 335-49.

Loessner MJ, Maier SK, Daubek-Puza H, Wendlinger G, Scherer S (1997). Three *Bacillus cereus* bacteriophage endolysins are unrelated but reveal high homology to cell wall hydrolases from different bacilli. *J Bacteriol* 179: 2845-51.

Loessner MJ, Wendlinger G, Scherer S (1995). Heterogeneous endolysins in *Listeria monocytogenes* bacteriophages: a new class of enzymes and evidence for conserved holin genes within the siphoviral lysis cassettes. *Mol Microbiol* 16: 1231-41.

Low LY, Yang C, Perego M, Osterman A, Liddington RC (2005). Structure and lytic activity of a *Bacillus anthracis* prophage endolysin. *J Biol Chem* 280: 35433-9.

Lu JZ, Fujiwara T, Komatsuzawa H, Sugai M, Sakon J (2006). Cell wall-targeting domain of glycylglycine endopeptidase distinguishes among peptidoglycan cross-bridges. *J Biol Chem* 281: 549-58.

Lu TK, Collins JJ (2007). Dispersing biofilms with engineered enzymatic bacteriophage. *Proc Natl Acad Sci U S A* 104: 11197-202.

Lukacik P, Barnard TJ, Keller PW, Chaturvedi KS, Seddiki N, Fairman JW, Noinaj N, Kirby TL, Henderson JP, Steven AC, Hinnebusch BJ, Buchanan SK (2012). Structural engineering of a phage lysin that targets gram-negative pathogens. *Proc Natl Acad Sci U S A* 109: 9857-62.

Mah TF, O'Toole GA (2001). Mechanisms of biofilm resistance to antimicrobial agents. *Trends Microbiol* 9: 34-9.

Manoharadas S, Witte A, Blasi U (2009). Antimicrobial activity of a chimeric enzybiotic towards *Staphylococcus aureus*. *J Biotechnol* 139: 118-23.

Matsushita I, Yanase H (2008). A novel thermophilic lysozyme from bacteriophage phiIN93. *Biochem Biophys Res Commun* 377: 89-92.

Matthews BW, Remington SJ (1974). The three dimensional structure of the lysozyme from bacteriophage T4. *Proc Natl Acad Sci U S A* 71: 4178-82.

Mayer MJ, Payne J, Gasson MJ, Narbad A (2010). Genomic sequence and characterization of the virulent bacteriophage phiCTP1 from *Clostridium tyrobutyricum* and heterologous expression of its endolysin. *Appl Environ Microbiol* 76: 5415-22.

McCullers JA, Karlstrom A, Iverson AR, Loeffler JM, Fischetti VA (2007). Novel strategy to prevent otitis media caused by colonizing *Streptococcus pneumoniae*. *PLoS Pathog* 3: e28.

Mikoulinskaia GV, Odinokova IV, Zimin AA, Lysanskaya VY, Feofanov SA, Stepnaya OA (2009). Identification and characterization of the metal ion-dependent L-alanoyl-D-glutamate peptidase encoded by bacteriophage T5. *FEBS J* 276: 7329-42.

Morin N, Lanneluc I, Connil N, Cottenceau M, Pons AM, Sable S (2011). Mechanism of bactericidal activity of microcin L in *Escherichia coli* and *Salmonella enterica*. *Antimicrob Agents Chemother* 55: 997-1007.

Morita M, Tanji Y, Orito Y, Mizoguchi K, Soejima A, Unno H (2001). Functional analysis of antibacterial activity of *Bacillus amyloliquefaciens* phage endolysin against Gram-negative bacteria. *FEBS Lett* 500: 56-9.

Nakagawa H, Arisaka F, Ishii S (1985). Isolation and characterization of the bacteriophage T4 tail-associated lysozyme. *J Virol* 54: 460-6.

Nakimbugwe D, Masschalck B, Atanassova M, Zewdie-Bosuner A, Michiels CW (2006). Comparison of bactericidal activity of six lysozymes at atmospheric pressure and under high hydrostatic pressure. *Int J Food Microbiol* 108: 355-63.

Navarre WW, Ton-That H, Faull KF, Schneewind O (1999). Multiple enzymatic activities of the murein hydrolase from staphylococcal phage phi11. Identification of a D-alanyl-glycine endopeptidase activity. *J Biol Chem* 274: 15847-56.

Nelson D, Loomis L, Fischetti VA (2001). Prevention and elimination of upper respiratory colonization of mice by group A streptococci by using a bacteriophage lytic enzyme. *Proc Natl Acad Sci U S A* 98: 4107-12.

Nelson D, Schuch R, Chahales P, Zhu S, Fischetti VA (2006). PlyC: a multimeric bacteriophage lysin. *Proc Natl Acad Sci U S A* 103: 10765-70.

Nikaido H (2003). Molecular basis of bacterial outer membrane permeability revisited. *Microbiol Mol Biol Rev* 67: 593-656.

Nikaido H, Vaara M (1985). Molecular basis of bacterial outer membrane permeability. *Microbiol Rev* 49: 1-32.

O'Flaherty S, Coffey A, Meaney W, Fitzgerald GF, Ross RP (2005). The recombinant phage lysin LysK has a broad spectrum of lytic activity against clinically relevant staphylococci, including methicillin-resistant *Staphylococcus aureus*. *J Bacteriol* 187: 7161-4.

Obeso JM, Martinez B, Rodriguez A, Garcia P (2008). Lytic activity of the recombinant staphylococcal bacteriophage PhiH5 endolysin active against Staphylococcus aureus in milk. *Int J Food Microbiol* 128: 212-8.

Oliveira H, Azeredo J, Lavigne R, Kluskens LD (2012). Bacteriophage endolysins as a response to emerging foodborne pathogens. *Trends in Food Science & Technology* 28: 103-115.

Oliveira H, Melo LD, Santos SB, Nobrega FL, Ferreira EC, Cerca N, Azeredo J, Kluskens LD (2013). Molecular aspects and comparative genomics of bacteriophage endolysins. *J Virol* 87: 4558-70.

Oren Z, Shai Y (1998). Mode of action of linear amphipathic alpha-helical antimicrobial peptides. *Biopolymers* 47: 451-63.

Pang T, Savva CG, Fleming KG, Struck DK, Young R (2009). Structure of the lethal phage pinhole. *Proc Natl Acad Sci U S A* 106: 18966-71.

Paradis-Bleau C, Cloutier I, Lemieux L, Sanschagrin F, Laroche J, Auger M, Garnier A, Levesque RC (2007). Peptidoglycan lytic activity of the *Pseudomonas aeruginosa* phage phiKZ gp144 lytic transglycosylase. *FEMS Microbiol Lett* 266: 201-9.

Park IY, Park CB, Kim MS, Kim SC (1998). Parasin I, an antimicrobial peptide derived from histone H2A in the catfish, *Parasilurus asotus*. *FEBS Lett* 437: 258-62.

Park T, Struck DK, Dankenbring CA, Young R (2007). The pinholin of lambdoid phage 21: control of lysis by membrane depolarization. *J Bacteriol* 189: 9135-9.

Payne KM, Hatfull GF (2012). Mycobacteriophage endolysins: diverse and modular enzymes with multiple catalytic activities. *PLoS One* 7: e34052.

Perez-Dorado I, Campillo NE, Monterroso B, Hesek D, Lee M, Paez JA, Garcia P, Martinez-Ripoll M, Garcia JL, Mobashery S, Menendez M, Hermoso JA (2007). Elucidation of the molecular recognition of bacterial cell wall by modular pneumococcal phage endolysin CPL-1. *J Biol Chem* 282: 24990-9.

Pier GB (2007). *Pseudomonas aeruginosa* lipopolysaccharide: a major virulence factor, initiator of inflammation and target for effective immunity. *Int J Med Microbiol* 297: 277-95.

Pisabarro AG, de Pedro MA, Vazquez D (1985). Structural modifications in the peptidoglycan of *Escherichia coli* associated with changes in the state of growth of the culture. *J Bacteriol* 161: 238-42.

Price WN, 2nd, Handelman SK, Everett JK, Tong SN, Bracic A, Luff JD, Naumov V, Acton T, Manor P, Xiao R, Rost B, Montelione GT, Hunt JF (2011). Large-scale experimental studies show unexpected amino acid effects on protein expression and solubility *in vivo* in *E. coli*. *Microb Inform Exp* 1: 6.

Pritchard DG, Dong S, Baker JR, Engler JA (2004). The bifunctional peptidoglycan lysin of *Streptococcus agalactiae* bacteriophage B30. *Microbiology* 150: 2079-87.

Pritchard DG, Dong S, Kirk MC, Cartee RT, Baker JR (2007). LambdaSa1 and LambdaSa2 prophage lysins of *Streptococcus agalactiae*. *Appl Environ Microbiol* 73: 7150-4.

Provencher SW, Glockner J (1981). Estimation of globular protein secondary structure from circular dichroism. *Biochemistry* 20: 33-7.

Raetz CR, Whitfield C (2002). Lipopolysaccharide endotoxins. *Annu Rev Biochem* 71: 635-700.

Rashel M, Uchiyama J, Ujihara T, Uehara Y, Kuramoto S, Sugihara S, Yagyu K, Muraoka A, Sugai M, Hiramatsu K, Honke K, Matsuzaki S (2007). Efficient elimination of multidrug-resistant *Staphylococcus aureus* by cloned lysin derived from bacteriophage phi MR11. *J Infect Dis* 196: 1237-47.

Raymond Schuch VAF, Daniel C. Nelson (2009). A Genetic Screen to Identify Bacteriophage Lysins. In: Clokie AMKMRJ (eds.) Bacteriophages - Methods in Molecular Biology, pp 307-319.

Remmert M, Biegert A, Hauser A, Soding J (2012). HHblits: lightning-fast iterative protein sequence searching by HMM-HMM alignment. *Nat Methods* 9: 173-5.

Rodriguez-Rubio L, Martinez B, Rodriguez A, Donovan DM, Gotz F, Garcia P (2013). The phage lytic proteins from the *Staphylococcus aureus* bacteriophage vB_SauS-phiIPLA88 display multiple active catalytic domains and do not trigger staphylococcal resistance. *PLoS One* 8: e64671.

Roe AJ, McLaggan D, Davidson I, O'Byrne C, Booth IR (1998). Perturbation of anion balance during inhibition of growth of *Escherichia coli* by weak acids. *J Bacteriol* 180: 767-72.

Roe AJ, O'Byrne C, McLaggan D, Booth IR (2002). Inhibition of *Escherichia coli* growth by acetic acid: a problem with methionine biosynthesis and homocysteine toxicity. *Microbiology* 148: 2215-22.

Rohwer F (2003). Global phage diversity. *Cell* 113: 141.

Rolfe MD, Rice CJ, Lucchini S, Pin C, Thompson A, Cameron AD, Alston M, Stringer MF, Betts RP, Baranyi J, Peck MW, Hinton JC (2012). Lag phase is a distinct growth phase that prepares bacteria

for exponential growth and involves transient metal accumulation. *J Bacteriol* 194: 686-701.

Saiz JL, Lopez-Zumel C, Monterroso B, Varea J, Arrondo JL, Iloro I, Garcia JL, Laynez J, Menendez M (2002). Characterization of EjI, the cell-wall amidase coded by the pneumococcal bacteriophage Ej-1. *Protein Sci* 11: 1788-99.

Sao-Jose C, Parreira R, Vieira G, Santos MA (2000). The N-terminal region of the *Oenococcus oeni* bacteriophage fOg44 lysin behaves as a bona fide signal peptide in *Escherichia coli* and as a cis-inhibitory element, preventing lytic activity on oenococcal cells. *J Bacteriol* 182: 5823-31.

Saren AM, Ravantti JJ, Benson SD, Burnett RM, Paulin L, Bamford DH, Bamford JK (2005). A snapshot of viral evolution from genome analysis of the *Tectiviridae* family. *J Mol Biol* 350: 427-40.

Sass P, Bierbaum G (2007). Lytic activity of recombinant bacteriophage phi11 and phi12 endolysins on whole cells and biofilms of *Staphylococcus aureus*. *Appl Environ Microbiol* 73: 347-52.

Scallan E, Hoekstra RM, Angulo FJ, Tauxe RV, Widdowson MA, Roy SL, Jones JL, Griffin PM (2011). Foodborne illness acquired in the United States - major pathogens. *Emerg Infect Dis* 17: 7-15.

Schleifer KH, Kandler O (1972). Peptidoglycan types of bacterial cell walls and their taxonomic implications. *Bacteriol Rev* 36: 407-77.

Schmelcher M, Powell AM, Becker SC, Camp MJ, Donovan DM (2012a). Chimeric phage lysins act synergistically with lysostaphin to kill mastitis-causing *Staphylococcus aureus* in murine mammary glands. *Appl Environ Microbiol* 78: 2297-305.

Schmelcher M, Shabarova T, Eugster MR, Eichenseher F, Tchang VS, Banz M, Loessner MJ (2010). Rapid multiplex detection and differentiation of *Listeria* cells by use of fluorescent phage endolysin cell wall binding domains. *Appl Environ Microbiol* 76: 5745-56.

Schmelcher M, Tchang VS, Loessner MJ (2011). Domain shuffling and module engineering of *Listeria* phage endolysins for enhanced lytic activity and binding affinity. *Microb Biotechnol* 4: 651-62.

Schmelcher M, Waldherr F, Loessner MJ (2012b). *Listeria* bacteriophage peptidoglycan hydrolases feature high thermoresistance and reveal increased activity after divalent metal cation substitution. *Appl Microbiol Biotechnol* 93: 633-43.

Schuch R, Nelson D, Fischetti VA (2002). A bacteriolytic agent that detects and kills *Bacillus anthracis*. *Nature* 418: 884-9.

Scudamore RA, Beveridge TJ, Goldner M (1979). Outer-membrane penetration barriers as components of intrinsic resistance to beta-lactam and other antibiotics in *Escherichia coli* K-12. *Antimicrob Agents Chemother* 15: 182-9.

Sheehan MM, Garcia JL, Lopez R, Garcia P (1997). The lytic enzyme of the pneumococcal phage Dp-1: a chimeric lysin of intergeneric origin. *Mol Microbiol* 25: 717-25.

Shen Y, Koller T, Kreikemeyer B, Nelson DC (2013). Rapid degradation of *Streptococcus* pyogenes biofilms by PlyC, a bacteriophage-encoded endolysin. *J Antimicrob Chemother* 68: 1818-24.

Sillankorva S, Pleteneva E, Shaburova O, Santos S, Carvalho C, Azeredo J, Krylov V (2010). *Salmonella* Enteritidis bacteriophage candidates for phage therapy of poultry. *J Appl Microbiol* 108: 1175-86.

Son JS, Lee SJ, Jun SY, Yoon SJ, Kang SH, Paik HR, Kang JO, Choi YJ (2010). Antibacterial and biofilm removal activity of a podoviridae *Staphylococcus aureus* bacteriophage SAP-2 and a derived recombinant cell-wall-degrading enzyme. *Appl Microbiol Biotechnol* 86: 1439-49.

Splith K, Neundorf I (2011). Antimicrobial peptides with cell-penetrating peptide properties and vice versa. *Eur Biophys J* 40: 387-97.

Sturino JM, Klaenhammer TR (2006). Engineered bacteriophage-defence systems in bioprocessing. *Nat Rev Microbiol* 4: 395-404.

Sudiarta IP, Fukushima T, Sekiguchi J (2010). *Bacillus subtilis* CwlP of the SP-{beta} prophage has two novel peptidoglycan hydrolase domains, muramidase and cross-linkage digesting DD-endopeptidase. *J Biol Chem* 285: 41232-43.

Sullivan L, Paredes CJ, Papoutsakis ET, Bennett GN (2007). Analysis of the clostridial hydrophobic with a conserved tryptophan family (ChW) of proteins in *Clostridium acetobutylicum* with emphasis on ChW14 and ChW16/17. *Enzyme and Microbial Technology* 42: 29-43.

Summers WC (2004). Bacteriophage research early history. In: Kutter E, Sulakvelidze A (eds.) Bacteriophages - Biology and Applications, CRC Press. pp 5-27.

Tamakoshi M, Murakami A, Sugisawa M, Tsuneizumi K, Takeda S, Saheki T, Izumi T, Akiba T, Mitsuoka K, Toh H, Yamashita A, Arisaka F, Hattori M, Oshima T, Yamagishi A (2011). Genomic and proteomic characterization of the large *Myoviridae* bacteriophage varphiTMA of the extreme thermophile *Thermus thermophilus*. *Bacteriophage* 1: 152-164.

Theron MM, Lues JFR (2011). Mechanisms of microbial inhibition. In: Theron MM, Lues JFR (eds.) Organic Acids and Food Preservation, CRC Press. pp 117-150.

Vaara M (1992). Agents that increase the permeability of the outer membrane. *Microbiol Rev* 56: 395-411.

Vaara M (1999). Lipopolysaccharide and the Permeability of the Bacterial Outer Membrane. In: Brade H, Opal SM, Vagel SN, Morrison DC (eds.) Endotoxin in Health and Disease, CRC Press. pp 31-39.

Vaara M, Vaara T (1983). Polycations sensitize enteric bacteria to antibiotics. *Antimicrob Agents Chemother* 24: 107-13.

van Stokkum IH, Spoelder HJ, Bloemendal M, van Grondelle R, Groen FC (1990). Estimation of protein secondary structure and error analysis from circular dichroism spectra. *Anal Biochem* 191: 110-8.

Vasala A, Valkkila M, Caldentey J, Alatossava T (1995). Genetic and biochemical characterization of the *Lactobacillus delbrueckii* subsp. *lactis* bacteriophage LL-H lysin. *Appl Environ Microbiol* 61: 4004-11.

Vincent PA, Delgado MA, Farias RN, Salomon RA (2004). Inhibition of *Salmonella enterica* serovars by microcin J25. *FEMS Microbiol Lett* 236: 103-7.

Vives E, Brodin P, Lebleu B (1997). A truncated HIV-1 Tat protein basic domain rapidly translocates through the plasma membrane and accumulates in the cell nucleus. *J Biol Chem* 272: 16010-7.

Vollmer W, Born P (2009). Bacterial cell envelope peptidoglycan. In: Moran AP, Holst O, Brennan P, Itzstein Mv (eds.) Microbial glycobiology - structures, relevance and applications, Elsevier Inc. pp 15–28.

Walmagh M, Briers Y, dos Santos SB, Azeredo J, Lavigne R (2012). Characterization of modular bacteriophage endolysins from *Myoviridae* phages OBP, 201phi2-1 and PVP-SE1. *PLoS One* 7: e36991.

Warnecke T, Gill RT (2005). Organic acid toxicity, tolerance, and production in *Escherichia coli*

biorefining applications. *Microb Cell Fact* 4: 25.

Weaver LH, Grutter MG, Matthews BW (1995). The refined structures of goose lysozyme and its complex with a bound trisaccharide show that the "goose-type" lysozymes lack a catalytic aspartate residue. *J Mol Biol* 245: 54-68.

Webb H, Tynan-Connolly BM, Lee GM, Farrell D, O'Meara F, Sondergaard CR, Teilum K, Hewage C, McIntosh LP, Nielsen JE (2010). Remeasuring HEWL pK(a) values by NMR spectroscopy: methods, analysis, accuracy, and implications for theoretical pK(a) calculations. *Proteins* 79: 685-702.

Whitmore L, Wallace BA (2004). DICHROWEB, an online server for protein secondary structure analyses from circular dichroism spectroscopic data. *Nucleic Acids Res* 32: W668-73.

Whitmore L, Wallace BA (2008). Protein secondary structure analyses from circular dichroism spectroscopy: methods and reference databases. *Biopolymers* 89: 392-400.

Wohlkonig A, Huet J, Looze Y, Wintjens R (2010). Structural relationships in the lysozyme superfamily: significant evidence for glycoside hydrolase signature motifs. *PLoS One* 5: e15388.

Wright GD, Molinas C, Arthur M, Courvalin P, Walsh CT (1992). Characterization of vanY, a DD-carboxypeptidase from vancomycin-resistant *Enterococcus faecium* BM4147. *Antimicrob Agents Chemother* 36: 1514-8.

Xu M, Struck DK, Deaton J, Wang IN, Young R (2004). A signal-arrest-release sequence mediates export and control of the phage P1 endolysin. *Proc Natl Acad Sci U S A* 101: 6415-20.

Yan L, Adams ME (1998). Lycotoxins, antimicrobial peptides from venom of the wolf spider *Lycosa carolinensis*. *J Biol Chem* 273: 2059-66.

Yoong P, Schuch R, Nelson D, Fischetti VA (2004). Identification of a broadly active phage lytic enzyme with lethal activity against antibiotic-resistant *Enterococcus faecalis* and *Enterococcus faecium*. *J Bacteriol* 186: 4808-12.

Yoong P, Schuch R, Nelson D, Fischetti VA (2006). PlyPH, a bacteriolytic enzyme with a broad pH range of activity and lytic action against *Bacillus anthracis*. *J Bacteriol* 188: 2711-4.

Young R (1992). Bacteriophage lysis: mechanism and regulation. *Microbiol Rev* 56: 430-81.

Young R, Blasi U (1995). Holins: form and function in bacteriophage lysis. *FEMS Microbiol Rev* 17: 191-205.

Zhang H, Bao H, Billington C, Hudson JA, Wang R (2012). Isolation and lytic activity of the *Listeria* bacteriophage endolysin LysZ5 against *Listeria monocytogenes* in soya milk. *Food Microbiol* 31: 133-6.

Zhu WL, Shin SY (2009). Antimicrobial and cytolytic activities and plausible mode of bactericidal action of the cell penetrating peptide penetratin and its lys-linked two-stranded peptide. *Chem Biol Drug Des* 73: 209-15.

Zimmer M, Vukov N, Scherer S, Loessner MJ (2002). The murein hydrolase of the bacteriophage phi3626 dual lysis system is active against all tested *Clostridium perfringens* strains. *Appl Environ Microbiol* 68: 5311-7.

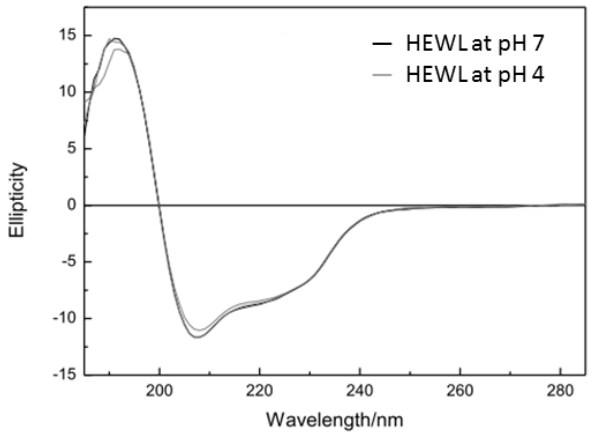

Figure S4.1. Circular dichroism spectrum of HEWL at pH (7.0) and acidic pH (4.0).

Table S4.1. Combinatorial effect of Lys68 with EDTA against different *Enterobacteriaceae* species. Overnight bacterial cells were 1:100 diluted in fresh LB, grown for approx. 3 h to reach exponential phase (OD_{600nm} of 0.6). Cells resuspended in 10 mM HEPES/NaOH (pH 7.2) were then 100-fold diluted to a final density of 10^6 CFU/mL. Each cell (50 µL) was incubated with 25 µL Lys68 (2 µM final concentration) together with 25 µL of EDTA (5 mM final concentration) for 30 min. Cells incubated with PBS (instead of Lys68) or with water (instead of EDTA) were used as a negative control. After incubation CFUs were counted. Averages ± standard deviations are given for n = 3 repeats.

Bacterial Species	Lys68/Water	PBS/EDTA	Lys68/EDTA
***S.* Tyhpimurium LT2**	0.08 ± 0.07	0.07 ± 0.08	0.18 ± 0.10
***E. coli* O157:H7 CECT 4782**	0.14 ± 0.05	0.11 ± 0.12	0.10 ± 0.00
***Cronobacter sakazakii* CECT 858**	0.09 ± 0.05	0.14 ± 0.05	0.13 ± 0.12

Figure S5.1. ClustalW multiple sequence alignment of ABgp46 with top five close-related sequences. The query ABgp46 (boxed) is aligned to five endolysin sequences belonging to *Acinetobacter* phages: phiAB2 (HM755898), phage AB3 (YP_008060133.1 and YP_008060134.1), phage ABP-01 (AHG30899.1) and phage ABP-04 (AHG30900.1). For each protein the accession numbers are given. Comparison shows conserved (*) and positive (:/.) amino acid matches. Highlighted at grey is the putative amphipathic helices region found in the C-terminus of the LysAB2 that matches 100% with ABgp46. Positively charged amino acids are shown are shown in bold.

1 MLTVSACGADPSASDHSAALDLAVNTATSLKRKLVVDFDLRVNTTTELDATLRIEGDGGAVQFSRSITATADIPIFTVKA 80

81 GFSSESSYFGKLMFKASTGGTATAFRSTSNGYLSQSTFDHCVFDRSLRYGIDANLILCDFQKCDFGTYMSTTNSIGFKAIR 160

161 SLGVVGTREPNANTFYNCIFRKGTDDCMIEWDSYGTQWHFFACDLEQ 208

Figure S5.2. Amino acid sequence of ABgp42. A depolymerase-related domain (Pectate_lyase_3), from the Pec lyase clan (CLO268), was found using HHpred webserver (URL: http://toolkit.tuebingen.mpg.de/hhpred.html) using Pfam, InterProScan and COG; with an E-value of 0.041 and 96.6% of query coverage (amino acids 4-207 underlined).